Structuring high-protein foods

Nanik Purwanti

Thesis committee

Thesis supervisor

Prof. dr. ir. R. M. Boom

Professor of Food Process Engineering

Wageningen University, The Netherlands

Thesis co-supervisor

Dr. ir. A.J. van der Goot

Associate Professor, Food Process Engineering Group

Wageningen University, The Netherlands

Other members

Prof. dr. ir. H. Gruppen

Wageningen University, The Netherlands

Prof. dr. P. Dejmek

Lund University, Sweden

Prof. dr. ir. P. M. M. Bongers

Eindhoven University of Technology, The Netherlands

Dr. ir. H. Luyten

Friesland Foods Corporate Research, Deventer, The Netherlands

This research was conducted under the auspices of the Graduate School of VLAG

Structuring high-protein foods

Nanik Purwanti

Thesis

submitted in fulfilment of the requirements for the degree of doctor
at Wageningen University
by the authority of the Rector Magnificus
Prof. dr. M. J. Kropff,
in the presence of the
Thesis Committee appointed by the Academic Board
to be defended in public
on Monday 12 March 2012
at 11 a.m. in the Aula.

Nanik Purwanti

Structuring high-protein foods,

192 pages.

Thesis, Wageningen University, Wageningen, NL (2012)

With summaries in English and Dutch

ISBN 978−94−6173−191−3

To Anton Ady Susanto

Pak Suharno & Bu Suwarti

Contents

Chapter 1

General introduction

1. Proteins in foods

Proteins are important biopolymers naturally present in foods that represent a major class of essential nutrients. Proteins are broken down in the body into amino acids that are used to resynthesize new proteins in the body, which are used to create for example new cells, hair, and tissue. In addition to being building blocks in the body, proteins can be used as an energy source. In addition to their physiological importance, proteins have important functions in food products, in which they stabilize or form a specific structure. For example, proteins stabilize foams and emulsions, they can act as binding agents and can induce gelation[1].

2. Health aspect of proteins

The amino acid composition differs for each protein source. Therefore, the recommended dietary intake is set for some reference proteins that are highly digestible and contain all essential amino acids. Typical examples of foods containing reference proteins are meat, milk, egg, and fish. The daily protein intake should be at least 0.75 g (kg body weight)$^{-1}$ day^{-1} for elderly people and young adults[2]. However, already in 1980s, researchers indicated that even higher protein intake could lead to health benefits for elderly people. Short-term and longer-term studies showed that a higher intake of protein can yield an improved, positive nitrogen balance[3, 4]. More recent studies indicate that a higher protein intake may suppress the progression of sarcopenia[5, 6].

An increased protein intake combined with heavy exercises stimulates muscle-development[7], which is important for athletes[8-11]. People that have overweight can also benefit from a diet with increased protein levels because proteins lead to an increased satiety compared with carbohydrates[12-18].

3. High-protein foods

The discerned benefits of high-protein intake have resulted in the development of high-protein products such as protein bars and protein drinks. Protein bars are often made from

protein mixtures and plasticizers, e.g. sugars or polyols. The latter components are used to keep the bars soft and pliable. Protein drinks are available in the form of ready-to-drink products or have to be reconstituted from powder. However, high-protein products often show lack of textural properties and subsequently, lead to shortcoming of sensorial properties[19-24]. Besides, high-protein products (especially solid products) are not stable upon storage, as their hardness tends to increase over time. Therefore, a further understanding on the role of the increased protein content on the textural attributes of the products is needed to allow further product development.

Most high-protein products contain whey protein. The main reason is that whey protein is a well available protein. An additional advantage is that it contains essential amino acids that are readily metabolised by the muscle[22, 25]. Whey protein isolate (WPI) contains more than 90% protein and most of it is β-lactoglobulin[26]. The protein composition of commercial WPI is listed in Table 1.

Table 1. Protein composition of commercial WPI determined with size-exclusion high-performance liquid chromatography[27].

Protein fraction	% total protein
Immunoglobulins	5.9–7.5
Bovine serum albumin	7.2–10.9
β-lactoglobulin	68.1–74.8
α-lactalbumin	8.3–17.5

4. The role of processing on high-protein food productions

A typical feature of high protein products is that their properties change over time. Often, the products become harder or tougher. Those changes are usually overcome by adding or varying ingredients. For example, the use of certain plasticizers or blended proteins instead of a single protein was found to lead to more stable product properties[28-35].

However, the role of processing has not received much attention. With appropriate process conditions, one has control over the exact distribution of proteins over the product, which will influence the properties of the product[36, 37].

One of the reasons for the undesired properties of high-protein foods is that the proteins form a strong network by forming intermolecular bonds[22, 30]. Inducing a non-homogenous distribution of the protein through processing could be a method to reduce long-range protein interactions. The reduced interactions may slow down the increasing strength of the network as a function of time. Fig. 1 gives an overview of possible structures in high-protein foods.

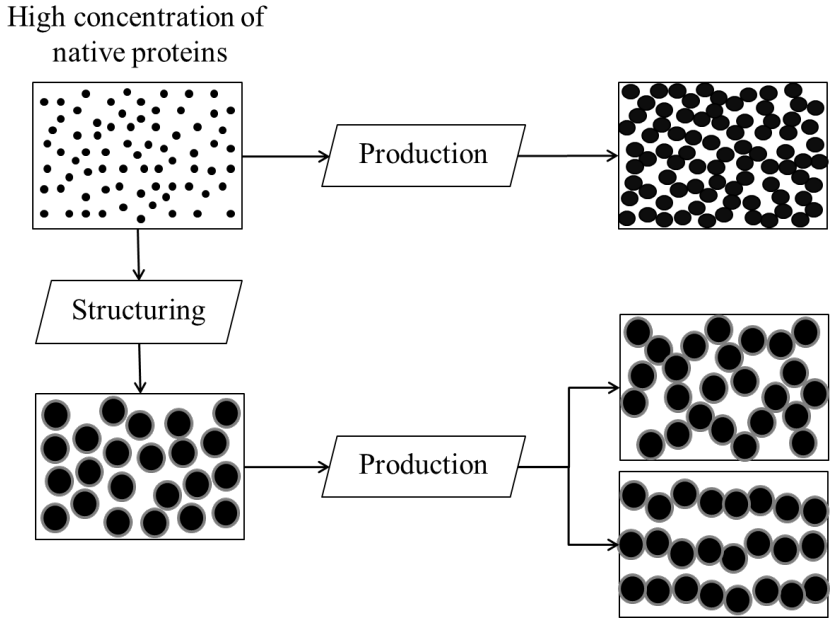

Figure 1. Schematic overview of possible structures in high-protein foods when production is done directly from native proteins or indirectly via structuring process.

In producing high-protein products, native proteins (i.e. as received from manufacturers) are generally blended with other ingredients. The production process may involve a heating process to ease mixing or solidification of the product. If a system contains a high protein concentration, it may jam; the system forms a solidified product before any interaction within the proteins, e.g. aggregation, completely occurs. The resulting product most likely will have a homogeneous and dense structure. However, unfinished

interactions in the proteins will continue and influence the product properties over time. If proteins are allowed to complete their interactions separated from the main process and then use them in the main process, the networks strength can be reduced and the resulting product is softer. The resulting network could be in isotropic or anisotropic form depending on the chosen processing method. Further, the protein interactions after the production process may also be less intensive.

Current industrial processes such as extrusion process have a limitation to allow modification of the detailed product structure to achieve the correct product properties. Almost a decade ago, it was found that application of well-defined flow fields (e.g. simple shear flow) could result in a better control on the product microstructure[38]. Simple shear was used to create new structures in wheat dough. Besides, a concentrated calcium caseinate could be made into fibrous structure[39]. Manski et al. (2007)[40] also showed that by altering the order of structuring and solidification of a mixture containing sodium caseinate and palm fat resulted in different product properties. In this thesis, it is studied how structuring techniques can be used to improve product properties and stability.

5. Objective and outline of the thesis

This thesis describes the exploration of structuring high-protein materials to control the product properties and stability. The scientific aim is to understand the relation between protein structure in the properties of high-protein products. A good understanding of this relation may guide us towards improving the quality of high-protein products using processing.

A literature study was performed and is described in **chapter 2.** This study provides routes to develop high-protein products with desirable structures, textures, and sensorial perceptions as well as stability over time.

Chapter 3 describes a first method to structure whey protein in which the protein molecules are clustered into protein aggregates by heat treatment at low protein

concentration. The protein concentration is increased by a concentration process. The effects of protein aggregation on rheological properties of high-protein gels are studied.

Chapter 4 describes a second method to structure whey protein. This method comprises gelling while mixing of a concentrated WPI suspension, followed by drying and milling the gels into microparticles. This chapter reports the properties of the microparticles and their potential application in the high-protein model product.

Chapter 5 further explores the potential of the WPI microparticles. Textural changes (i.e. hardening) in high-protein gels over time are reported. The influence of the internal structure on the hardening process is studied in detail.

The abovementioned methods result in isotropic structures. Previous research showed that it is possible to create an anisotropic structure using flow-induced structuring[39]. **Chapter 6** describes some first steps towards understanding structure formation in a model dispersion. The behaviour of model particles dispersed in a weakly viscoelastic medium under torsional flow in a shearing device (simple shear flow) is described extensively and the role of the various driving forces is evaluated.

Chapter 7 provides the overall conclusions of this thesis and it evaluates the scientific approaches described in the preceding chapters. The possibility to structure WPI microparticles using a shearing device is assessed, including its potential for future applications. Chapter 7 ends with a discussion about the importance of further understanding phenomena responsible for hardening of high-protein foods.

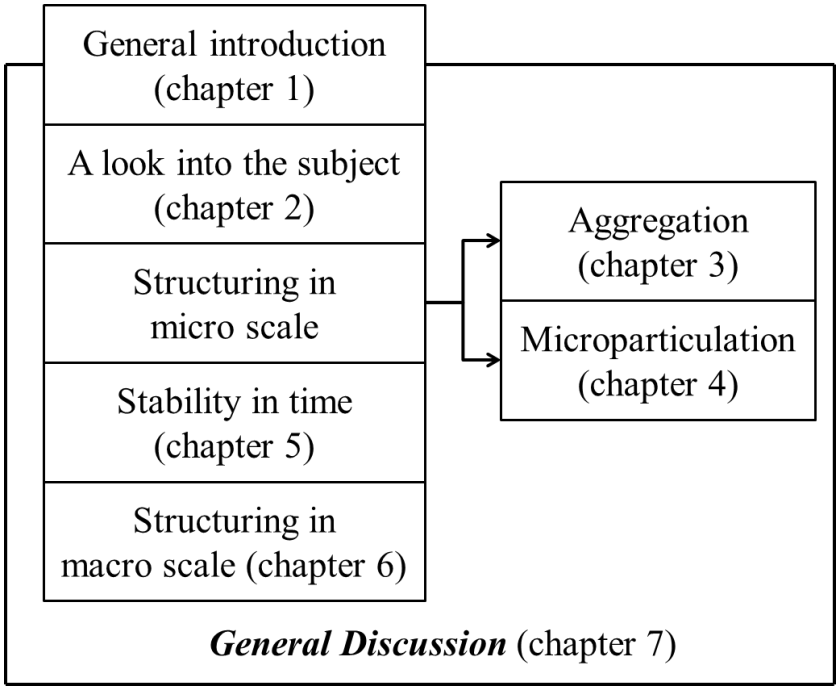

Figure 2. Schematic overview of the thesis entitled Structuring high-protein foods.

References

1. Fennema, O. R. (1996). Food Chemistry (3rd ed.). New York: Marcel Dekker, Inc.
2. Food and Nutrition Board, N. R. C. (1989). Recommended Dietary Allowances (10th ed.). Washington, D. C.: National Academy of Science.
3. Uauy, R., Scrimshaw, N. S., & Young, V. R. (1978). Human protein requirements: nitrogen balance response to graded levels of egg protein in elderly men and women. *American Journal of Clinical Nutrition*, *31*, 779-785.
4. Gersovitz, M., Motil, K., Munro, H. N., Scrimshaw, N. S., & Young, V. R. (1982). Human protein requirements: assessment of the adequacy of the current Recommended Dietary Allowance for dietary protein in elderly men and women. *American Journal of Clinical Nutrition*, *35*(1), 6-14.
5. Campbell, W. W. & Leidy, H. J. (2007). Dietary protein and resistance training effects on muscle and body composition in older persons. *Journal of the American College of Nutrition*, *26*(6), 696S-703S.
6. Paddon-Jones, D., Short, K. R., Campbell, W. W., Volpi, E., & Wolfe, R. R. (2008). Role of dietary protein in the sarcopenia of aging. *American Journal of Clinical Nutrition*, *87*(5), 1562S-1566S.
7. Lemon, P. W. R. (1997). Dietary protein requirements in athletes. *Nutritional Biochemistry*, *8*, 52-60.
8. Meredith, C. N., Zackin, M. J., Frontera, W. R., & Evans, W. J. (1989). Dietary protein requirements and body protein metabolism in endurance-trained men. *Journal of Applied Physiology*, *66*(6), 2850-2856.
9. Tarnopolsky, M. A. (2004). Protein requirements for endurance athletes. *Nutrition*, *20*, 662-668.
10. Tipton, K. D. & Wolfe, R. R. (2004). Protein and amino acids for athletes. *Journal of Sports Sciences*, *22*(1), 65-79.

11. Hayes, A. & Cribb, P. J. (2008). Effect of whey protein isolate on strength, body composition and muscle hypertrophy during resistance training. *Current Opinion in Clinical Nutrition and Metabolic Care*, *11*(1), 40-44.

12. Lejeune, M. P. G. M., Kovacs, E. M. R., & Westerterp-Plantenga, M. S. (2005). Additional protein intake limits weight regain after weight loss in humans. *British Journal of Nutrition*, *93*(2), 281-289.

13. Luhovyy, B. L., Akhavan, T., & Anderson, G. H. (2007). Whey proteins in the regulation of food intake and satiety. *Journal of the American College of Nutrition*, *26*(6), 704S-712S.

14. Halton, T. L. & Hu, F. B. (2004). The effects of high protein diets on thermogenesis, satiety and weight loss: a critical review. *Journal of the American College of Nutrition*, *23*(5), 373-385.

15. Westerterp-Plantenga, M. S., Luscombe-Marsh, N., Lejeune, M. P. G. M., Diepvens, K., Nieuwenhuizen, A., Engelen, M. P. K. J., Deutz, N. E. P., Azzout-Marniche, D., Tome, D., & Westerterp, K. R. (2006). Dietary protein, metabolism, and body-weight regulation: dose-response effects. *International Journal of Obesity*, *30*, S16-S23.

16. Veldhorst, M., Smeets, A., Soenen, S., Hochstenbach-Waelen, A., Hursel, R., Diepvens, K., Lejeune, M., Luscombe-Marsh, N., & Westerterp-Plantenga, M. (2008). Protein-induced satiety: effects and mechanisms of different proteins. *Physiology and Behavior*, *94*(2), 300-307.

17. Fischer, K., Colombani, P. C., & Wenk, C. (2004). Metabolic and cognitive coefficients in the development of hunger sensations after pure macronutrient ingestion in the morning. *Appetite*, *42*(1), 49-61.

18. Bertenshaw, E. J., Lluch, A., & Yeomans, M. R. (2008). Satiating effects of protein but not carbohydrate consumed in a between-meal beverage context. *Physiology & Behavior*, *93*(3), 427-436.

19. Allen, K. E., Carpenter, C. E., & Walsh, M. K. (2006). Influence of protein level and starch type on an extrusion-expanded whey product. *International Journal of Food Science and Technology*, *42*, 953-960.

20. Areas, J. A. (1992). Extrusion of food proteins. *Critical Reviews in Food Science and Nutrition*, *32*(4), 365-392.

21. Onwulata, C. I., Konstance, R. P., Smith, P. W., & Holsinger, V. H. (1998). Physical properties of extruded products as affected by cheese whey. *Journal of Food Science*, *63*(5), 814-818.

22. Labuza, T. P., Zhou, P., & Davis, L. (2007). Whey to go. *The World of Food Ingredients* Vol. October/November, 108-112.

23. Childs, J. L., Yates, M. D., & Drake, M. A. (2007). Sensory properties of meal replacement bars and beverages made from whey and soy proteins. *Journal of Food Science*, *72*(6).

24. Guinee, T. P., Auty, M. A. E., & Fenelon, M. A. (2000). The effect of fat content on the rheology, microstructure and heat-induced functional characteristics of cheddar cheese. *International Dairy Journal*, *10*(4), 277-288.

25. Ha, E. & Zemel, M. B. (2003). Functional properties of whey, whey components, and essential amino acids: mechanisms underlying health benefits for active people (Review). *Journal of Nutritional Biochemistry*, *14*, 251-258.

26. Siso, M. I. G. (1996). The biotechnological utilization of cheese whey: a review. *Bioresource Technology*, *57*, 1-11.

27. Morr, C. V. & Foegeding, E. A. (1990). Composition and functionality of commercial whey and milk protein concentrates and isolates: a status report. *Food Technology* Vol. 44, 100-112.

28. Zhou, P. & Labuza, T. P. (2007). Effect of water content on glass transition and protein aggregation of whey protein powders during short-term storage. *Food Biophysics*, *2*(2), 108-116.

29. Zhou, P., Liu, X., & Labuza, T. P. (2008). Moisture-induced aggregation of whey proteins in a protein/buffer model system. *Journal of Agricultural and Food Chemistry*, *56*(6), 2048-2054.

30. Zhou, P., Liu, X., & Labuza, T. P. (2008). Effects of moisture-induced whey protein aggregation on protein conformation, the state of water molecules, and the microstructure and texture of high-protein-containing matrix. *Journal of Agricultural and Food Chemistry*, *56*(12), 4534-4540.

31. Liu, X., Zhou, P., Tran, A., & Labuza, T. P. (2009). Effects of polyols on the stability of whey proteins in intermediate-moisture food model systems. *Journal Agricultural Food and Chemistry*, *57*, 2339-2345.

32. Li, Y., Szlachetka, K., Chen, P., Lin, X., & Ruan, R. (2008). Ingredient characterization and hardening of high-protein food bars: an NMR state diagram approach. *Cereal Chemistry*, *85*(6), 780-786.

33. McMahon, D. J., Adams, S. L., & McManus, W. R. (2009). Hardening of high-protein nutrition bars and sugar/polyol-protein phase separation. *Journal of Food Science*, *74*(6), E312-E321.

34. Loveday, S. M., Hindmarsh, J. P., Creamer, L. K., & Singh, H. (2009). Physicochemical changes in a model protein bar during storage. *Food Research International*, *42*, 798-806.

35. Loveday, S. M., Hindmarsh, J. P., Creamer, L. K., & Singh, H. (2010). Physicochemical changes in intermediate-moisture protein bars made with whey protein or calcium caseinate. *Food Research International*, *43*, 1321-1328.

36. Aguilera, J. M. & Stanley, D. W. (1999). Microstructural principles of food processing and engineering. Gaithersberg, MD: Aspen Publishers, Inc.

37. Aguilera, J. M. (2000). Microstructure and food product engineering. *Food Technology* Vol. 54, 56-64.

38. Peighambardoust, S. H., van der Goot, A. J., Hamer, R. J., & Boom, R. M. (2004). A new method to study simple shear processing of wheat gluten-starch mixtures. *Cereal Chemistry*, *81*, 714-721.

39. Manski, J. M., van der Goot, A. J., & Boom, R. M. (2007). Formation of fibrous materials from dense calcium caseinate dipersions. *Biomacromolecules*, *8*(4), 1271-1279.

40. Manski, J. M., van der Goot, A. J., & Boom, R. M. (2007). Influence of shear during enzymatic gelation of caseinate-water and caseinate-water-fat systems. *Journal of Food Engineering*, *79*(2), 706-717.

Chapter 2

New directions towards structure formation and stability of protein-rich foods from globular proteins

Abstract

Concentrated protein-rich foods have strong potential to be developed in terms of health and well-being roles. Unfortunately, limitations in creating products with the right texture and stability hinder the use of those products by consumers. Main reason is that the formation of micro- and macrostructures in concentrated protein systems is not fully understood yet and hence not controlled. As a result, their multi-level structures are not optimal. This paper overviews possible routes to produce protein-rich foods with emphasis on options to produce protein-rich materials that have the potential to be stable and desirable in terms of the combination structure-texture-sensory. The main conclusion is that these demands could be met by introducing of well-defined heterogeneity in the product using new plasticizing components and innovative production methods.

This chapter has been published as: Purwanti, N., van der Goot, A., Boom, R. and Vereijken, J. **2010**. New directions towards structure formation and stability of protein-rich foods from globular proteins. *Trends in Food Science & Technology*, *21*(2), 85-94.

1. Introduction to protein-rich foods

Proteins in food products have both nutritive and technical functionality. Examples of their technical functionality are their foaming, emulsifying, thickening/gelling and texturizing properties. The nutritional functions of proteins have been extensively investigated. Recent studies, however, indicate more advantages of protein-rich diets. Intake of a protein-rich food gives a stronger feeling of satiety compared to a carbohydrate-based product with the same caloric value. Intake of dairy fruit drink enriched with protein before lunch triggered less energy consumption at lunch compared to the same drink enriched with carbohydrate[1]. Specific on the type of protein, whey protein seems to induce a satiety signal that influences both short term and long term food intake[2]. Lower subsequent food intake due to high protein diets[2-4] led to a statistically significant decrease in total body weight in case of long term diets (6 months or longer). A group of people with higher protein intake experienced lower weight regain and a decreased waist circumference compared to a control group[5]. The satiety effect is influenced by the source of the proteins but this effect varies with dose, product form, treatment and formulation, the duration to the next meal, and the presence of other macronutrients[2]. The satiety effect also increases with concentrations of satiety hormones, energy expenditure, concentrations of amino acids, and gluconeogenesis process[6]. In addition, a higher dietary protein intake by elderly people may slow the progression of sarcopenia[7]. The recommended dietary allowance of proteins, i.e. 0.8 g $kg^{-1}d^{-1}$, is generally not enough for elderly people to maintain their fat-free mass, in particular their muscle mass[7-9].

These findings concerning health effects are drivers for food industries to develop and provide more and better protein-rich products. However, protein-rich foods generally have low stability. The stability problem arises because protein-protein interactions upon storage may give rise to strong and tight networks, product hardening and syneresis of water. The additional formation of intermolecular disulphide bonds and/or non-covalent interactions lead to increased protein aggregation[10, 11]. The changes in properties of

protein-rich products seem unavoidable because they are related to inherent properties of proteins. The product hardening is further favoured by moisture redistribution and the Maillard reaction[10, 12, 13]. This reaction, initiated by the reaction between reducing sugars and amine groups in proteins, contributes to the formation of covalent bonds between protein molecules resulting in hardening during long-term storage[10]. The physical-chemical changes in properties of protein-rich products thus lead to changes in textures and, subsequently, the sensory properties. These physical-chemical changes also depend on the protein sources added to the product. As an illustration, the addition of whey protein in meal replacement bars (100% whey bar) gave dense products with strong cohesiveness and adhesiveness. The use of soy protein (100% soy bar), however, led to products that were less dense, more sticky and showed increased hardening over time[14].

The shortcomings of the current protein-rich foods impose several challenges to product development. Unfortunately, most production processes for protein-rich foods are rather empirical and innovations are limited by lack of scientific insight. Therefore, the main goal of this paper is to map possible pathways towards structuring of protein-rich foods. We will focus on the use of dairy globular proteins with concentration higher than 10% w/w that mostly give soft solid products. These proteins are chosen because these are often used to enrich the protein content of food products. The outline of the paper is as follows. Section 2 provides an overview of the existing literatures with main focus on the existing food products. Section 3 describes how recently developed scientific insights can be translated to improve the stability and properties of protein-rich foods.

2. Production of protein-rich foods

Protein-rich foods are often produced using a thermal treatment, leading to protein denaturation. Denaturation is generally defined as uni-molecular process in which a protein molecule unfolds. Protein denaturation has to precede protein aggregation, being the process in which unfolded proteins form larger structures. This makes aggregation minimally a bi-molecular process. It has been reported that random networks formed upon protein aggregation can lead to gelled systems (or at least thickening) for soy protein

isolate (SPI)[15] and pea legumin[16]. Protein denaturation offers many possibilities to produce foods but also pose limitations to process globular proteins in terms of the texture to be obtained[17]. The use of only a high concentration of globular protein in the native form to create high-protein foods is challenging because above the critical concentration (C_g) of this protein, e.g. C_g of whey protein is 12 % w/v[18, 19], gelation may already occur below the denaturation temperature. A highly concentrated protein dispersion might give rise to a dense network, which becomes even denser at elevated temperatures. Below, we describe a number of scientific approaches that are applied to relieve the abovementioned problems. The potential of ingredients and processing are described to create product structures with higher protein content, providing acceptable textural and sensorial properties[20].

2.1. Ingredients

Ingredients are often used to soften the product texture. The use of whey protein hydrolysate (WPH) instead of whey protein isolate (WPI) in nutritional bars leads to a softer and more flexible product, and lowers the hardening to a minimum over time[10, 14]. The protein matrix in low-fat cheese has low porosity leading to a more compact matrix[21, 22]. As a result, the cheese becomes more viscous and hence, it is less-spreadable. The cheese also has an increase in firmness and fracture stress compared with full-fat cheese[22]. A great variety of ingredients has been investigated to improve structures and textures of low fat cheese by increasing the moisture content, e.g. by using fat replacers and exopolysaccharide (EPS)-producing starter culture[23, 24]. Higher moisture content in low-fat cheese reduces the density in cheese by inducing a higher porosity in the protein matrix. Rodríguez (1998) summarized that the use of fat replacers in low fat cheese, i.e. Simplesse®, Dairy-Lo® (protein-based fat replacers), Stellar™ and Novagel™ (carbohydrate-based fat replacers), resulted in higher moisture content than that in the control cheese and more porosity in the protein matrix of the cheese. To increase moisture content in reduced-fat cheese, capsular and ropy exopolysaccharide (EPS)-producing

strains of *Lactococcus lactis ssp. cremoris* were used in the starter culture[25]. This led to better textures and structures of reduced-fat cheese.

2.2. Processing

Different processes exist to create protein-rich foods with good microstructure, such as extrusion and spinning. This sub-section describes the processes used for globular proteins.

2.2.1. Extrusion

Extrusion of protein is used to texturize the protein (in case of a protein-based product), to increase protein content in the end product (in case of a protein-enriched product), to create an anisotropic structure, and probably to obtain better expansion in the case of porous products. Often, other biopolymers are added to the protein. During extrusion, protein structure changes following the sequence of activation, structuring and solidification. Activation is induced by protein denaturation. Then, structuring takes place through protein association and deformation by heat and shear. In addition to colloidal interactions, covalent bonds may be formed at high temperature. Solidification then takes place by cooling, which leads to the formation of non-covalent and further covalent bounds, and glassification at low moisture content[26].

Most studies have been performed using a twin-screw extruder for texturization of whey protein[27-29]. Initial mixing of whey protein with 40% moisture content in the extruder led to paste or slurries with irregular aggregates (string and granules), ranging from 10-200 nm. The extruder-denatured insoluble protein showed a dense and compact structure at nanometre scale[29]. The starch up to 25% was replaced by whey protein to increase the protein content of corn puffs from 2% to 20%. However, some trade-offs on snack properties became evident because the addition of whey protein led to un-expanded products with higher breaking strength[27]. Similar findings were reported by other researchers. A high protein content (16%, 32%, and 40%) in extrudates of starch-protein system resulted in a reduced expansion ratio, reduced product diameter, increased product

density and increased breaking force[30]. The reduction in expansion ratio was attributed to the water held by whey protein, which was needed for gelatinization of starch[31]. Hence, the gelatinization of the starch was reduced. An alternative hypothesis to explain the reduced expansion is that amylose and whey protein have a certain physico-chemical interactions, leading to the formation of amylose-protein complexes[32]. In general, above a certain protein concentration, products obtained from extrusion become hard, resistant to disruption by water and, therefore, less suitable for direct consumption[26].

Process modifications could partly compensate for the effects mentioned above. For an example, a twin screw extruder that was designed with specialized die holes and a pressure chamber, maintaining the pressure at the die end below atmospheric pressure, was claimed to produce consistent texture of product and better product expansion than that obtained using a super-atmospheric pressure chamber[33]. In addition, a certain degree of alignment was achieved in the cooling die as a result of laminar flow, especially when the product was phase separated[34].

Unfortunately, it is still difficult to predict the structures and textures resulted from an extrusion process, especially in combination with variation of product formulation. As an illustration, different volumes of food are subjected to different flows being elongation, rotational and simple shear flows at different areas, due to chaotic nature of the extrusion process. This includes inhomogeneous distribution of temperature, shear, elongation rates, and the coupled effects of the process parameters that can be adjusted[35]. Thus, the effects of process parameters on the structure formation of protein-rich extrudates are complex and the available knowledge is still rather empirical.

2.2.2. Spinning

Spinning is applied for a specific purpose, e.g. to create yarns, fibrous materials, or films. It is hardly used for food production, except for the production of edible or biodegradable films for instance casein films[36]. Spinning generally results in anisotropy at the level of the fibres. A globular protein still retains its globular shape in the network formed from random aggregation[15]. Therefore, there is no preferential orientation of the protein

network in the film. However, the physical properties of food that are perceived as texture by consumers are dependent on the structure from molecular scales and up[20, 37]. Thus, this process might not yield the desired product microstructure especially for globular proteins. At the same time, the process does not lend itself easily to scaling up to large volume throughputs, which further hampers its development.

3. Trends of new design technologies for structuring protein-rich foods

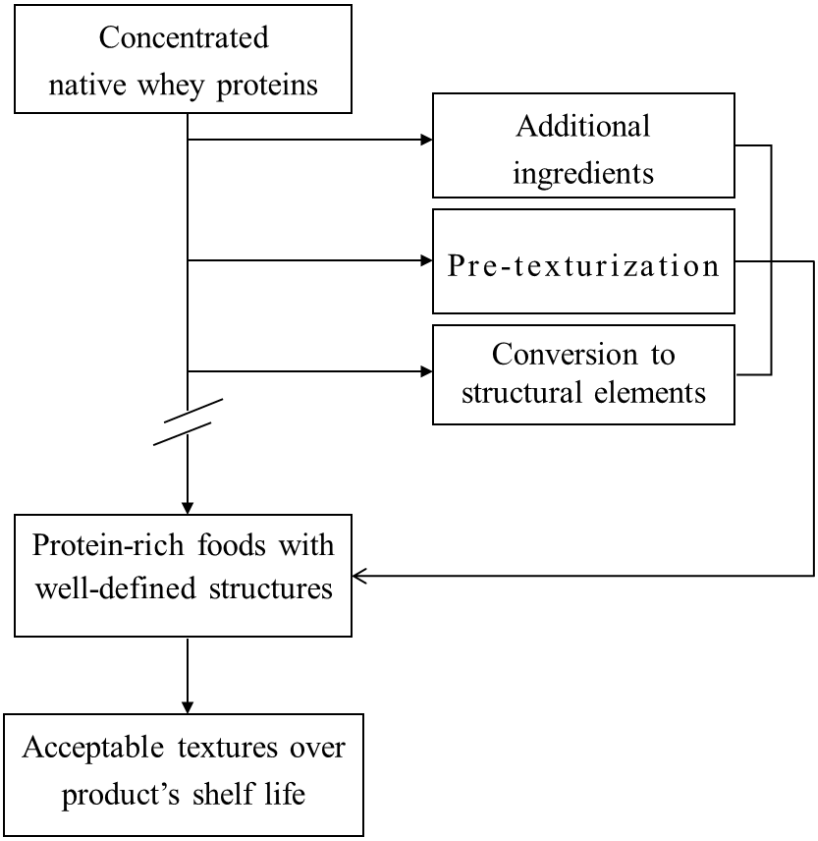

Figure 1. Overview of conceptual strategies to use concentrated globular proteins, illustrated with whey proteins, to produce protein-rich products having acceptable textures over time.

In this section, emerging trends to improve the structures of protein-rich foods from globular proteins are discussed. This is done because protein-rich products with a homogeneous and dense microstructure are not stable. Here, we describe how the inclusion of new ingredients, the creation of heterogeneity by pre-texturization and the use

of structure elements, and novel processing concepts may help to solve the problems of protein-rich foods. A brief overview on possibilities of concentrated protein result in protein-rich product that is acceptable for consumers is depicted in Fig. 1. Whey proteins are used as the illustration for globular proteins.

3.1. Ingredients

Hardening in protein-rich bars involves solvent rearrangement, disulphide bonds formation, non-covalent interactions, and Maillard reaction[10]. To relieve this problem, ingredients that oppose these negative aspects can be used. Plasticizers are often used to soften the products and to retard the hardening. In addition, plasticizers may also influence other mechanical properties of the products, e.g. change the formulation at which it is glassy, brittle, rubbery or viscous[38]. Plasticizers such as reducing sugars are often used but the use of these sugars may lead to hardening due to the Maillard reaction[10]. Therefore, non-reducing sugars are preferred as plasticizers. Some researchers also indicated the possibility of using WPH to partially replace WPI in WPI-based nutritional bars, as mentioned in 2.1. Protein hydrolysates may have different gelling properties[39]. It has been shown that particular whey protein peptides can affect gelation of whey proteins[18, 40, 41], either promote stronger gels or inhibit gel formation. Some of these peptides have been identified and were shown to affect aggregation of WPI in mixed hydrolysates/WPI systems if sufficient aggregating peptides are present[42]. Unfortunately, the interaction of these peptides with the intact protein during gelation and the properties of the resulting gel are still largely unknown. Furthermore, deeper knowledge about whey protein peptides inhibiting gelation will be useful for production of protein-rich foods.

The influence of plasticizer rearrangement on the hardening of protein-rich products might also be related to the hydration state of the protein in the matrix. Zhou and co-workers indicated that whey protein with moisture content below 30% did not aggregate at a temperature below 35 °C[43]. Aggregation reached maximum at a moisture content between 70 and 80%, however, it reduced upon further dilution. Moisture-induced aggregation of whey protein was later recognized as an important factor influencing

microstructure and texture of high-protein food matrix during storage[13]. The facts described above might suggest that hardening process of protein-rich foods could also be related to changes in the hydration state of the protein upon storage.

Another possibility to avoid hardening of protein-rich foods is to inhibit the formation of additional disulphide bonds. Addition of a disulphide reducing agent, i.e. dithiothreitol (DTT), resulted in a brittle gel with strain values of 0.30-0.39 and a stress value of 44% of that of a gel without DTT at pH 7.0[44]. The use of a free-thiol group blocking agent, i.e. N-ethylmaleimide (NEM) was also effective to reduce hardness of whey protein gels[45, 46]. Nevertheless, to perform this kind of inhibition by using food grade ingredients that ally with consumer preferences remains a challenge.

3.2. Structural elements

The use of structural elements may play important roles to create desirable structures from concentrated globular proteins. We aim for protein-based structural elements for this purpose and we define these structural elements as domains (from only protein or in combination with other ingredients), in the shape of particles, fibres, etc., in the size range of nm until μm. By using structural elements, colloidal scale interaction will play an important role. The interactions might be among the structure elements themselves and between the elements and continuous phase.

In Fig. 2, two modes of structural elements in a product are depicted. Structural elements prepared from low protein concentration may act as structural breakers in a high-protein matrix (Fig. 2A). These structure elements create weak spots in a relatively strong matrix and can act as nuclei for cracks, reducing the product strength. This effect is already prominent in cheeses, in which fat droplets act as structural breakers. The effect of hardening of the protein phase in cheeses is suppressed by the structural breaker function of the fat droplets. Reducing the number of fat droplets reduces the suppression, which probably causes low-fat cheeses to have more problems with texture and stability. Thus, the presence of sufficient structural breakers will retard and reduce the effect of protein phase hardening.

Structural elements that contain a high-protein concentration may act as structural builders in a low protein or non-protein matrix (Fig. 2B). The storage stability may increase because an additional increase in strength of these elements will probably not influence the overall sensory perception if the continuous phase remains constant. The perceived increase in strength depends on the size of structural elements. Nonetheless, additional increase in strength of the concentrated protein domains in Fig. 2B is much lower compared with that of the concentrated protein matrix in Fig. 2A. In both conditions (2A & 2B), the structural elements may act as inert fillers. This type of filler may result in more brittle product. When the structural elements tend to aggregate to some extent, or the continuous matrix is viscoelastic, different networks may be formed such as mixed, bi-continuous or phase separated. When shear is applied on such a system, anisotropy may be obtained.

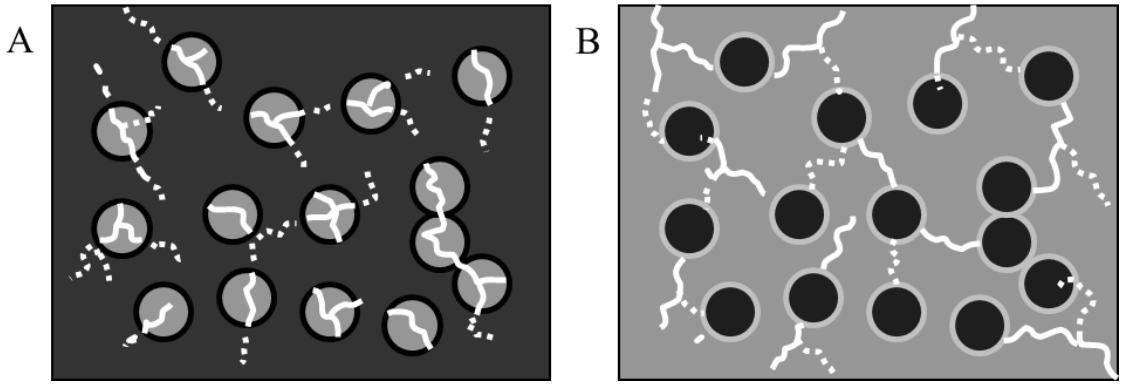

Figure 2. Overview of structural elements having low-protein concentration as structural breakers in a high-protein matrix (A) and protein-rich structural elements as structural builders in a low-protein matrix (B).

Below, we describe two processes to create protein-based structural elements from solely protein (pre-texturization) and from combination of ingredients.

3.2.1. Pre-processing and structuring of single protein systems

Pre-texturization induces a first change in protein properties with process conditions that differ from the final structuring process. Unfolded state of whey protein can be achieved

through shear at 50 °C[29], which is below the denaturation temperature, i.e. 70-80 °C[47]. A gel that was prepared from pre-texturized WPI, processed between 35 and 50 °C to induce partial denaturation, resulted in significantly increased gel strength. In contrast, a complete loss of gelling properties was obtained when pre-texturized WPI was processed at 75 °C or higher in the extruder[29]. Thus, controlling the denaturation level during pre-texturization of whey proteins is important for tuning the functional properties. Under extrusion conditions, some of the proteins can become insoluble and act as a dispersed phase within the melt phase[26] and thus, may induce an anisotropic microstructure. The combination of native whey protein with aggregated whey protein at a total protein concentration of 10% w/v (pH 7) led to a decrease of pore and strand size in the gel microstructures[48]. This aggregated whey protein was prepared by heating a WPI solution (11% w/w, pH 7.4) in a water bath at 80 °C for 1 h. This concentration produced aggregates with a high intrinsic viscosity, an indication for larger and non-spherical aggregates[49]. This type of aggregates is known as reactive protein aggregates[50] or whey protein aggregates[47]. Their properties can be varied using different time-temperature profiles. It was reported that the presence of more aggregates produced a stronger gel[46, 51]. Protein fibrils with a typical length of 1-10 μm and a diameter 1-10 nm were used to modify structuring properties of concentrated WPI solutions[52]. WPI/fibrils dispersion showed complex behaviour. Both shear thickening and shear thinning were observed at increasing shear rates. The addition of the fibrils increased the viscosity and the gel strength. While, the matrix became more porous when shear flow was applied.

Generally, the globular proteins behave as inert particles in diluted solutions or dispersion. They lack the natural ability to interact with each other to form more complex structures in which this ability is reflected in the Newtonian behaviour of e.g. whey protein concentrate (WPC) in the range of 4-12% w/w. However, the behaviour of globular proteins depends on the concentration, temperature, and pH to a certain extent. WPC was pseudoplastic at intermediate concentrations (14-16%) and featured a yield point with thixotropic behaviour at even higher concentrations (> 40% w/w) at 20-40 °C[53]. At higher temperatures, these solutions became rheopectic[54]. Pseudoplastic behaviour was

also reported for WPI at 20 % w/w[55]. An individual globular whey protein, such as β-lactoglobulin, showed a strong shear thinning behaviour at concentrations of 23% w/w and 27% w/w but the dispersion became less shear thinning at 45% w/w and 52% w/w[56]. This could be explained by the reduced solvent mobility at higher concentrations due to solvated layers formed by the interaction of the dispersed system and the solvent[57]. Even with these deviations from Newtonian behaviour at certain concentrations, it is unlikely that the use of globular proteins only will result in heterogeneous structure. Gels with homogenous structures are expected. Shear flow with practical intensities is simply not sufficient to induce arrangement on the molecular scale.

For better results, the original structure-function relationships of globular proteins have to be changed. This can be done in concentrated as well as in diluted systems. In general, it can be stated that pre-texturization aims for a continuous process with the main process, i.e. the formation of well-defined domains and the subsequent interactions to form the final product structure. Pre-texturization should make use the potential of proteins to be able to create desirable interactions in the main processing[26]. In concentrated protein systems without other polymers involved, phase separation or non-linearity within the systems can be utilized to create structural elements. However, even though phase separation in diluted systems is a popular subject, this phenomenon is hardly studied in concentrated systems. Liquid-liquid phase separation for *β*-lactoglobulin at pH 5.1 in 10 mM buffer without addition of salt was observed at mass fraction < 27% w/w[56]. Under supersaturated condition, a two-phase liquid region existed as an intrinsic feature of globular proteins[58]. Nevertheless, more researches on concentrated systems are needed to obtain better understanding of the phase behaviour and its potential to be used in structuring processes.

3.2.2. Formation of structural elements (protein-dispersed phase)

A number of methods exist to create protein-rich structural elements. These methods are microparticulation, double emulsification, or in combination with other biopolymers through phase separation. These options are mainly explored to create products with a

dispersed protein-rich phase. The protein content of the final product is then to a large extent determined by the protein content of the proteinaceous structural elements in combination with protein content in the rest of the product. Still, the overall textural-sensory properties will be determined mostly by the continuous phase.

The most pragmatic way to create structural elements is by microparticulation. Several methods for microparticulation have been described. Microparticulation of WPC-sucrose was done by high shear homogenization at 34 °C for 2, 4, and 6 min, ending up with 16.7% protein content in the syrups which were formed after evaporation of microparticulated slurries at 45 °C, 5.2 MPa[59]. Reduction of particle sizes was observed by increasing processing time but re-aggregation was observed at longer microparticulation time. Microparticulation was also done by dissolving a protein gel prepared from 16.7% w/w WPC into alkaline solutions at temperature up to 60 °C with or without agitation[60]. In another study, whey protein microparticles were obtained by homogenizing a 25% w/w WPC solution at pH 5.8, 690 MPa for 5 min at room temperature[61]. Addition of 5% w/w WPC microparticles obtained from ultra-high pressure treatment to a low-fat processed cheese resulted in high melt-ability and acceptable firmness, yet an undesirable grainy texture was obtained that was attributed to the presence of WPC microparticles.

Surh and co-workers[62] presented double emulsification as an alternative method to produce protein particles. A w/o emulsion was prepared by dispersing protein in water (up to 15% w/w) followed by emulsification of the aqueous phase into oil that contained PGPR as emulsifier. This mixture was re-dispersed in water. Then, a heating step was applied to gel the protein phase, which led to protein particles inside each oil droplet. The protein particles had a Sauter diameter ($d_{3,2}$) of 1.95 ± 0.07 μm and $d_{4,3}$ of 10.5 ± 1.6 μm, indicating a rather polydisperse particle size. The oil droplets were large and contained a number of protein particles. Unfortunately, the overall protein content in the system will remain rather low due to the presence of oil.

Another method to prepare structural elements is by utilizing phase separation between biopolymers, e.g. between proteins and polysaccharides. Two driving forces for phase separation are mentioned, i.e. temperature reduction, which reduces the mixture entropy and increases incompatibility in the system, and molecular ordering as well as molecular weight increase, which result in reduced entropy of the mixture[63]. The de-mixing process here may follow a nucleation and growth mechanism, or it may follow spinodal decomposition, depending on the exact interactions and phase behaviour. Especially, spinodal decomposition (de-mixing by deepening of concentration fluctuations, followed by a coarsening process) is known to yield domains with rather uniform size. Gelation during de-mixing process is often used to solidify the domains[64, 65]. In that situation, the phase separation process has to start from a homogeneous protein/carbohydrate solution. Therefore, the typical protein concentration for this application is low[66-68]. Phase separation can be induced by a change in temperature or by a (slow) change in pH through the use of glucono delta-lactone (GDL). At high concentration of β-lactoglobulin in the mixture (e.g. 14% w/w), phase separation occurred with still high concentration of β-lactoglobulin in the carbohydrate phase, implying that phase separation was not complete[69]. Nevertheless, general application of phase separation in biopolymers to get protein-rich domains only occurs in metastable region at the diluted side of the critical point. For protein, the critical point is situated at low protein concentrations. This fact raises a challenge to use phase separation method to produce protein-rich structural elements.

3.3. Towards new processes for protein structuring

Recently, well-defined deformation was introduced for inducing novel structures in concentrated biopolymer systems[70]. Hierarchically structured, fibrous materials from concentrated Calcium-caseinate (CaCas) dispersions processed under well-defined shear flow were obtained[71-73]. The same composition gave an isotropic material upon mixing. The fibrillization process was based on a specific CaCas property, i.e. the dispersion tends to phase separate upon simple shearing. This behaviour was confirmed through the

rheological properties and was dependent on the physical properties. Shearing of the material having certain rheological and physical properties may lead to shear banding that can result in an anisotropic, fibrillar-like morphology. Similarly, a combination of fibrillized WPI with 'native' WPI into a solution of 22.5% total protein showed rheological evidence of being phase separated, which was confirmed with microscopy[52].

The behaviour of proteins under simple shear flow is very dependent on the molecular size and the colloidal interactions[72]. Caseinates are proteins in the form of random coils, assembled into micelles with typical radius of gyration 22-27 nm for Na-Cas[74] and 100-500 nm (or 100-300 nm of hydrodynamic radius) for caseinate sub-micelles with addition of calcium[75]. In addition, native casein micelles have a maximum hydrodynamic diameter distribution of 200 nm, measured with a combination of field flow fractionation and dynamic light scattering and predicted with adhesive hard sphere (AHS) model[76, 77]. On the other hand, dairy globular proteins, i.e. whey proteins, have a mean particle size of around 8 nm at pH 7[51]. The Brownian motion of particles with this size will be too high to permit alignment due to mild shear flow. Hence, one cannot directly translate the use of shear flow with caseinate micellar suspensions towards the use with globular proteins.

The use of well-defined shear flow is often applied to create shear-induced structure formation in model systems[73, 78-80]. Those studies confirmed that structure formation in a heterogeneous mixture is a result of physical properties of phases in the mixture in combination with the deformation applied. Structure formation in a heterogeneous material is often ascribed to shear banding. Shear banding is the ability of a flowing liquid to form adjacent regions that have a shear-rate discontinuity at their interface. This can occur if the flow curve (shear stress versus shear rate relation) has a negative slope over some range of shear rates[81]. This type of flow curve was observed in concentrated CaCas dispersions[72].

It can, therefore, be concluded that the introduction of well-defined shear flow as a process parameter might create new possibilities to induce interesting structures in concentrated biopolymer systems. The thought behind this is described in Fig. 3. This is

especially true if the protein dispersion contains structural elements having colloidal size. The structural elements might be naturally present or created by the methods described in sub-section 3.2. By applying well-defined shear flow as a process parameter to be controlled, the understanding on the structure developments in the product matrices during processing might be revealed.

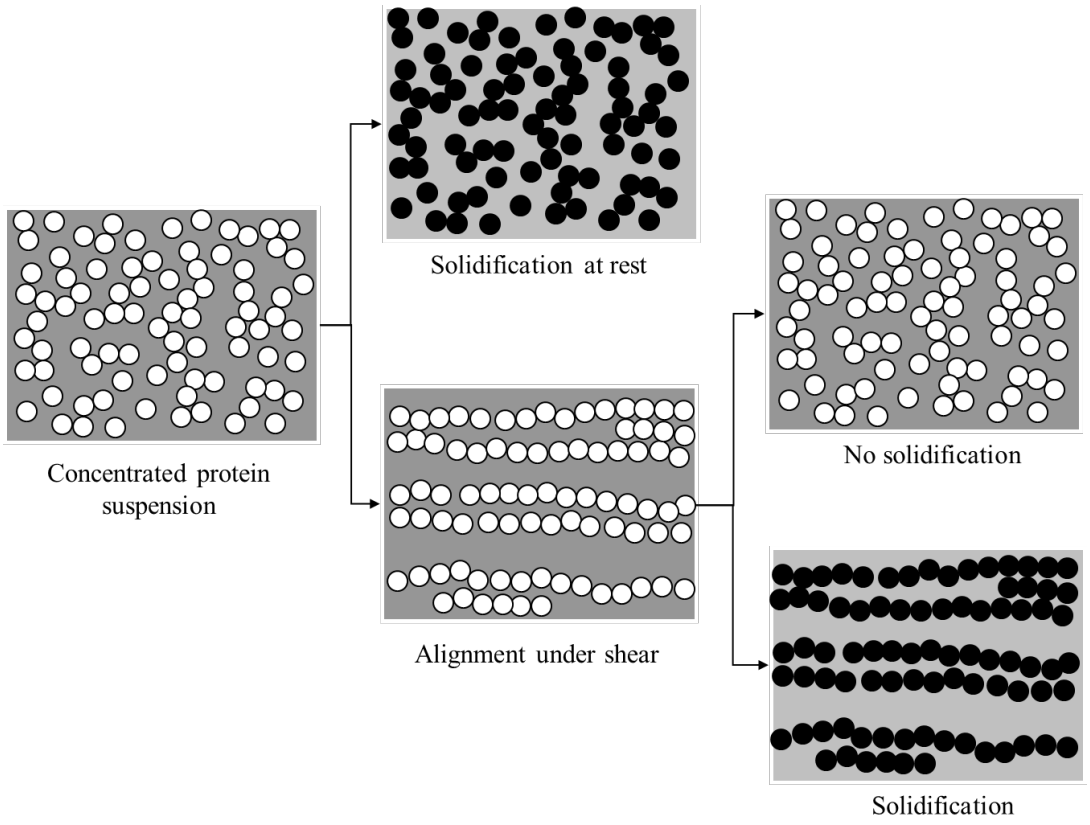

Figure 3. Schematic picture of how well-defined flow might induce new structures in a concentrated protein system.

4. Conclusion and future trends

High-protein foods attract much attention due to their relevance to society such as balanced nutrition for the elderly and the combat against obesity. Unfortunately, till now the properties for concentrated protein systems are hardly studied contrary to diluted protein solutions. Hence, structuring high-protein products is still firmly rooted in empirical approaches. However, for the development of those products with better sensory attributes regarding their textures, we need better structured products that retain their structures for sufficient times to allow preparation and distribution. Thus, insight in the properties and processing of concentrated protein systems is needed.

There is a promising trend to create more structures of protein-rich foods and to understand their formation. Two options show potential in order to improve stability of protein-rich foods, i.e.

a. The addition of plasticizers may modify the rheological properties of the starting protein system, by which its final structure and morphology may be predicted. Different plasticizers can have different roles and interactions with the protein matrix. The main role is softening the protein matrix. A more advanced option is the use of a plasticizer that may suppress disulphide bond formation. But, such a plasticizer is not available yet for food applications.

b. The use of structural elements. The addition of protein particles, known as structural elements, in a protein/non-protein matrix, may give freedom in optimizing the properties of the product. Hardening might be controlled by the use of a low-protein matrix around high-protein structural elements. Alternatively, the use of structural breakers (low-protein domains in a high-protein matrix) would modulate the mechanical behaviour of the matrix and reduce the effects of hardening by facilitating breakage. Different methods for preparing structural elements can be applied depending on the functional properties to be achieved.

It is clear that the development of these complex products needs a bridge between fundamental understanding and the technique developments to prepare them. By using simple shear flow instead of complex mixing processes, one may be able to bridge those two aspects. In addition to the different methods that exist to form the structural elements, outlining them into a structured morphology in our view has to take place using well-defined shear flow. The fact that simple shear flow can also be utilized to induce phase separation and tune domain sizes, indicates the central role of well-defined flow in further endeavours towards structured high-protein foods.

References

1. Bertenshaw, E. J., Lluch, A., & Yeomans, M. R. (2008). Satiating effects of protein but not carbohydrate consumed in a between-meal beverage context. *Physiology & Behavior*, *93*(3), 427-436.

2. Luhovyy, B. L., Akhavan, T., & Anderson, G. H. (2007). Whey proteins in the regulation of food intake and satiety. *Journal of the American College of Nutrition*, *26*(6), 704S-712S.

3. Halton, T. L. & Hu, F. B. (2004). The effects of high protein diets on thermogenesis, satiety and weight loss: a critical review. *Journal of the American College of Nutrition*, *23*(5), 373-385.

4. Westerterp-Plantenga, M. S., Luscombe-Marsh, N., Lejeune, M. P. G. M., Diepvens, K., Nieuwenhuizen, A., Engelen, M. P. K. J., Deutz, N. E. P., Azzout-Marniche, D., Tome, D., & Westerterp, K. R. (2006). Dietary protein, metabolism, and body-weight regulation: dose-response effects. *International Journal of Obesity*, *30*(S3), S16-S23.

5. Lejeune, M. P. G. M., Kovacs, E. M. R., & Westerterp-Plantenga, M. S. (2005). Additional protein intake limits weight regain after weight loss in humans. *British Journal of Nutrition*, *93*(2), 281-289.

6. Veldhorst, M., Smeets, A., Soenen, S., Hochstenbach-Waelen, A., Hursel, R., Diepvens, K., Lejeune, M., Luscombe-Marsh, N., & Westerterp-Plantenga, M. (2008). Protein-induced satiety: effects and mechanisms of different proteins. *Physiology and Behavior*, *94*(2), 300-307.

7. Campbell, W. W. & Leidy, H. J. (2007). Dietary protein and resistance training effects on muscle and body composition in older persons. *Journal of the American College of Nutrition*, *26*(6), 696S-703S.

8. Gersovitz, M., Motil, K., Munro, H. N., Scrimshaw, N. S., & Young, V. R. (1982). Human protein requirements: assessment of the adequacy of the current Recommended Dietary Allowance for dietary protein in elderly men and women. *American Journal of Clinical Nutrition*, *35*(1), 6-14.

9. Kurpad, A. V. & Vaz, M. (2000). Protein and amino acid requirements in the elderly. *European Journal of Clinical Nutrition*, *54*(3), S131-S142.

10. Labuza, T. P., Zhou, P., & Davis, L. (2007). Whey to go. *The World of Food Ingredients* Vol. October/November, 108-112.

11. Zhou, P. & Labuza, T. P. (2006). Hardening of whey protein based nutritional bars resulting from protein-protein interactions. *Tech News Quarterly of American Dairy Products Institute* Vol. XX.

12. Labuza, T. P. (2008). Influence of moisture on aggregation of protein during storage. Abstact for oral presentation on 5th conference on Water in Food. April 6-8, Nürtingen, Germany.

13. Zhou, P., Liu, X., & Labuza, T. P. (2008). Effects of moisture-induced whey protein aggregation on protein conformation, the state of water molecules, and the microstructure and texture of high-protein-containing matrix. *Journal of Agricultural and Food Chemistry*, *56*(12), 4534-4540.

14. Childs, J. L., Yates, M. D., & Drake, M. A. (2007). Sensory properties of meal replacement bars and beverages made from whey and soy proteins. *Journal of Food Science*, *72*(6), S425-S434.

15. Rampon, V., Robert, P., Nicolas, N., & Dufour, E. (1999). Protein structure and network orientation in edible films prepared by spinning process. *Journal of Food Science*, *64*(2), 313-316.

16. O'Kane, F. E., Happe, R. P., Vereijken, J. M., Gruppen, H., & van Boekel, M. A. J. S. (2004). Heat-induced gelation of pea legumin: comparison with soybean glycinin. *Journal of Agricultural and Food Chemistry*, *52*(16), 5071-5078.

17. Schmitt, C. J. E., Lionel, B., Frederich, R., & Matthieu, P. (2007). Whey protein micelles. EP 1839492 A1.

18. Otte, J., Ju, Z. Y., Skriver, A., & Qvist, K. B. (1996). Effects of limited proteolysis on the microstructure of heat-induced whey protein gels at varying pH. *Journal of Dairy Science*, *79*(5), 782-790.

19. Hongsprabhas, P. & Barbut, S. (1997). Protein and salt effects on Ca^{2+}-induced cold gelation of whey protein isolate. *Journal of Food Science*, *62*(2), 382-385.

20. Foegeding, E. A. (2007). Rheology and sensory texture of biopolymer gels. *Current Opinion in Colloid & Interface Science*, *12*(4-5), 242-250.

21. Bryant, A., Ustunol, Z., & Steffe, J. (1994). Texture of cheddar cheese as influenced by fat reduction. *Journal Food Science*, *60*(6), 1216-1219

22. Guinee, T. P., Auty, M. A. E., & Fenelon, M. A. (2000). The effect of fat content on the rheology, microstructure and heat-induced functional characteristics of cheddar cheese. *International Dairy Journal*, *10*(4), 277-288.

23. Rodríguez, J. (1998). Recent advances in the development of low-fat cheeses. *Trends in Food Science & Technology*, *9*(6), 249-254.

24. Perry, D. B., McMahon, D. J., & Oberg, C. J. (1998). Our Industry Today: manufacture of low fat mozzarella cheese using exopolysaccharide-producing starter cultures. *Journal of Dairy Scence*, *81*, 563-566.

25. Dabour, N., Kheadr, E., Benhamou, N., Fliss, I., & LaPointe, G. (2006). Improvement of texture and structure of reduced-fat cheddar cheese by exopolysaccharide-producing lactococci. *Journal of Dairy Science*, *89*(1), 95-110.

26. Areas, J. A. (1992). Extrusion of food proteins. *Critical Reviews in Food Science and Nutrition*, *32*(4), 365-392.

27. Onwulata, C. I., Konstance, R. P., Smith, P. W., & Holsinger, V. H. (1998). Physical properties of extruded products as affected by cheese whey. *Journal of Food Science*, *63*(5), 814-818.

28. Onwulata, C. I., Smith, P. W., Konstance, R. P., & Holsinger, V. H. (2001). Incorporation of whey products in extruded corn, potato or rice snacks. *Food Research International*, *34*(8), 679-687.

29. Onwulata, C. I., Konstance, R. P., Cooke, P. H., & Farrell Jr, H. M. (2003). Functionality of extrusion - texturized whey proteins. *Journal of Dairy Science*, *86*(11), 3775-3782.

30. Allen, K. E., Carpenter, C. E., & Walsh, M. K. (2006). Influence of protein level and starch type on an extrusion-expanded whey product. *International Journal of Food Science and Technology*, *42*, 953-960.

31. Onwulata, C. & Tomasula, P. (2004). Whey texturization: a way forward. *Food Technology* Vol. 58(7), 50-54.

32. Matthey, F. P. & Hanna, M. A. (1997). Physical and functional properties of twin-screw extruded whey protein concentrate-corn starch blends. *Lebensmittel-Wissenschaft und-Technologie*, *30*(4), 359-366.

33. Bohner, H. F. & Reynolds, K. J. (2006). Extrusion apparatus and method for extruding high protein foodstuffs. WO2006019320.

34. Cheftel, J. C., Kitagawa, M., & Queguiner, C. (1992). New protein texturization processes by extrusion cooking at high moisture levels. *Food Reviews International*, *8*(2), 235-275.

35. van den Einde, R. (2004). Molecular modification of starch during thermomechanical treatment. PhD thesis, Wageningen University and Research, Wageningen.

36. Frinault, A., Gallant, D. J., Bouchet, B., & Dumont, J. P. (1997). Preparation of casein films by a modified wet spinning process. *Journal of Food Science*, *62*(4), 744-747.

37. Aguilera, J. M. & Stanley, D. W. (1993). The microstructure of food protein assemblies. *Food Reviews International*, *9*(4), 527-550.

38. Roos, Y. H., Jouppila, K., & Söderholm, E. S. (1998). Crystallization of amorphous food components and polymers In *Water Management in the Design and Distribution of Quality*

Foods (Proceedings). International symposium on the Properties of Water in Foods-ISOPOW 7, May 30-June 4, Helsinki.

39. Panyam, D. & Kilara, A. (1996). Enhancing the functionality of food proteins by enzymatic modification. *Trends in Food Science & Technology*, *7*(4), 120-125.

40. Doucet, D., Gauthier, S. F., & Foegeding, E. A. (2001). Rheological characterization of a gel formed during extensive enzymatic hydrolysis. *Journal of Food Science*, *66*(5), 711-715.

41. Doucet, D., Gauthier, S. F., Otter, D. E., & Foegeding, E. A. (2003). Enzyme-induced gelation of extensively hydrolyzed whey proteins by alcalase: comparison with the plastein reaction and characterization of interactions. *Journal of Agricultural and Food Chemistry*, *51*(20), 6036-6042.

42. Creusot, N., Gruppen, H., van Koningsveld, G. A., de Kruif, C. G., & Voragen, A. G. J. (2006). Peptide-peptide and protein-peptide interactions in mixtures of whey protein isolate and whey protein isolate hydrolysate. *International Dairy Journal*, *16*, 840-849.

43. Zhou, P., Liu, X., & Labuza, T. P. (2008a). Moisture-induced aggregation of whey proteins in a protein/buffer model system. *Journal of Agricultural and Food Chemistry*, *56*(6), 2048-2054.

44. Errington, A. D. & Foegeding, E. A. (1998). Factors determining fracture stress and strain of fine-stranded whey protein gels. *Journal of Agricultural and Food Chemistry*, *46*(8), 2963-2967.

45. Matsudomi, N., Rector, D., & Kinsella, J. E. (1991). Gelation of bovine serum albumin and betalactoglobulin: effects of pH, salts and thiol reagents. *Food Chemistry*, *40*(1), 55-69.

46. Alting, A. C., Hamer, R. J., de Kruif, C. G., Paques, M., & Visschers, R. W. (2003). Number of thiol groups rather than the size of the aggregates determines the hardness of cold set whey protein gels. *Food Hydrocolloids*, *17*(4), 469-479.

47. Ju, Z. Y., Hettiarachchy, N., & Kilara, A. (1999). Thermal properties of whey protein aggregates. *Journal of Dairy Science*, *82*, 1882-1889.

48. Vardhanabhuti, B., Foegeding, E. A., McGuffey, M. K., Daubert, C. R., & Swaisgood, H. E. (2001). Gelation properties of dispersions containing polymerized and native whey protein isolate. *Food Hydrocolloids*, *15*(2), 165-175.

49. Vardhanabhuti, B. & Foegeding, E. A. (1999). Rheological properties and characterization of polymerized whey protein isolates. *Journal of Agricultural and Food Chemistry*, *47*(9), 3649-3655.

50. Alting, A. C., Hamer, R. J., de Kruif, C. G., & Visschers, R. W. (2000). Formation of disulfide bonds in acid-induced gels of preheated whey protein isolate. *Journal of Agricultural and Food Chemistry*, *48*(10), 5001-5007.

51. Ju, Z. Y. & Kilara, A. (1998). Gelation of pH-aggregated whey protein isolate solution induced by heat, protease, calcium salt, and acidulant. *Journal of Agricultural and Food Chemistry*, *46*(5), 1830-1835.

52. Akkermans, C., van der Goot, A. J., Venema, P., van der Linden, E., & Boom, R. M. (2008). Properties of protein fibrils in whey protein isolate solutions: microstructure, flow behaviour and gelation. *International Dairy Journal*, *18*(10-11), 1034-1042.

53. Hermansson, A.-M. (1975). Functional properties of proteins for foods - flow properties. *Journal of Texture Studies*, *5*, 425-439.

54. Alizadehfrad, M. R. & Wiley, D. E. (1996). Non-newtonian behaviour of whey protein solutions. *Journal of Dairy Research*, *63*, 315-320.

55. Bazinet, L., Trigui, M., & Ippersiel, D. (2004). Rheological behavior of WPI dispersion as a function of pH and protein concentration. *Journal of Agricultural and Food Chemistry*, *52*(17), 5366-5371.

56. Parker, R., Noel, T. R., Brownsey, G. J., Laos, K., & Ring, S. G. (2005). The nonequilibrium phase and glass transition behavior of betalactoglobulin. *Biophysics Journal*, *89*, 1227-1236.

57. Tung, M. A. (1978). Rheology of protein dispersions. *Journal of Texture Studies*, *9*, 3-31.

58. Muschol, M. & Rosenberger, F. (1997). Liquid-liquid phase separation in supersaturated lysozyme solutions and associated precipitate formation/crystallization. *The Journal of Chemical Physics*, *107*(6), 1953-1962.

59. Onwulata, C. I., Konstance, R. P., & Tomasula, P. M. (2002). Viscous properties of microparticulated dairy proteins and sucrose. *Journal of Dairy Science*, *85*(7), 1677-1683.

60. Yoo, J. Y., Chen, X. D., Mercadé-Prieto, R., & Ian, W. D. (2007). Dissolving heat-induced protein gel cubes in alkaline solutions under natural and forced convection conditions. *Journal of Food Engineering*, *79*(4), 1315-1321.

61. Lee, W., Clark, S., & Swanson, B. G. (2006). Low fat process cheese food containing ultrahigh pressure-treated whey protein. *Journal of Food Processing and Preservation*, *30*(2), 164-179.

62. Surh, J., Vladisavljevic, G. T., Mun, S., & McClements, D. J. (2007). Preparation and characterization of water/oil and water/oil/water emulsions containing biopolymer-gelled water droplets. *Journal of Agricultural and Food Chemistry*, *55*(1), 175-184.

63. Norton, I. T. & Frith, W. J. (2001). Microstructure design in mixed biopolymer composites. *Food Hydrocolloids*, *15*(4-6), 543-553.

64. Edelman, M. W., van der Linden, E., de Hoog, E., & Tromp, R. H. (2001). Compatibility of gelatin and dextran in aqueous solution. *Biomacromolecules*, *2*(4), 1148-1154.

65. Williams, M. A. K., Fabri, D., Hubbard, C. D., Lundin, L., Foster, T. J., Clark, A. H., Norton, I. T., Loren, N., & Hermansson, A. M. (2001). Kinetics of droplet growth in gelatin/maltodextrin mixtures following thermal quenching. *Langmuir*, *17*(11), 3412-3418.

66. Tromp, R. H., Edelman, M. W., & van der Linden, E. (2004). Gelatine/dextran solutions - a model system for food polymer mixtures. In *Gums and Stabilisers for the Food industry*, Vol. 12, 201-210. Royal Society of Chemistry.

67. van den Berg, L., Carolas, A. L., van Vliet, T., van der Linden, E., van Boekel, M. A. J. S., & van de Velde, F. (2008). Energy storage controls crumbly perception in whey proteins/polysaccharide mixed gels. *Food Hydrocolloids*, *22*(7), 1404-1417.

68. de Jong, S. & van de Velde, F. (2007). Charge density of polysaccharide controls microstructure and large deformation properties of mixed gels. *Food Hydrocolloids*, *21*(7), 1172-1187.

69. Wang, Q. & Qvist, K. B. (2000). Investigation of the composite system of betalactoglobulin and pectin in aqueous solutions. *Food Research International*, *33*(8), 683-690.

70. van der Goot, A., Peighambardoust, S., Akkermans, C., & van Oosten-Manski, J. (2008). Creating novel structures in food materials: the role of well-defined shear flow. *Food Biophysics*, *3*(2), 120-125.

71. Manski, J. M., van der Zalm, E. E. J., van der Goot, A. J., & Boom, R. M. (2008). Influence of process parameters on formation of fibrous materials from dense calcium caseinate dispersions and fat. *Food Hydrocolloids*, *22*(4), 587-600.

72. Manski, J. M., van Riemsdijk, L. E., van der Goot, A. J., & Boom, R. M. (2007). Importance of intrinsic properties of dense caseinate dispersions for structure formation. *Biomacromolecules*, *8*(11), 3540-3547.

73. Manski, J. M., van der Goot, A. J., & Boom, R. M. (2007). Formation of fibrous materials from dense calcium caseinate dipersions. *Biomacromolecules*, *8*(4), 1271-1279.

74. Lucey, J. A., Srinivasan, M., Singh, H., & Munro, P. A. (2000). Characterization of commercial and experimental sodium caseinates by multiangle laser light scattering and size-exclusion chromatography. *Journal of Agricultural and Food Chemistry*, *48*(5), 1610-1616.

75. Dickinson, E., Semenova, M. G., Belyakova, L. E., Antipova, A. S., Il'in, M. M., Tsapkina, E. N., & Ritzoulis, C. (2001). Analysis of light scattering data on the calcium ion sensitivity of caseinate solution thermodynamics: relationship to emulsion flocculation. *Journal of Colloid and Interface Science*, *239*(1), 87-97.

76. de Kruif, C. G. & Holt, C. (2003). Casein micelle structure, functions and interactions. In *Advanced Dairy Chemistry* (3rd ed., Vol. 1: Proteins, pp. 233-276). New York: Kluwer Academic/Plenum Publishers.

77. de Kruif, C. G. (1998). Supra-aggregates of casein micelles as a prelude to coagulation. *Journal of Dairy Science*, *81*(11), 3019-3028.

78. Won, D. & Kim, C. (2004). Alignment and aggregation of spherical particles in viscoelastic fluid under shear flow. *Journal of Non-Newtonian Fluid Mechanics*, *117*(2-3), 141-146.

79. Lyon, M. K., Mead, D. W., Elliott, R. E., & Leal, L. G. (2001). Structure formation in moderately concentrated viscoelastic suspensions in simple shear flow. *Journal of Rheology*, *45*(4), 881-890.

80. Hobbie, E. K., Lin-Gibson, S., Wang, H., Pathak, J. A., & Kim, H. (2004). Ubiquity of domain patterns in sheared viscoelastic fluids. *Physical Review E - Statistical, Nonlinear, and Soft Matter Physics*, *69*(6 Pt 1), 061503: 1-5.

81. Vermant, J. (2001). Large-scale structures in sheared colloidal dispersions. *Current Opinion in Colloid and Interface Science*, *6*(5-6), 489-495.

Chapter 3

Modulation of rheological properties by heat-induced aggregation of whey protein solution

Abstract

Heat-induced protein aggregation at low protein concentrations generally leads to higher viscosities. We here report that aggregated protein can yield weaker gels than those from native protein (i.e. as received from the manufacturer) at the same concentration. Aggregated protein was produced by heating a solution of whey protein isolate (WPI) at 3% and 9% w/w. The higher protein concentration resulted in a larger aggregate size and a higher intrinsic viscosity. The protein fraction in native WPI had the smallest size and the lowest intrinsic viscosity. The same trend was observed for the shear viscosity after concentrating the suspensions containing aggregates to around 15% w/w. Suspensions containing aggregates that were produced from a higher concentration possessed a higher viscosity. After reheating the concentrated suspensions, the suspension from the 9% w/w aggregate system produced the weakest gel, followed by the one from 3% w/w, while the native WPI yielded the strongest gel. Reactivity of the aggregates was also an important factor that influenced the resulting gel properties. We conclude that aggregation of whey protein solution is a feasible route to manipulate the gel strength of a concentrated protein system, without having to alter the concentration of the protein.

This chapter has been published as: Purwanti, N., Smiddy, M., van der Goot, A., de Vries, R., Alting, A. and Boom, R. **2011**. Modulation of rheological properties by heat-induced aggregation of why protein solution. *Food Hydrocolloids*, *25*(6), 1482-1489.

1. Introduction

Recent studies describe positive health benefits of whey protein and the importance of higher dietary protein intake[1-3]. Unfortunately, high protein foods are often associated with poor sensory properties. Whey protein bars that consisted up to 28.5% whey protein in different forms had a dense and cohesive texture, which required more chews prior to swallowing[4]. In addition, incorporating whey protein isolate (WPI) in bars also led to hardening in time[5]. This effect might be attributed to the segregation of protein aggregates from the rest of the matrix, followed by interactions between those aggregates creating networks[6].

A possible solution to minimize the formation of dense protein networks could be by pre-processing native whey protein[7]. Through clustering whey protein into protein aggregates, intra-molecular bonds are created in the first place followed by short-range inter-molecular bonds. This could be a method to reduce the total long-range interactions (i.e. inter-molecular bonds) in the material and as a result, a reduced strength in the overall network. Clustering of WPI into whey protein aggregates has previously been used to increase the water holding capacity of WPI at relatively low concentrations in applications such as a thickening agent. The applications of these aggregates at high concentrations and their consequences for the rheological properties after final preparation of the concentrated products have not been investigated yet. WPI heat-aggregated at 4% w/v at pH 8 resulted in a viscosity that was similar to that of 1% w/v solutions of carbohydrate-based hydrocolloids[8]. The addition of WPI aggregates to yoghurt up to a total protein content of 30–38 g/L increased the product viscosity[9], which was not observed when 3–12% native WPI was added to the yoghurt[10]. Whey protein aggregates are often applied for their cold gelling properties. Gelation of 3% whey protein aggregates using $CaCl_2$ or glucono-δ-lactone (GDL) as gelling or acidification agent yielded a stronger gel when the preceding aggregation was produced from a higher protein concentration[11, 12].

Generally, the protein aggregates are produced by heating a whey protein solution below its critical gelation concentration, which is about 12% w/w. Heating causes protein

unfolding and subsequent aggregation. The unfolding changes the number of accessible sulfhydryl groups and thereby the reactivity of the aggregates, which is defined as the tendency of the aggregates to form inter-aggregate bonds[13]. A stronger reactivity through a higher prevalence of sulfhydryl groups yielded stronger acid-induced protein networks[13]. The reactivity can be manipulated depending on the concentration of whey protein, heating temperatures, heating time, pH, and ionic strength[13-16]. A higher protein concentration during aggregation not only yields larger aggregates[11, 17-20] but it also influences interactions between aggregates. Aggregates that were produced from a higher protein concentration showed an increased viscosity[8] and thickening capacity[21] at similar concentration as those from low protein concentration.

Mostly, the effects of protein aggregation have been investigated at relatively low concentrations. The aim of this paper is to investigate the use of WPI aggregates at concentrations above the gelling concentration to *reduce* the protein–protein interactions, leading to a final gel that is *less* firm than would be obtained with the same protein in the native form (i.e. as received from the manufacturer).

2. Materials and methods

2.1. Materials

WPI (BIPRO) lot no. JE 034-7-440 was obtained from DAVISCO Food International Inc. (Le Sueur, MN), with a reported protein content of 97.9%. Other chemicals used were sodium hydroxide (NaOH), hydrochloric acid (HCl), disodium hydrogen phosphate (Na_2HPO_4) and sodium dihydrogen phosphate (NaH_2PO_4) (Merck, Germany); Bis-Tris, 5,5'-dithiobis-(2-nitrobenzoic acid) (DTNB), urea, sodium citrate, acetonitrile, trifluoroacetic acid (TFA) and dithriothreitol (DTT) (Sigma, USA); lactic acid (BDH Lab. Supplies, UK).

2.2. Preparation of WPI aggregates and the concentrated aggregate suspensions

WPI solutions with protein concentrations of 3% w/w and 9% w/w were prepared by dissolving WPI powder in Milli-Q water (Millipore, France) and stirring at room temperature for at least 2 h. The solutions were then stirred at 4°C for at least 12 h to allow complete hydration. The WPI solutions were centrifuged (~ 20,000×*g*, 30 min, 20 °C) and the supernatant was filtered (0.45 μm, Millex-HV, Millipore, Ireland) to remove any insoluble materials. The pH was set to 7.0 with NaOH. Suspensions of WPI aggregates (WPIA) were prepared by heating the WPI solutions in the water bath for 2 h or 24 h after the solutions reached 68.5 °C. This particular heating condition was chosen based on the previous study[13]. The WPIA were also prepared at a higher temperature, i.e. 90 °C for 30 min, to induce faster aggregation at a shorter time. The suspensions of WPIA were cooled down in ice water to room temperature before further use.

To increase the aggregate concentration, the WPIA suspensions produced from 3% and 9% w/w WPI solutions were concentrated to 15% w/w with a rotor evaporator (Heidolph Laborota 4001), with an operating temperature of 40 °C. The concentration process took approximately 4 h for aggregates originating from 9% and 6–8 h for those produced at 3%. The concentration changes in times were determined based on weight changes. Therefore, it was difficult to obtain the exact protein concentration of 15% w/w. After the process, the final protein concentration was checked using Dumas analysis (Nitrogen Analyzer, FlashEA 1112 series, Thermo Scientific, Interscience) using a conversion factor of 6.38 for whey protein. Dumas measurements were done in triplicate and the result was presented as an average protein concentration. In this paper, the WPIA suspensions obtained after concentrating the 3% and 9% WPIA suspensions are named the "concentrated WPIA suspension".

2.3. Analyses of whey protein isolate aggregates

2.3.1. Determination of the conversion

The conversion of native whey protein into aggregates was determined by a reversed-phase HPLC (RP-HPLC). All WPIA suspensions were diluted to 1.5% w/w. The diluted suspensions were brought to pH 4.6 using a lactic acid/acetate buffer after which the suspensions were centrifuged at 14680 rpm for 15 min (Eppendorf centrifuge). The supernatant was taken and added with buffer E^+ (8 M urea, 135 mM Bis–Tris, 44 mM sodium citrate (1.3%), pH 7 with HCl added with DTT). After incubation for 2 h at room temperature, buffer D (6 M urea, 2% acetonitrile, pH 2.7 with TFA) was added. Components were eluted with a linear gradient of solvent B in A with a flow rate of 0.8 ml/min. Solvent A was a mixture of acetonitrile–water–TFA (20:980:1, v/v/v) and solvent B contained the same component (900:100:0.8). The absorbance of the eluent was monitored at 220 nm. A 250 x 4.6 mm Widepore C18 column (Grace) was used with a C18 cartridge (Grace) as a guard column. Column temperature was 30 °C. The equipment was linked to a data acquisition and processing system (Turbochrom, Perkin-Elmer). The conversion (%) was determined by calculating the peak area of WPIA compared with that of native WPI.

2.3.2. Intrinsic viscosity measurement

The WPIA suspensions prepared from 3% to 9% w/w WPI solutions were diluted to 0.25, 0.5, 0.75, and 1% with 10 mM phosphate buffer at pH 7.0. The viscosity of each dilution was measured using Ubbelohde viscometers (Poulten Selfe and Lee Ltd, USA), tube number 0B 30451 (constant 0.004639) or 0B 39709 (constant 0.005045), in a controlled water bath at 25°C ± 0.1 (TV 4000, Tamson). Each dilution was measured in triplicate. The specific viscosity (η_{sp}) was calculated with the following equation:

$$\eta_{sp} = (t - t_0)/t_0 \qquad (1)$$

where t_0 is the time needed for the solvent to flow through the capillary in the Ubbelohde, and t is the time for the suspension. The intrinsic viscosity $[\eta]$ (L/g) was determined by extrapolating the reduced viscosity, i.e. η_{sp}/C, to zero concentration[22].

2.3.3. Size measurement

Hydrodynamic sizes of the protein aggregates were measured by using Zetasizer nano series (Zetasizer Nano ZS, Malvern Instruments) using 173° backscattering light from a laser with a wavelength of 633 nm. The aggregate suspensions were diluted to 0.25% or 0.1% using 10 mM phosphate buffer pH 7 and measured at 20 °C. The measurement for each dilution was repeated five times and the data was analysed using Malvern DTS 5.03 software. The size values reported are the average of effective hydrodynamic diameter of the largest intensity peak as found in the distribution analysis.

2.3.4. Accessibility of thiol groups

The reactivity of the aggregates was determined by measuring the number of accessible thiol groups using Ellman's reaction[23]. 50 mM Bis-Tris buffer (pH 7) was added to 0.25 ml DTNB solution (1 mg/ml Bis-Tris buffer) and 0.2 ml of aggregates at final protein concentration of 2% was added. The mixture was incubated at room temperature for 15 min. The absorbance of this mixture was measured at 412 nm with spectrophotometer (Carry UV–VIS 4000). The measurement showed good reproducibility in duplicate, except for the aggregates produced at 68.5 °C for 2 h, which were measured five times. The number of thiol groups was calculated using a molar extinction coefficient of 13600 M^{-1} cm^{-1}[24].

2.4. Rheological characterizations of concentrated WPIA suspension

2.4.1. Shear rate sweep

A freshly prepared concentrated WPIA suspension was subjected to a shear rate sweep in a cone–plate geometry at 20 °C (Rheometer Anton paar 301, CP75–1: diameter 75 mm, angle of 1°). A rest time of 15 min was applied after the geometry was subjected to the

sample. The 15% w/w native WPI solution, which was not pre-processed, was measured as a reference. Shear rates ranging from 1–300 s^{-1} were measured within 5 s per point with 10 points per shear rate. Below 1 s^{-1}, a duration of 10 s per point was applied with 25 points per shear rate to avoid transient effects. For the reference, 10 s per point with 60 points per shear rate were applied below 1 s^{-1} because the transient effects of the solution were still too high when 25 points per shear rate were applied. The measurement was done in triplicate, with the time gap between one measurement and another was around 1.5 h.

2.4.2. Dynamic oscillatory tests

A freshly prepared concentrated WPIA suspension was subjected to a heat treatment to form a heat-induced gel. The heat treatment was done *in situ* in a Couette geometry (CC–17) with the following temperature profiles: heating up from 20 to 90 °C with 1 °C/min, then 30 min at 90 °C, followed by cooling from 90 to 20 °C with 1 °C/min and finally 30 min at 20 °C. Paraffin oil was used to cover the protein suspension to avoid evaporation during heating. The properties of the gel formed were characterized following the heat treatment through frequency sweep and strain sweep at 20 °C. The frequency sweep was performed at 0.1–100 Hz with a constant strain of 0.1%. Subsequently, the strain sweep was applied using a strain of 0.1–100% at a constant frequency of 1 Hz. All tests were done in duplicate.

The frequency dependence of storage modulus (G'), which used to indicate gel firmness was described using power law parameters, i.e. a and b[25] as follow

$$G' = a\omega^b \qquad (2)$$

A frequency range of 0.1–10 Hz was used to determine a and b. The damping factor was determined from frequency sweep at 1 Hz.

The ultimate yield point of the gel was determined from the strain sweep. Straight lines were drawn from independent-strain moduli and the dependent-strain moduli. The point at which these lines cross is defined as the yield point.

3. Results

3.1. WPIA properties

The amount of native protein converted into aggregates was determined with RP-HPLC. The calculation results showed that all heat treatments of 3% and 9% w/w WPI solutions yielded in almost complete aggregation (>95%), except for 3% w/w WPI that was treated at 68.5 °C for 2 h (see Table 1). Complete aggregation assures that behaviour of the aggregate suspension in further application is not influenced by the remaining native protein. That is why the WPIA suspensions prepared at 68.5 °C for 2 h, both from 3% and 9% WPI, are excluded further in the remaining of this paper.

Different WPI concentrations yielded different aggregate sizes and different intrinsic viscosities. A higher WPI concentration resulted in larger aggregates and a higher intrinsic viscosity. It was difficult to maintain the size or the viscosity without changing the other physical properties. A higher WPI concentration yielded a higher number of available thiol groups when the solutions were heated at 68.5 °C for 24 h (see Table 1). It indicates that the aggregates produced from 9% WPI solution had a higher reactivity than those produced from 3% WPI solution. This confirmed the previous results shown by Alting et al. (2003)[13]. This trend seems also the case when the solutions were heated at 90 °C for 30 min. However, the reactivity difference between the two concentrations was not statistically significant.

Fig. 1 shows the size distributions of the WPI aggregates. A higher initial protein concentration resulted in somewhat larger aggregates by heating at 90 °C or 68.5 °C. The average size of the aggregates originating from 3% and 9% WPI solutions heated at 90 °C were 49.3 nm and 62.7 nm, respectively. Those from 3% and 9% WPI solutions heated at 68.5 °C were 32.7 nm and 49.2 nm, respectively. Those sizes confirmed aggregation because native WPI mostly consists of un-aggregated protein with a reported size of 8 nm[11]. The larger aggregate size obtained from a higher WPI concentration was also shown by Alting et al. (2003)[13] when WPI solution was heated at 68.5 °C. Furthermore, Fig. 1 shows that the aggregate size from 3% WPI heated at 90 °C coincided with those

from 9% heated at 68.5 °C. It might suggest that the number of the aggregates from 9% WPI heated at 68.5 °C was larger than those from 3% heated at 90 °C, giving the fact that the density was lower.

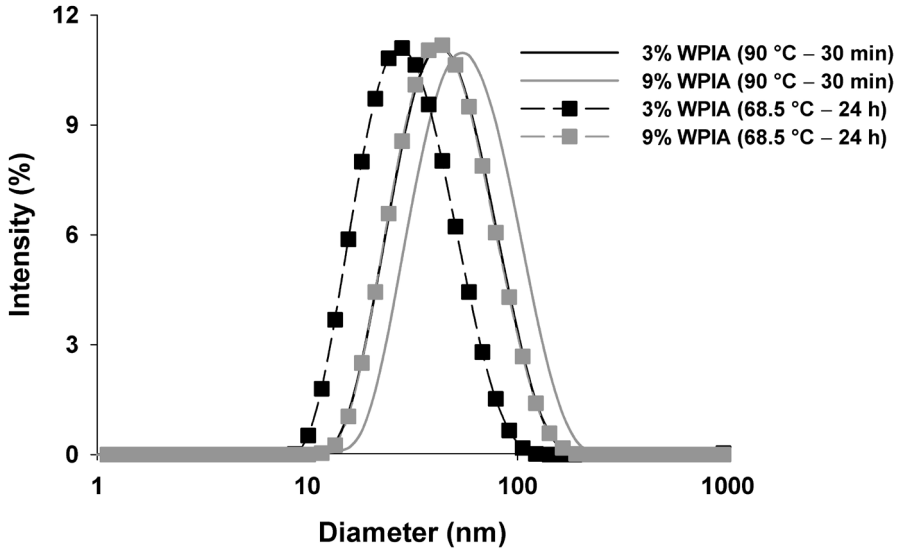

Figure 1. The size distributions of aggregates originating from 3% and 9% w/w WPI solutions heated at 90 °C for 30 min (black and grey solid lines, respectively) and those heated at 68.5 °C for 24 h (black and grey squares, respectively).

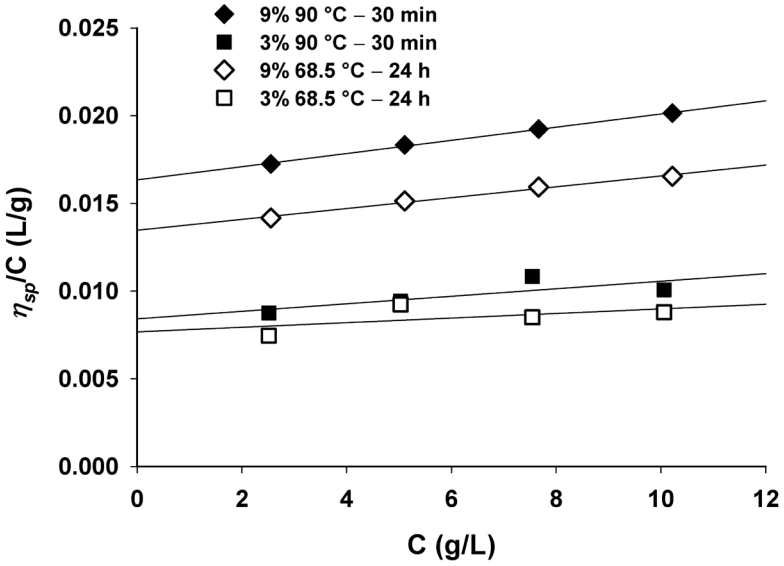

Figure 2. The reduced viscosity, η_{sp}/C, versus the concentrations of diluted WPIA suspensions originating from 3% and 9% w/w WPI solutions. The lines are linear fits; the intercepts yield the intrinsic viscosities.

The values of the intrinsic viscosity can be derived from Fig. 2. The intrinsic viscosity was always higher for the aggregates produced from 9% WPI than those from 3% WPI under both heating conditions. The values for intrinsic viscosity are listed in Table 1. The results were in-line with the trend described earlier that the intrinsic viscosity increased with the initial protein concentration[20]. Since the intrinsic viscosity is inversely related to the internal density of the aggregates, it can be stated that heat-induced aggregation of a 9% WPI solution yielded a lower protein density than that of a 3% WPI solution. The intrinsic viscosity of native WPI was reported as 5 mL/g[20]. This means that native WPI is the smallest and the densest compared to the other protein aggregates.

Table 1. Properties of WPI aggregates from various heating conditions.

No	WPI concentrations (w/w) and heat treatments	Conversion (%)[a]	*[η]* (ml/g)[b]	Hydrodynamic diameter (nm)[c]	Number of thiol groups (mM)[c]
1	3%, 68.5 °C – 2 h	62.9	–	36.5 (±2.8)	0.35 (±0.01)
2	3%, 68.5 °C – 24 h	95.1	7.7	32.8 (±0.9)	0.20 (±0.01)
3	3%, 90 °C – 30 min	95.5	8.4	49.3 (±1.4)	0.49 (±0.07)
4	9%, 68.5 °C – 2 h	96.5	12.8	49.6 (±1.9)	0.49 (±0.05)
5	9%, 68.5 °C – 24 h	99.9	13.5	49.2 (±1.8)	0.33 (±0.01)
6	9%, 90 °C – 30 min	99.7	16.3	62.7 (±0.9)	0.54 (±0.01)

[a]The percentages were calculated based on the ratio of area between the remaining native protein after and before heat treatments. The area was calculated from the chromatograms of RP-HPLC.

[b]*[η]* given for ≥95% aggregation.

[c]Mean ± standard deviation.

3.2. Rheological properties of concentrated WPIA suspensions

The rheological properties of concentrated aggregates were directly characterized after the concentration process.

3.2.1. The aggregates produced at 90 °C for 30 min

The concentration process resulted in protein contents of 14.1% w/w (±0.1%) and 14.9% w/w (±0.3%) for 3% and 9% WPIA suspensions, respectively, according to Dumas analysis. The shear viscosities of the concentrated WPIA suspensions before reheating were compared to those of a 15% w/w native WPI solution as a reference solution (Fig. 3). The reference solution showed Newtonian behaviour with a slight deviation at shear rates below 0.44 s^{-1}, which can probably be attributed to large transient effects and other experimental inaccuracies. The aggregated systems showed markedly higher viscosities. The system aggregated at 9% w/w was about five to ten times as high as the system aggregated at 3% w/w. The later was approximately 10 times higher than the reference solution. Since all systems had more or less the same concentration, the differences reflected the fact that the aggregates prepared at 9% w/w were less dense and hence included a higher effective solvent volume fraction. This observation was in agreement with previous studies for 8–11% WPI[20]. While the behaviour of the system from 3% w/w WPI was relatively Newtonian, the system from 9% w/w showed a certain extent of non-Newtonian behaviour. The slightly shear thickening at shear rates below 1 s^{-1} is related to transient effects.

The viscosities of the concentrated aggregate suspensions increased with time. As a result, the viscosities as function of shear rates in the next replications were always higher than the previous ones. That is why only the first run of each type of concentrated aggregates was plotted in Fig. 3. The viscosities of the reference solution were the average of triplicate measurements. The viscosity increase over time resulted even in a gel after storage at room temperature overnight, which was probably a result of the aggregates forming additional disulphide bonds over time.

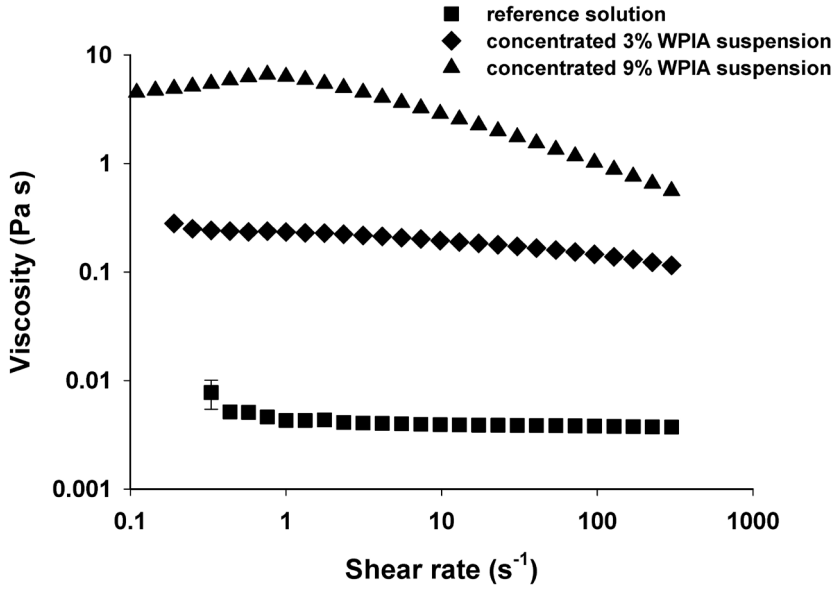

Figure 3. Shear viscosities of 15% w/w native WPI as the reference (■), 14.1% w/w WPIA that were aggregated at 3% w/w WPI (♦), and 14.9% w/w WPIA aggregated at 9% w/w WPI (▲) under 90 °C for 30 min.

The freshly prepared concentrated WPIA suspensions were subjected to reheating inside the rheometer to obtain high protein gels. After the reheating (and re-cooling) treatment, frequency and strain sweeps were used to analyse the gel properties.

The power law parameters that indicate the dependency of G' to frequency for each gel can be derived from frequency sweep. These parameters are listed in Table 2. Constant *a* represents the magnitude of storage modulus at a given frequency, while constant *b* indicates the frequency dependence of the modulus[25]. The reference gel from native WPI showed the highest value of *a* and the lowest of *b,* indicating the strongest gel with a relatively constant modulus over the frequencies. The gel prepared from 9% WPIA had lower *a* and higher *b* than that from 3% WPIA, which indicates a weaker gel that hardened with frequency.

Table 2. Power law parameters of protein gels from aggregates produced at 90 °C for 30 min.

Samples	***a**** **(kPa Hz^{-b})**	***b**** **× 1000 (–)**
15% w/w native WPI	8.9 (± 0.2)	52.5 (±0.4)
14.1% w/w WPIA from 3% WPIA	5.8 (± 0.2)	58.1 (±1.6)
14.9% w/w WPIA from 9% WPIA	3.5 (± 0.2)	78.8 (±5.9)

* Mean ± standard deviation.

Similar effects can be seen from the damping factors (tan δ), which is the ratio of loss modulus over storage modulus (Fig. 4). All gels had damping factors < 1, indicating solid gels. The reference gel had the lowest value meaning the most solid-like gel. The higher values are shown by the gels from concentrated aggregate suspensions, with the suspension produced from 9% w/w WPI having the highest value.

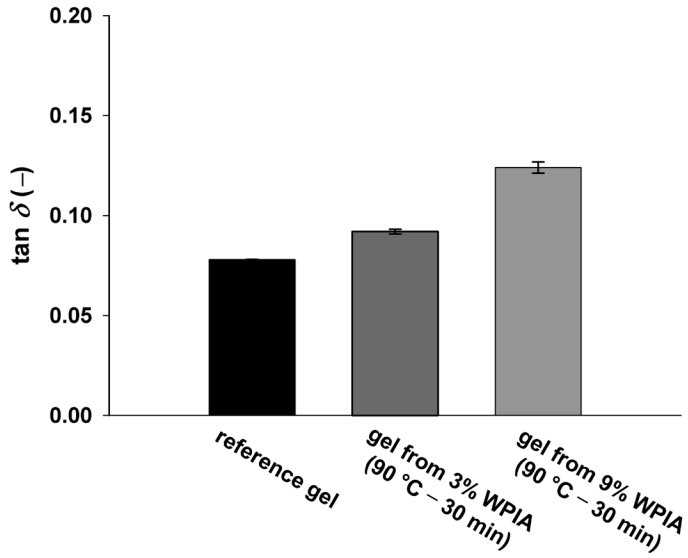

Figure 4. Damping factors of protein gels from aggregates produced at 90 °C for 30 min.

The storage moduli of gels that were subjected to strain deformation in the range of 0.1–100% are depicted in Fig. 5. Also here, the reference protein gel was the firmest gel compared to the gels from concentrated WPIA. Concentrated 9% WPIA created a weaker

gel than that from concentrated 3% WPIA. The ultimate yield point occurred at a strain around 12.5% for the reference gel, 10.0% for the gel from concentrated 3% WPIA suspension, and 7.9% for the gel from concentrated 9%WPIA suspension.

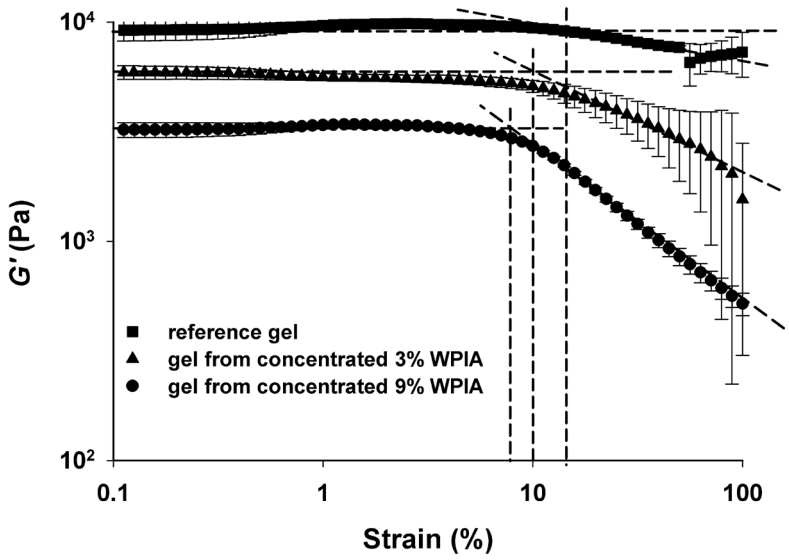

Figure 5. Solid properties of the protein gels: native WPI as the reference (■), concentrated aggregates from 3% WPIA (90 °C – 30 min) (▲), and concentrated aggregates from 9% WPIA (90 °C – 30 min) (●). The vertical dashed-lines indicate the ultimate yield point of the gels.

3.2.2. The aggregates produced at 68.5 °C for 24 h

The concentration process of the aggregates that were produced at 68.5 °C for 24 h resulted in protein contents of 14.3% w/w (±0.2%) and 13.8% w/w (±0.1%) for 3% and 9% WPIA, respectively, according to Dumas analysis. Since the protein concentration of concentrated 9% WPIA was below 14% w/w, the concentration process was repeated. This resulted in protein contents of 15.5% w/w (±0.5%) and 16.0% w/w (±0.4%) for 3% and 9% WPIA, respectively. Both results of concentration processes were used for rheological analysis. Results of concentrated aggregates from the first and second processes are indicated by "1" and "2", respectively.

Fig. 6 shows shear viscosities of the concentrated WPIA suspensions and the reference solution, i.e. 15% w/w native WPI solution, before reheating. The trends observed here

are comparable to those from aggregates that were produced by heating at 90 °C for 30 min. The viscosities of aggregates produced from 9% WPI were higher than those from 3% WPI, while viscosities of the reference solution remained the lowest. However, both aggregates systems showed relatively Newtonian behaviour as observed in the reference system. Shear thinning was observed at shear rates below 0.19 s^{-1} for 3% WPIA suspensions and 9% WPIA suspension 1. Slightly shear thinning was also observed at relatively higher shear rates in the 9% WPIA suspensions.

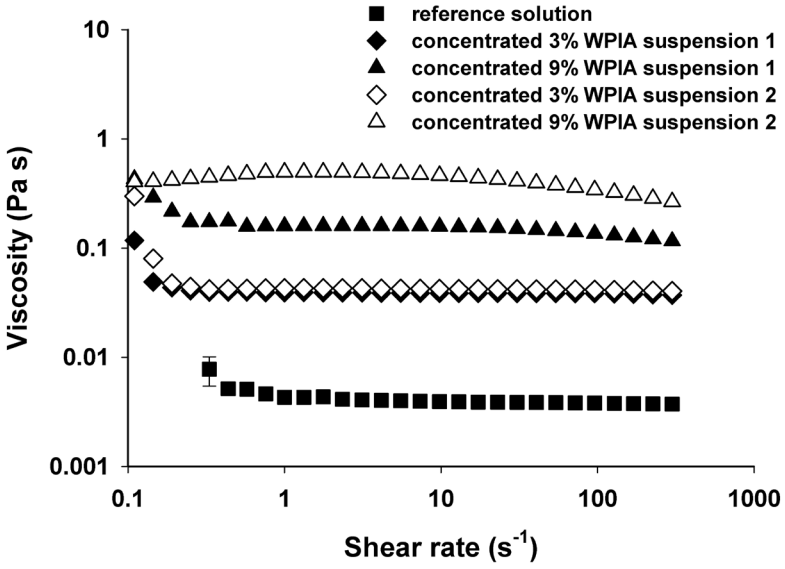

Figure 6. Shear viscosities of concentrated 3% WPIA at 14.3% w/w (♦) and 15.5% w/w (◊) and concentrated 9% WPIA at 13.8% w/w (▲) and 16.0% w/w (Δ) prepared from WPI solutions that were aggregated at 68.5 °C for 24 h, and also the reference solution at 15% w/w (■).

As observed previously, the viscosities of these aggregate suspensions also changed over time. Higher viscosities were observed in the replication experiments. That is why only the initial runs were plotted in Fig. 6, as in the case of Fig. 3. Fig. 6 shows that the viscosities of the concentrated 3% WPIA between the first and the second concentration processes were comparable although the protein concentration difference was around 1%. But, a concentration effect was observed when the protein content difference was more than 2%, as in the concentrated 9% WPIA. The 3% WPIA suspensions contained white-insoluble aggregates after storage at room temperature overnight. This was also observed

with the suspension originating from 9% WPIA having protein content of 13.8% w/w. However, a gel was formed at room temperature with the higher protein content (i.e. 16.0% w/w).

Power law parameters of the heat-induced gels originating from the concentrated aggregate suspensions are listed in Table 3. The gel from 9% WPIA had a lower value for *a* and a higher value for *b* than the gel from 3% WPIA. The trends observed here are similar to those observed when the aggregates were produced at 90 °C for 30 min. The trends remained when the gel was produced for the second time with a freshly prepared aggregate suspension. These observations were confirmed by values of damping factor of the gels (Fig. 7). It should be noted that a distinct difference was observed in the values *a* and *b* for the gel originating from 9% WPIA with lower concentration. The values were 0.4 (kPa Hz^{-b}) and 0.228 (–), respectively. These values indicate a much weaker gel compared to the one produced for the second time. This seems to be related to a low protein content, i.e. 13.8% w/w. Nevertheless, the gel was rather weak because lowering the concentration in the native WPI solution to 14.1% w/w (not listed in Table 3) resulted in a firm gel. Here, the values of the constants were 7.4 (kPa Hz^{-b}) and 0.049 (–) for *a* and *b*, respectively. The big difference in gel strength was, therefore, a result of the presence of protein aggregates. It seems that a critical concentration for gelling is increased when the proteins are aggregated.

Fig. 7 shows that the gels produced originating from the concentrated 9% WPIA suspensions had the highest values of damping factor, followed by those from concentrated 3% WPIA, and then the reference. It means that the gels originating from 9% WPIA showed the least solid-like behaviour. These trends are comparable to those observed in gels from aggregated WPI at 90 °C for 30 min. Fig. 7 also shows a distinct damping factor of the gel originating from 9% WPIA produced for the first time, i.e. around 0.38. This confirmed what has been presented in Table 3.

Table 3. Power law parameters of protein gels from aggregates produced at 68.5 °C for 24 h.

Samples	a^* (kPa Hz^{-b})	$b^* \times 1000$ (–)
15% w/w native WPI	8.9 (± 0.2)	52.5 (±0.4)
14.3% w/w WPIA from 3% WPIA (68.5 °C–24 h)[1]	3.3 (± 0.4)	80.1 (±6.5)
15.5% w/w WPIA from 3% WPIA (68.5 °C–24 h)[2]	5.9 (±1.0)	63.9 (±3.4)
13.8% w/w WPIA from 9% WPIA (68.5 °C–24 h)[1]	0.4 (±0.1)	228.0 (±1.2)
16.0% w/w WPIA from 9% WPIA (68.5 °C–24 h)[2]	4.4 (±0.2)	79.8 (±0.0)

* Mean ± standard deviation.

[1] First concentration process.

[2] Second concentration process.

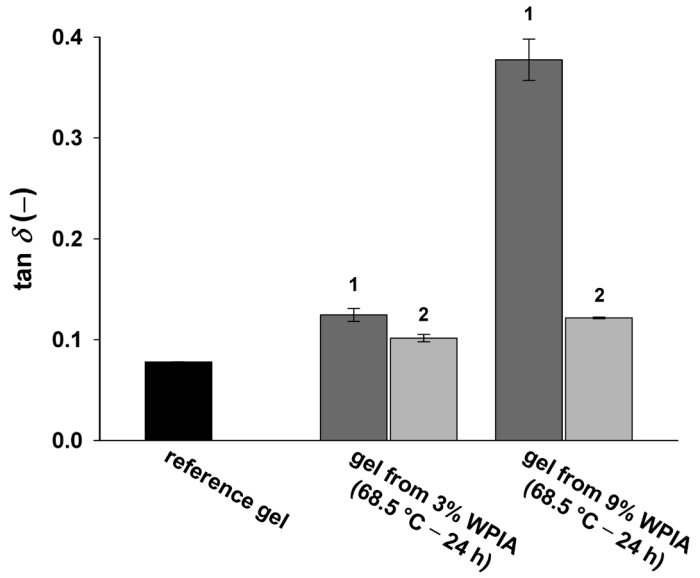

Figure 7. Damping factors of protein gels from aggregates produced under 68.5 °C for 24 h.

Storage moduli of the gels as function of strain deformation are shown in Fig. 8. Also here, the concentrated 9% WPIA suspension resulted in a weaker gel than that originating from the concentrated 3% WPIA suspension. Further, the gels originating from aggregates were weaker than the reference gel. This can also be observed in Table 3 and Fig. 7.

Again, a much weaker gel at 13.8% w/w originating from 9% WPIA can be observed in Fig. 8. This was suggested as the effect of aggregate properties, although, protein content might play a role. This was also confirmed in the gels produced for the second time. The gel originating from 9% WPIA still resulted in a weaker gel at a higher concentration, i.e. 16.0% w/w, than the gel at 15.5% w/w originating from 3% WPIA.

The ultimate yield points occurred at strains around 7.9% and 9.4% for the gels from concentrated 3% WPIA and 9%WPIA, respectively, that were obtained from the first concentration process. Higher concentrations obtained in the second concentration process resulted in gels with yield points at a strain around 10 % and 9.4% for the gels containing aggregates originating from 3% and 9% WPIA, respectively. The trends of those results did not in line with the trend observed in the gels originating from aggregates produced at 90 °C. Nevertheless, there were different yield points between the aggregated systems and the reference. However, the differences within the aggregated systems were relatively small.

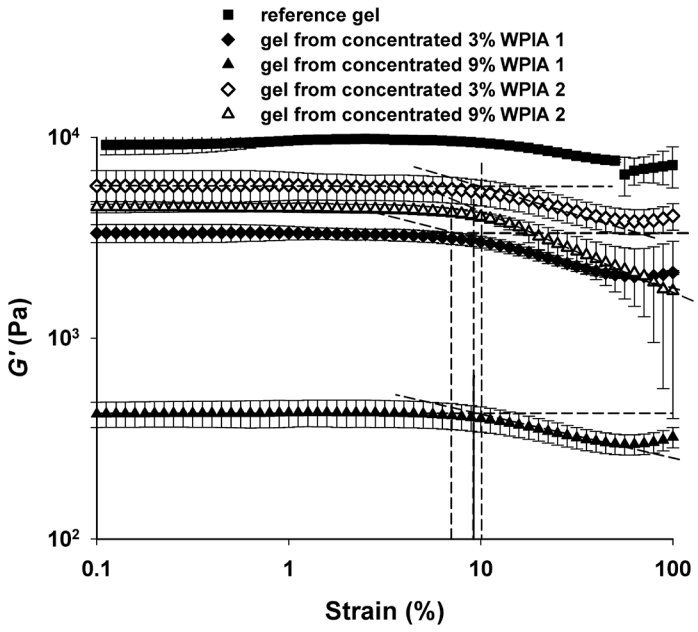

Figure 8. Solid properties of the protein gels from concentrated 9% WPIA (68.5 °C – 24 h) (▲, Δ), concentrated aggregates from 3% WPIA (68.5 °C – 24 h) (♦, ◊), and native WPI as the reference (■). The vertical dashed-lines indicate the ultimate yield point of the gels.

4. Discussion

We showed that pre-processing WPI into aggregates followed by concentrating the aggregates is a method to modulate the rheological properties of a WPI gel. The measurements showed that the aggregates originating from 9% w/w WPI solution prepared under specific heating conditions were relatively open (low density), while those originating from a 3% w/w WPI solution prepared under the same heating treatment had a denser structure and were smaller. These denser aggregates will include less solvent. The aggregates suspension originating from the 3% WPI solution showed Newtonian behaviour with a low apparent viscosity. Suspensions containing larger and lower-density aggregates were more viscous. When all systems were reheated to form gels, the order of gel firmness was reversed compared with the order of viscosities. The native protein that has the lowest viscosities showed the strongest gel. Even if the measurements might not be conclusive, we may speculate on what causes this trend reversal using the aggregate structures. Because the larger aggregates have a lower specific surface area, there are less contact points between aggregates per m^3 gel. Assuming that the inter-aggregate bonds are the weakest links in the gel, one would expect that the system with the largest aggregates would yield earlier to stress than a system with smaller aggregates, simply because the stress can be distributed over fewer inter-aggregate bonds. Thus, it seems that the mere fact of aggregation necessarily leads to a change in rheological behaviour, which can be easily tuned by choosing different aggregate sizes.

Fig. 9 depicts a schematic mechanism of the reversal of gelation properties (not to scale). The top row is the schematic representation of the protein suspensions before they undergo the heat treatment. The bottom row is the resulting networks formed after heat treatment. The aggregates are depicted as particles with different sizes. The small particles give many contact points per m^3 of gel (left hand figure). When the size of the particles increases (by reduction of the density of the particles), there is a large decrease of the number of contact points per m^3 resulting in a decrease of the gel strength (central figure). The larger the particles become, while the strength per contact point remains the same, the

stronger the effect is (right hand figure). The observation that smaller particles lead to stronger networks was also reported for colloidal gelatine particles[26]. Smaller particle size aggregated into clusters giving more resistance to deformation. The strength, size, and number of the clusters depend on the attraction forces and contact area between particles[27].

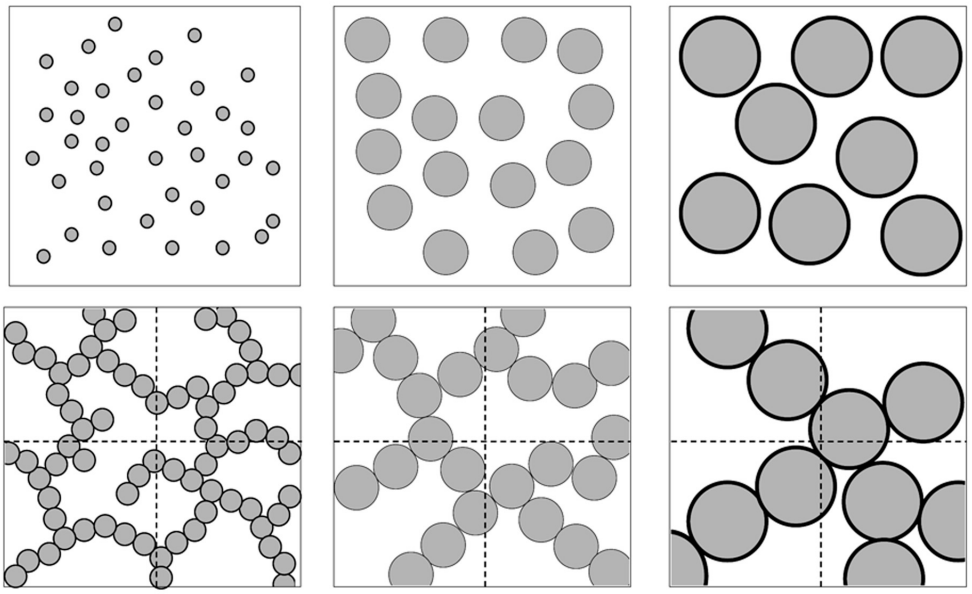

Figure 9. Schematic depiction of the mechanism of the reversal of gelation properties (not to scale). Top to bottom: before and after re-heating, left to right: native WPI, concentrated aggregates from 3% WPIA, and from 9% WPIA.

The effect of the number of contact points is counteracted by the particle density. Due to the lower particle density, the suspension created from the 9% includes more solvent volume, which would have a positive effect on the gel strength. However, the results suggest that the number of particle contact points dominates the include volume effect.

The other effect relates to the reactivity of the aggregates, next to the aggregate size and density. The gel obtained from native protein might have become a bit stronger by the (latent) reactivity of the protein. On the other hand, the aggregated WPI can only use the remaining reactivity at the surface of the aggregates. The aggregates formed at 90 °C possessed a similar reactivity. The reactivity of aggregates produced at 68.5 °C was lower

than those produced at 90 °C. It seems that a higher reactivity leads to firmer gels. However, due to the fact that the final gel strength depends on the size, density and reactivity, the overall effect is difficult to predict. For example, the aggregates produced from 3% WPI under heating at 90 °C for 30 min had comparable size as those from 9% WPI under heating at 68.5 °C for 24 h. This implies that number of contact points in the gel networks between the two systems should be similar, which could lead to the similar gels strength. However, the gel from the 9% WPIA produced at 68.5 °C was weaker than that from the 3% WPIA produced at 90 °C. This might be contributed by a lower reactivity in the 9% WPIA, i.e. a smaller number of remaining thiol groups available to create disulphide bonds. The importance of the ability of particles to form disulphide bonds on the network strength has been reported for colloidal whey protein particles[28]. However, a higher reactivity does not necessarily result in a stronger gel. When the size of the aggregates forming the network is larger, the resulting gel might also be weaker as observed for the aggregate systems produced by heating at 68.5 °C for 24 h.

5. Conclusion

The results of this study show that it is possible to alter the properties of a WPI gel at a relatively high protein concentration by using aggregated WPI. WPI aggregates were produced at diluted conditions and subsequently concentrated to the target concentration, prior to the final gelling using a heat treatment. The results in this study suggest that WPIA properties, especially size, density and reactivity, determine the strength of resulting protein gel. It can be derived that most pronounced weakening effects in the gel can be expected when using large, dense and non-reactive aggregates. Overall, it can be concluded that the preparation of products containing aggregated protein may well open the road towards food products with higher protein content and good textural properties.

Acknowledgements

The authors would like to thank to Emmelie Jacobsen for assisting the analysis of WPI aggregates, Charles Slagen and Esther van der Meulen for performing RP-HPLC.

References

1. Krissansen, G. W. (2007). Emerging health properties of whey proteins and their clinical implications. *Journal of the American College of Nutrition*, *26*(6), 713S-723S.

2. Luhovyy, B. L., Akhavan, T., & Anderson, G. H. (2007). Whey proteins in the regulation of food intake and satiety. *Journal of the American College of Nutrition*, *26*(6), 704S-712S.

3. Hayes, A. & Cribb, P. J. (2008). Effect of whey protein isolate on strength, body composition and muscle hypertrophy during resistance training. *Current Opinion in Clinical Nutrition and Metabolic Care*, *11*(1), 40-44.

4. Childs, J. L., Yates, M. D., & Drake, M. A. (2007). Sensory properties of meal replacement bars and beverages made from whey and soy proteins. *Journal of Food Science*, *72*(6), S425-S434.

5. Labuza, T. P., Zhou, P., & Davis, L. (2007). Whey to go. *The World of Food Ingredients* Vol. October/November, 108-112.

6. Zhou, P., Liu, X., & Labuza, T. P. (2008). Effects of moisture-induced whey protein aggregation on protein conformation, the state of water molecules, and the microstructure and texture of high-protein-containing matrix. *Journal of Agricultural and Food Chemistry*, *56*(12), 4534-4540.

7. Purwanti, N., van der Goot, A. J., Boom, R., & Vereijken, J. (2010). New directions towards structure formation and stability of protein-rich foods from globular proteins. *Trends in Food Science and Technology*, *21*(2), 85-94.

8. Mleko, S. & Foegeding, E. A. (1999). Formation of whey protein polymers: effects of properties a two-step heating process on rheological. *Journal of Texture Studies*, *30*, 137-149.

9. Britten, M. & Giroux, H. J. (2001). Acid-induced gelation of whey protein polymers: effects of pH and calcium concentration during polymerization. *Food Hydrocolloids*, *15*(4-6), 609-617.

10. Guggisberg, D., Eberhard, P., & Albrecht, B. (2007). Rheological characterization of set yoghurt produced with additives of native whey proteins. *International Dairy Journal*, *17*(11), 1353-1359.

11. Ju, Z. Y. & Kilara, A. (1998). Effects of preheating on properties of aggregates and of cold-set gels of whey protein isolate. *Journal of Agricultural and Food Chemistry*, *46*(9), 3604-3608.

12. Hongsprabhas, P. & Barbut, S. (1997). Protein and salt effects on Ca^{2+}-induced cold gelation of whey protein isolate. *Journal of Food Science*, *62*(2), 382-385.

13. Alting, A. C., Hamer, R. J., de Kruif, C. G., Paques, M., & Visschers, R. W. (2003). Number of thiol groups rather than the size of the aggregates determines the hardness of cold set whey protein gels. *Food Hydrocolloids*, *17*(4), 469-479.

14. Hoffmann, M. A. M. & van Mil, P. J. J. M. (1997). Heat-induced aggregation of betalactoglobulin: role of the free thiol group and disulfide bonds. *Journal of Agricultural and Food Chemistry*, *45*(8), 2942-2948.

15. Monahan, F. J., German, J. B., & Kinsella, J. E. (1995). Effect of pH and temperature on protein unfolding and thiol/disulfide interchange reactions during heat-induced gelation of whey proteins. *Journal of Agricultural and Food Chemistry*, *43*(1), 46-52.

16. Schmitt, C., Bovay, C., Rouvet, M., Shojaei-Rami, S., & Kolodziejczyk, E. (2007). Whey protein soluble aggregates from heating with NaCl: physicochemical, interfacial, and foaming properties. *Langmuir*, *23*(8), 4155-4166.

17. Boulet, M., Britten, M., & Lamarche, F. (2000). Aggregation of some food proteins in aqueous dispersions: effects of concentration, pH and ionic strength. *Food Hydrocolloids*, *14*(2), 135-144.

18. Hoffmann, M. A. M., Roefs, S. P. F. M., Verheul, M., van Mil, P. J. J. M., & de Kruif, K. G. (1996). Aggregation of betalactoglobulin studied by in situ light scattering. *Journal of Dairy Research*, *63*(3), 423-440.

19. Roefs, S. P. F. M. & de Kruif, C. G. (1994). A model for the denaturation and aggregation of betalactoglobulin. *European Journal of Biochemistry*, *226*, 883-889.

20. Vardhanabhuti, B. & Foegeding, E. A. (1999). Rheological properties and characterization of polymerized whey protein isolates. *Journal of Agricultural and Food Chemistry*, *47*(9), 3649-3655.

21. Mudgal, P., Daubert, C. R., & Foegeding, E. A. (2009). Cold-set thickening mechanism of betalactoglobulin at low pH: concentration effects. *Food Hydrocolloids*, *23*(7), 1762-1770.

22. Harding, S. E. (1997). The intrinsic viscosity of biological macromolecules: progress in measurement, interpretation and application to structure in dilute solution. *Progress in Biophysic and Molecular Biology*, *68*(2-3), 207-262.

23. Ellman, G. L. (1959). Tissue sulfhydryl groups. *Archives of Biochemistry and Biophysics*, *82*(1), 70-77.

24. Alting, A. C., Hamer, R. J., de Kruif, C. G., & Visschers, R. W. (2000). Formation of disulfide bonds in acid-induced gels of preheated whey protein isolate. *Journal of Agricultural and Food Chemistry*, *48*(10), 5001-5007.

25. Resch, J. J. & Daubert, C. R. (2002). Rheological and physicochemical properties of derivatized whey protein concentrate powders. *International Journal of Food Properties*, *5*(2), 419 - 434.

26. van Riemsdijk, L. E., Snoeren, J. P. M., van der Goot, A., Boom, R., & Hamer, R. J. (2010). New insights on the formation of colloidal whey protein particles. *Journal of Food Engineering*, *101*(4), 394-401.

27. Osman, M. A. & Atallah, A. (2006). Effect of the particle size on the viscoelastic properties of filled polyethylene. *Polymer*, *47*, 2357-2368.

28. van Riemsdijk, L. E., Snoeren, J. P. M., van der Goot, A. J., Boom, R., & Hamer, R. J. (2011). New insights on the formation of colloidal whey protein particles. *Food Hydrocolloids*, *25*(3), 333-339.

Chapter 4

Reducing the stiffness of concentrated whey protein isolate (WPI) gels by using WPI microparticles

Abstract

Concentrated protein gels were prepared using native (i.e. as received from the manufacturer) whey protein isolate (WPI) and WPI-based microparticles. WPI microparticles were produced by making gel pieces from a concentrated WPI suspension (40% w/w), which were dried and milled. The protein within the microparticles was denatured and the protein concentration after drying was similar to the native WPI powder. WPI microparticles had irregular shape with an average size of about 70 μm. They absorbed water when dispersed in water but the dispersion did not gel upon heating. Replacing part of the native WPI powder with WPI microparticles in the protein gel resulted in lower gel stiffness compared with a gel with the same overall protein concentration but without microparticles. However, microparticles also strengthened the continuous phase because they take up water from this phase. This might increase gel stiffness more than would be expected from an inert particle/filler. There was also good bonding between the microparticles and the WPI continuous phase in the gel, which contributed to gel stiffness.

This chapter has been published as: Purwanti, N., Moerkens, M., van der Goot, A. and Boom, R. **2012**. Reducing the stiffness of concentrated whey protein isolate (WPI) gels by using WPI microparticles. *Food Hydrocolloids*, *26*(1), 240-248.

1. Introduction

A number of studies have reported health benefits of a diet high in whey protein. Such a diet induces a feeling of satiety that could influence subsequent food intake and, thus, control body weight[1]. It is also reported that a high intake of whey protein can increase muscle strength and hypertrophy during resistance training[2]. However, whey protein forms a gel at a moderate concentration (about 12% w/w). A higher whey protein content in a product might increase the firmness of the product, which could result in rubbery mouth-feel and undesirable texture changes in time (hardening)[3, 4]. To circumvent these problems, modification of whey protein is proposed as an interesting solution[5-7].

Whey protein can be modified in various ways to suppress its ability to increase viscosity or form a gel. One option is to create whey protein particles. A few studies have used 12% w/w whey protein concentrate (WPC) or whey protein isolate (WPI) solution at pH 3.35[8, 9] to make protein particles. This solution was heated at 80 °C for 3 h to allow complete denaturation of the acidic whey solution. The gel obtained was freeze dried, crushed and ground into a powdery material. After rehydration in water, the protein particles formed a weak gel at ambient or chilled temperature. Whey-based particles could also be prepared using 8–30% w/v WPC at pH 6.0–8.5 with added divalent ions (calcium, magnesium and zinc) according to a patent by Havea (2007)[10]. The whey solution was heated to 90 °C for 7 min through direct steam injection, followed by cooling to about 60 °C. Dried particles were obtained by spray drying. The process resulted in protein particles ranging from 12 to 73 μm. The protein content was around 85% and more than 94% of the protein was denatured. These particles did not precipitate at 8% w/w when retorted in water at 121 °C for 10 min, which makes them suitable for beverages. The application of those particles in processed cheese using a protein content up to 20% resulted in cheese with a higher meting index than cheese with native WPC. Another study showed that a 15% w/w suspension of WPI particles resulted in a weaker gel than native WPI at the same concentration[11]. The particles were produced by heat-aggregating 3% w/w and 9% w/w WPI solutions at pH 7.0.

In this article, we present a simplified method based on previous studies[8, 10] to produce WPI microparticles. In addition, we describe the physical properties, including gelling properties of the microparticles and their behaviour in water and protein matrix. In this study, a concentrated WPI suspension was taken as the starting material without changing the pH or adding salts. This study reviews the potential of microparticles to improve the textural properties of the model of high-protein food, i.e. protein gel. The textural properties of *composite gels* containing native WPI (i.e. as received from the manufacturer) and WPI microparticles are compared with *WPI gels* containing native WPI only.

2. Materials and methods

2.1. Materials

WPI (BIPRO) lot no. JE 034-7-440 (DAVISCO Food International Inc., Le Sueur, MN), with a reported protein content of 97.9% on a dry basis, was used to prepare WPI microparticles. Isopropanol Emplura® (Merck, Germany) was used as carrier fluid for WPI microparticles during size measurements. D-Methionine (Acros Organics, Belgium) was used as a protein standard in the Dumas analysis. Milli-Q water (resistivity of 18.2 MΩ cm at 25 °C, total oxidizable carbon <10 ppb, Millipore, France) was used in all experiments, unless mentioned otherwise.

2.2. Preparation of WPI microparticles

A 40% w/w WPI suspension was prepared by suspending WPI powder in reverse-osmosis water. The suspension was stirred vigorously using a mixer blade connected to a laboratory overhead mixer at room temperature. The suspension was then kept at 4 °C under gentle stirring for at least 12 h. The pH of the suspension was not controlled, leading to a pH of around 6.8. The suspension was centrifuged in 1-L centrifuge tubes at 1500×*g* for 10 min to remove air bubbles. The resulting foam at the surface was removed manually. The protein suspension was then heated to 90 °C in approximately 30 min. The suspension was kept at this temperature for an additional 50 min while mixing in a 40-L

Stephan cutter mixer (Stephan, Germany). The scraping blade and knife in the mixer were operated at 800 rpm. After heating, the temperature was decreased to 30 °C, which took about 45 min. The process resulted in small pieces of gel. The gel was then dried in an oven at 50–60 °C (Rational, UK) until the moisture content of the gel was below 10% w/w. The dried gel was ground using an ultracentrifuge mill (Retsch ZM 1000) equipped with a 24-tooth stainless steel rotor at 15,000 rpm for 120 s. A sieve with 80-μm pore size was attached to the rotor. The resulting powder consists of the so-called WPI microparticles.

2.3. Size measurement of microparticles

The size distribution of microparticles was measured using static light scattering (Mastersizer 2000, Malvern Instruments). The stirring speed in the vessel of carrier fluid was set at 1600 rpm. The microparticle size was measured with two types of carrier fluid, namely isopropanol and water. Isopropanol was used to measure the original size because the microparticles do not swell in this solvent. Water was used to measure the size of hydrated microparticles. The particle size was measured directly after dispersing microparticles in the carrier fluid. We also measured microparticle size after 24 h in water. Refractive indices of 1.545, 1.33 and 1.39 were taken for the WPI microparticles[12], water and isopropanol, respectively. The absorption of microparticles during the measurement was set to 0.001 following Walkenstrom et al. (1999)[12]. In addition, we measured the effect of heating on the microparticle size. A 10% w/w dispersion of microparticles was heated at 90 °C for 30 min while stirring. The heated dispersion was cooled using an ice–water mixture and tempered at room temperature before measurement. The measurements were done four times for each condition tested, except for direct hydration microparticles in the carrier fluid. The latter were repeated eleven times to determine the final water absorption.

2.4. Microscopy observation

2.4.1. Light microscopy

A light microscope was used (Zeiss, Axiovert 200 MAT) to visualize the morphology of the microparticles in dry and hydrated conditions. Dry and hydrated microparticles were placed in a counting glass chamber (0.1 mm depth, 0.0025 mm^2, Optik Labor, Germany). The morphology of the microparticles was observed using 200× magnification.

2.4.2. Ultra high resolution scanning electron microscopy

Scanning electron microscopy (SEM; FEI™, Magellan 400) was operated at ultra-high resolution (UHR), i.e. 0.5 nm, to observe the morphology of the particle surface in more detail. Prior to observation, the microparticles were sputter-coated with 2 nm of tungsten (Leica EM Med 020). Pictures of the microparticles were taken at a working distance of 3 mm using magnifications of 4000× and 400,000×.

2.4.3. Normal resolution SEM

The arrangement of WPI microparticles in the composite gel was observed with SEM (FEI™, Magelan 400) at normal resolution, i.e. 4–5 nm. Two composite gels containing 12.5% w/w native WPI−2.5% w/w microparticles and 12.5% w/w native WPI−7.5% w/w microparticles were prepared for SEM observation according to the method described by Muller et al. (2000)[13], except that 50 mM phosphate buffer at pH 6.8 was used as the medium during fixation. The composite gels were dehydrated using acetone series after freeze fracturing. Critical point drying was performed after freeze fracturing and the cross-sections of the gels were examined at a magnification of 700× at a working distance of 4 mm.

2.5. Differential scanning calorimetry

The degree of denaturation of a 40% w/w WPI suspension and the gel pieces obtained after heating and mixing were measured using differential scanning calorimetry (DSC, Perkin-Elmer Diamond). A WPI suspension of about 25 mg was loaded into an aluminium

cup. This sample was measured within one day after preparation. The gel pieces with excess water (about 25 mg) were incubated for 96 h to allow equilibration before measurement. Heating and cooling ramps of 20–120 °C and 120–20 °C were applied with heating and cooling rates of 10 °C/min, after which a second heating ramp was run to check whether the first heating ramp denatured the protein completely. Five good measurements were analyzed using Start Pyris Software. The normalized peak area to the weight of protein measured was used to determine the degree of denaturation.

2.6. Protein concentration

The protein concentration of native WPI powder and WPI microparticles was analyzed using Dumas analysis (Nitrogen analyzer, FlashEA 1112 series, Thermo Scientific, Interscience). A conversion factor of 6.38 for whey protein[14] was used. The measurements were done in triplicate for native WPI powder and ten times for microparticles.

2.7. Density determination

The density of WPI microparticles was measured using an automatic, manometric gas expansion pycnometer (Quanta Chrome, Ultrapycnometer 1000). As a reference, the density of native WPI powder was also determined. For all measurements, approximately 1 g of sample was used. The measurements were done in triplicate.

2.8. Water holding capacity

The water holding capacity (WHC) of WPI microparticles was determined using a centrifugation procedure[15]. Microparticles were hydrated in water at 10% w/w at room temperature for about 3 h. The dispersions were centrifuged at 845×*g* (Eppendorf-Centrifuge 5424) at room temperature for 20 min. The weight difference between the dried microparticles and the pellet of microparticles after centrifugation was used to calculate the WHC.

We also measured the WHC of heated microparticles. A dispersion of 10% w/w microparticles was heated at 90 °C for 30 min. The dispersion was subsequently cooled in an ice–water mixture and tempered at room temperature before centrifugation.

The WHC of unheated and heated microparticles was measured in eight samples for each condition. The WHC per gram of powder and the WHC per gram of protein were calculated based on the equations used by Hudson and Daubert (2002)[16].

2.9. Thermal treatment of microparticle dispersions

A dispersion of microparticles in water was heated to check the ability of microparticles to form a heat-induced gel. Concentrations of microparticle dispersions based on the weight of the microparticles were prepared, i.e. 15, 20, and 30% w/w. We defined this concentration as the total protein concentration. The dispersions were stirred on a stirring plate while heating at 90 °C for 30 min. This was done in a closed glass vessel with double walls through which hot water was circulated. The dispersions were cooled in an ice–water mixture for 20 min. The heated dispersion was visually inspected and compared with unheated dispersion.

2.10. Production of protein gels

2.10.1. Replacement of native WPI by WPI microparticles

Whey protein gel was used as a model for high-protein food. Our aim was to investigate the effect of replacement of native WPI in the model product by WPI microparticles on the properties of the product. The protein gels contained 12.5–20% w/w WPI, in the form of native WPI only (WPI gel) or a combination of native WPI and microparticles (composite gel). The range of concentrations prepared is listed in Table 1.

The composite gel was prepared by dispersing microparticles in a native WPI solution. The dispersion was stirred for about 30 min before heating. The dispersion was placed in several glass containers (40 mL of dispersion per container) and then stirred with a magnetic stirrer on a stirring plate while heating at 90 °C for 30 min. The stirring prevented sedimentation of the microparticles. Stirring stopped once the viscosity of the

continuous phase had increased, therefore stirring did not result in broken gels. After heating, the composite gels were cooled first in warm water and then in an ice–water mixture for 5 and 20 min, respectively, to avoid glass breakage due to temperature shock. After the cooling process, the gels were subjected to a large deformation test. The temperature in the centre of the gels was 4–8 °C after cooling.

WPI gel was prepared using the same procedure as composite gel, except that native WPI was not replaced by microparticles.

Table 1. A range of concentrations for WPI and composite gels when microparticles replaced native WPI.

Native WPI (% w/w)	WPI microparticles (% w/w)	Total protein concentration (% w/w)
12.5	–	12.5
14.0	–	14.0
11.5[a]	2.5	14.0
15.0	–	15.0
12.5[a]	2.5	15.0
17.5	–	17.5
15.0[a]	2.5	17.5
12.5[a]	5.0	17.5
20.0	–	20.0
17.5[a]	2.5	20.0
15.0[a]	5.0	20.0
12.5[a]	7.5	20.0
10.0[a]	10.0	20.0

[a] Composite gels in which part of the native WPI was replaced by WPI microparticles at the same total protein concentration as the gel without replacement.

2.10.2. Addition of WPI microparticles to WPI gel

In addition to the effect of replacement of WPI, we were interested in how the mechanical properties of the gel changed upon addition of microparticles. Therefore, a new series of WPI gels was made. Each WPI gel had the same concentration as the native WPI in the continuous phase of the composite system. The preparation procedure was identical to that described in the previous section. The composition of all gels tested is listed in Table 2.

Table 2. Concentration of WPI gel and the corresponding composite gel.

Native WPI (% w/w)	WPI microparticles (% w/w)	Total protein concentration (% w/w)
12.8	–	12.8
12.8[a]	2.5	15.0
13.2	–	13.2
13.2[a]	5.0	17.5
15.4	–	15.4
15.4[a]	2.5	17.5
15.8	–	15.8
15.8[a]	5.0	20.0

[a] Gel to which WPI microparticles were added, leading to a higher total protein concentration than the gel without addition of microparticles.

2.11. Large deformation test and the data analysis

Large deformation tests were used to probe the textural properties, i.e. gel stiffness, of the WPI gels and the composite gels. The protein gels were subjected to uniaxial compression tests (Instron 5564) inside the glass containers. A stainless steel cylindrical probe with a flat base of diameter 11.25 mm was attached to the moving crosshead. The ratio between the diameter of the gel and the probe was 3.6:1. This ratio ensures that the diameter of the sample is at least three times the diameter of the probe to exclude boundary or wall effects

on the compressive force[17]. The gels were compressed at a constant speed of 1 mm/s up to 15 mm depth (50% of the initial height), with data acquisition every 10 ms. A load cell of 50 N was used for weak gels and a load cell of 2000 N was used for firmer gels. The measurement for each concentration of the gel was repeated four or five times. The gel stiffness was determined as the increment of the force with the compressive strain from 0.3 to 1%. Determination of gel stiffness using this method gives a value closely correlated to Young's modulus. The main purpose of these measurements was to compare gels rather than allow an exact mechanistic interpretation of the data.

3. Results

3.1. Structural aspect of microparticles

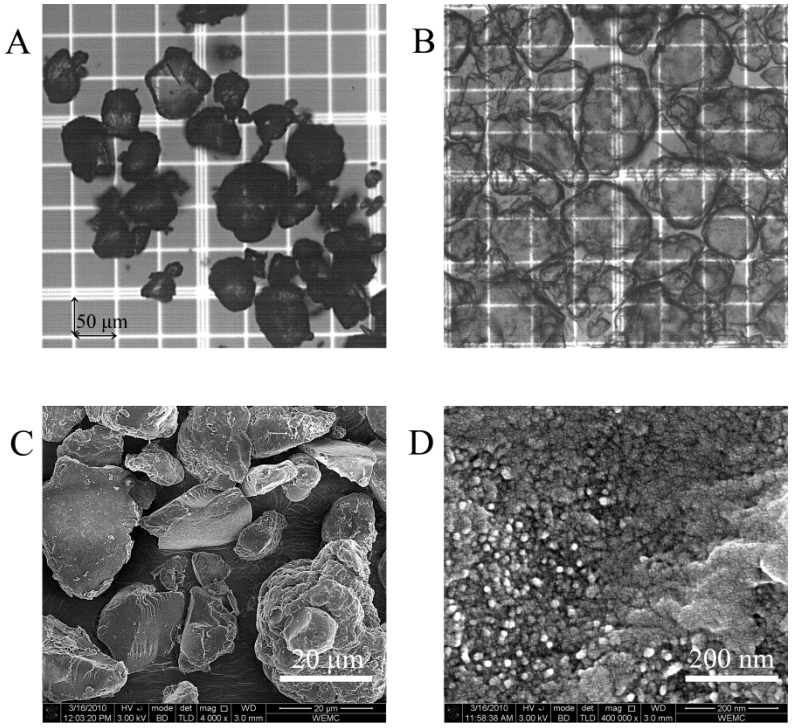

Figure 1. Morphology of microparticles observed with a light microscope at 200× magnification: (A) dry; (B) hydrated; (C) in dry form with UHR-SEM 4000× magnification; (D) 400,000× magnification.

The morphology of the microparticles, both dry and hydrated, was visualized using light microscopy (Fig. 1A, B). The morphology of the dry microparticles was visualized using UHR-SEM (Fig. 1C and 1D). The microparticles had an irregular shape (Fig. 1A and 1C) and swelled significantly on hydration (Fig. 1B). Mixing the 40% w/w WPI suspension while heating resulted in irregularity, i.e. fractured gels in irregular form[18]. The milling step also contributed to the irregularity of the particles obtained.

The image of single microparticle at high resolution shows a non-porous and rather dense structure (Fig. 1D). This dense structure was due to the use of a high concentration of WPI suspension as the starting material.

3.2. Particle size

The size distribution of the microparticles in different conditions are depicted in Fig. 2. The size of unswollen microparticles was measured using isopropanol as the inert carrier fluid. The size changed when the microparticles were measured in water, suggesting particle swelling. The extent of swelling was calculated by the ratio of the diameter between hydrated microparticles in water, d_h, and unswollen (dry) microparticles, d_d. This ratio was about 1.3, i.e. a swelling ratio by volume of around 2.4. A comparable swelling ratio for diameter was reported for WPI microparticles in a previous study[19]. Microparticles swelled further after being dispersed in water for 24 h compared with those that were directly measured in water. This indicates that some time is required to allow complete hydration of the particles at room temperature. However, this time effect can be overruled by heating. Understanding the effect of heating is important as pasteurization or sterilization is often required when applying those microparticles in a real food product. A short heating time resulted in an increase in microparticle size, leading to a swelling ratio by diameter of about 1.7. This implies a swelling of the volume by a factor of 5. It can be concluded that the changes in the size of the microparticles due to water absorption depend on time and temperature (see Table 3 for the details).

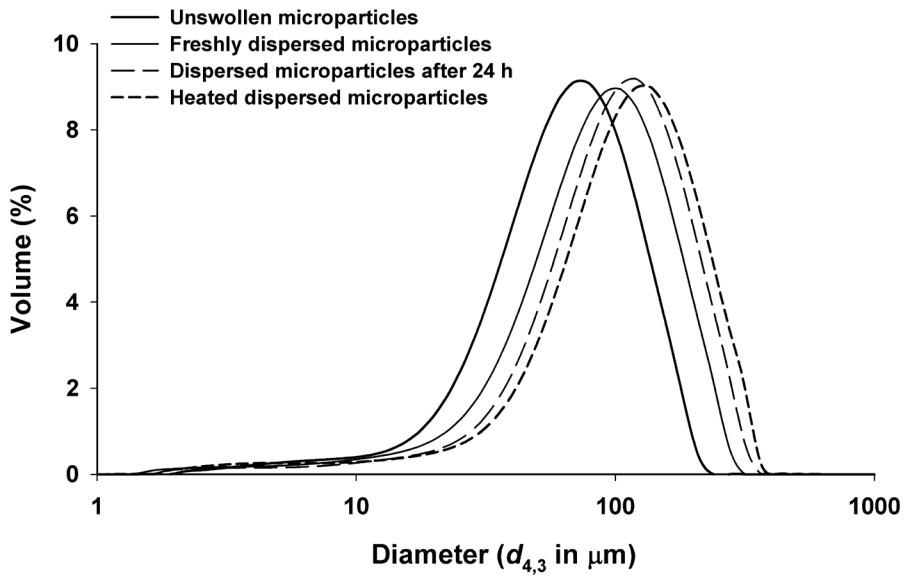

Figure 2. Size distribution of microparticle dispersions under different conditions.

3.3. Protein denaturation

Information about the denaturation level of microparticles is important to ensure that microparticles are not influenced by the presence of native protein in any application. DSC measurements can be used to reveal protein denaturation. In Fig. 3, a denaturation peak for a 40% w/w native WPI suspension can be clearly observed. This peak was no longer observed in the second heating ramp, which indicates that the protein was completely denatured in the first heating ramp. Pieces of protein gel obtained after heating and mixing showed only a small denaturation peak in the first heating ramp. Compared with native WPI, the denaturation level of WPI after heating and mixing was at least 95%. Thus, it can be concluded that denaturation has occurred during the first heating process of microparticle production.

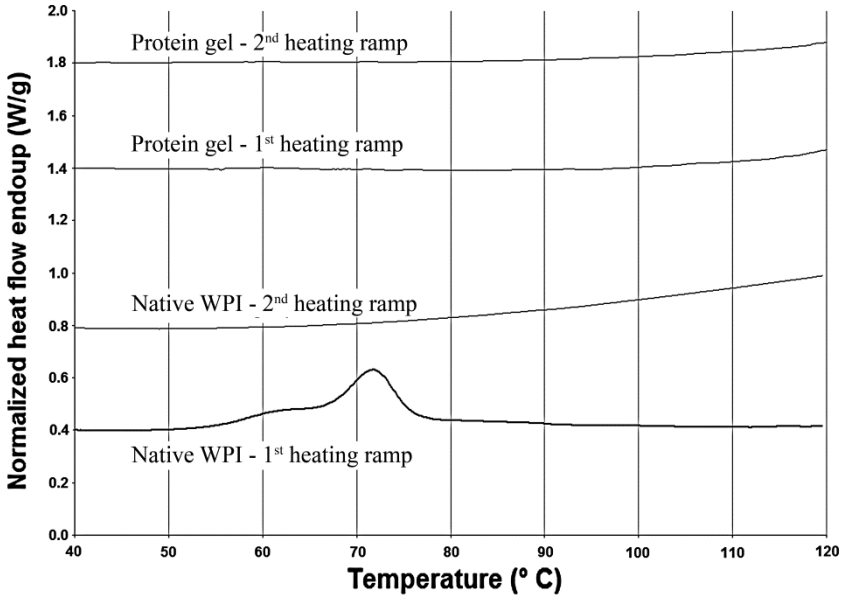

Figure 3. Typical denaturation peaks for a 40% w/w native WPI suspension and the protein gel obtained after heating and mixing.

3.4. Protein density

The density of the microparticle powder was somewhat higher than that of the native WPI powder (Table 3). Nevertheless, the values for both powders are similar to the results reported by Daubert et al. (2006)[19].

3.5. Protein concentration

The protein concentration of microparticles was around 93% w/w, which is close to the protein concentration of native WPI (96% w/w).

3.6. WHC

The WHC of the microparticles during hydration at room temperature for about 3 h was 2.76 g water/g powder. This gave 2.97 g water/g protein according to the protein content as measured. This capacity increased when the hydrated microparticles were further heated. The WHC became 4.56 g water/g powder, giving 4.9 g water/g protein. These

water absorption values are in line with the changes in particle sizes (see Fig. 2 and Table 3).

3.7. Thermal treatment of microparticle dispersions

Heat treatment of microparticle dispersion was used to check the ability of the dispersion to form a heat-induced gel. Visual observation showed that microparticle dispersions did not gel upon heating in the range of concentrations tested. Unheated dispersions showed a thickening effect of microparticles with concentrations (see Fig. 4). The thickening is probably caused by the ability of microparticles to take up water from the continuous phase. This lowers the solvent in the continuous phase and increases the volume fraction of microparticles in the system, which explains an increased viscosity. The thickening effect was more pronounced after heating. This was the result of further solvent absorption by microparticles upon heating (see Fig. 2 and Table 3).

These observations showed the altered behaviour of WPI microparticles compared with native WPI. Microparticles do not form a gel upon heating at a concentration >12% w/w, unlike native WPI. However, microparticles have a thickening capacity.

% w/w	Unheated	Heated
15	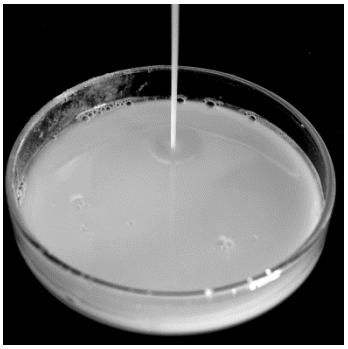 Thick dispersion, sediment of microparticles formed after stirring was stopped.	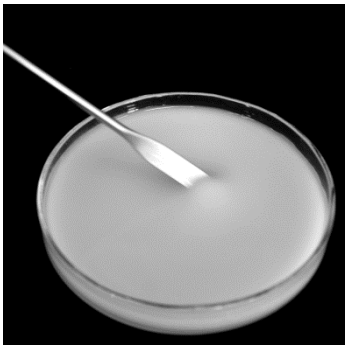 Thicker dispersion, flow-able, syneresis after some time.
20	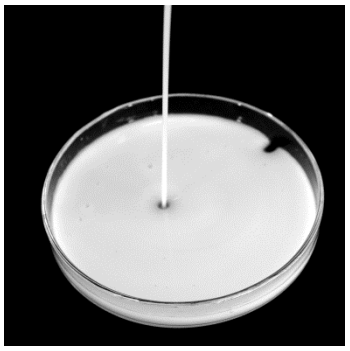 Thick dispersion, slurry-like and thick sediment of microparticles formed.	 Sticky wet lumps, weak clay-like, crushable by hand without crumbles observed.
30	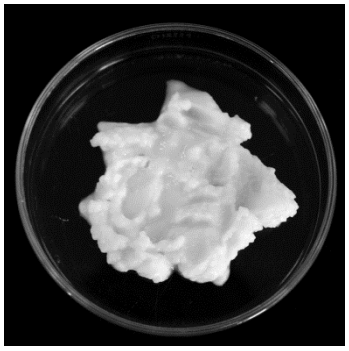 Thick paste which was not flow-able and showed syneresis after some time.	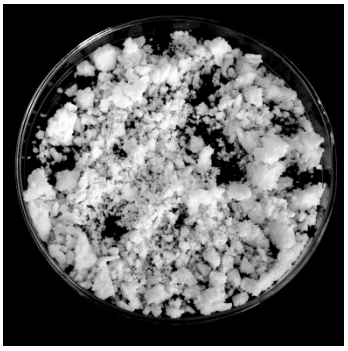 Dry, soft powder which crumbled into sand-like particles.

Figure 4. Unheated and heated microparticle dispersions at different conditions.

Table 3. Physical properties of microparticles.

Properties	**Values**[a]
Protein concentration (% w/w)	92.8 ± 0.5
Density (*g/cm*^{3})	
WPI (dry)[b]	1.1 ± 0.01
Microparticles (dry)	1.3 ± 0.00
Particle size distribution by diameter (*μm*) ($d_{0.1}$–$d_{0.9}$)	
Unswollen microparticles	25 ± 1.1–122 ± 5.6
Freshly dispersed microparticles	30 ± 1.6–164 ± 4.5
Dispersed microparticles after 24 h	38 ± 3.0–191 ± 6.1
Heated dispersed microparticles	39 ± 4.6–212 ± 4.6
Average microparticle size by diameter (*μm*) ($d_{4,3}$)	
Unswollen microparticles	68 ± 2.5
Freshly dispersed microparticles	90 ± 2.7
Dispersed microparticles after 24 h	107 ± 3.4
Heated dispersed microparticles	117 ± 4.1

[a] Average ± standard deviation.

[b] The reference.

3.8. Replacement of native WPI by WPI microparticles

It has been shown that a dispersion of WPI microparticles does not gel upon heating. This property could be beneficial in a product formulation that requires a high concentration of protein. The application of microparticles could lead to a product with a softer texture. This section describes the effects of partial replacement of native WPI in a model product, i.e. protein gel, by microparticles. The protein concentration of microparticles is

comparable with native WPI powder, hence the microparticles can be readily used to replace native WPI. Therefore, the composite gel and the WPI gel were compared at similar total protein concentrations using a compression test.

Fig. 5 shows typical data obtained from the compression tests for a WPI gel and composite gels at 20% w/w protein concentration. The force needed to compress the WPI gel was higher than that needed to compress the composite gels, i.e. the WPI gel was the strongest gel. Replacing part of the native WPI by microparticles led to a reduction in gel strength, shown by lower forces needed to compress the gel. A further replacement of WPI by microparticles resulted in an even further reduction in the compression force needed.

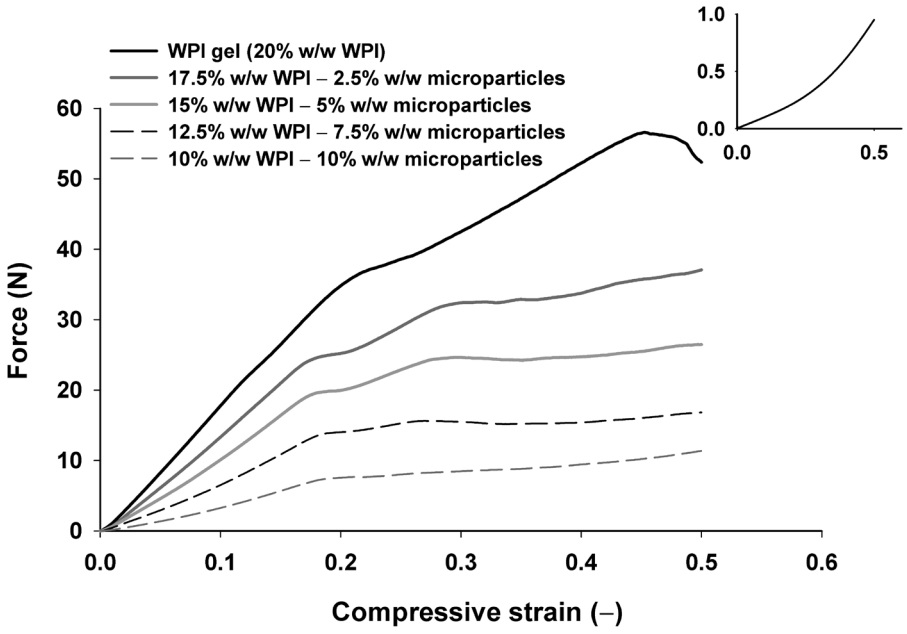

Figure 5. The data of WPI gel and composite gels at 20% w/w total protein concentration obtained from the compression tests. Inset: data of 12.5% w/w WPI gel.

The data from the compression tests were analysed and expressed as gel stiffness of the gels. The typical data shown in Fig. 5 were analysed by taking the initial slope of the curves, i.e. from compressive strain 0.003 to 0.01. These values were divided by the value of the slope related to a 12.5% w/w WPI gel. The raw data for this gel are shown in the

inset in Fig. 5. We defined the resulting values as normalized gel stiffness. These values are plotted in Fig. 6.

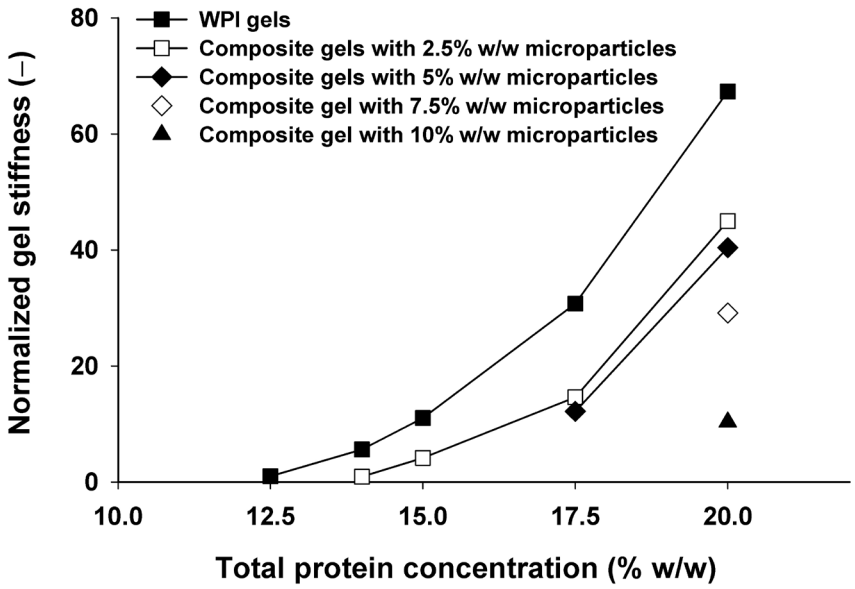

Figure 6. Normalized gel stiffness of WPI and composite gels at different protein concentrations.

Fig. 6 shows that WPI gels were stiffer than composite gels for all concentrations tested. Replacement of native WPI by microparticles resulted in a weaker gel. Replacement of 2.5%, 5%, 7.5%, or 10% w/w native WPI by microparticles clearly led to a weaker gel. This effect is probably caused by the fact that microparticles do not gel upon heating. Fig. 6 also shows that WPI gels stiffened with total protein concentration. This is typical behaviour of protein gels[20-22]. Composite gels also stiffened with total protein concentration. This could be simply the effect of increased overall protein concentration in the system, as mentioned previously for protein gels. Specifically, increased protein concentration in the continuous phase due to moisture transport from the continuous phase to the particles could also have a stiffening effect. In addition, the stiffening of composite gels with protein concentration could be the result of a filling effect of the microparticles, which have good bonding with the continuous phase.

The SEM images of composite gel containing 12.5% w/w WPI–2.5% w/w microparticles and 12.5% w/w WPI−7.5% w/w microparticles (see Fig. 7) show good bonding between

the microparticles and the continuous phase. The microparticles are not isolated from the continuous phase in Fig. 7A but seem well bonded to it. The microparticles cannot be easily differentiated from the continuous phase in Fig. 7A. At a higher concentration of microparticles, they become more visible (see Fig. 7B) and the bonding seems good. This type of figure has been shown for starch−zein blends when there was good adhesion between the two materials[23].

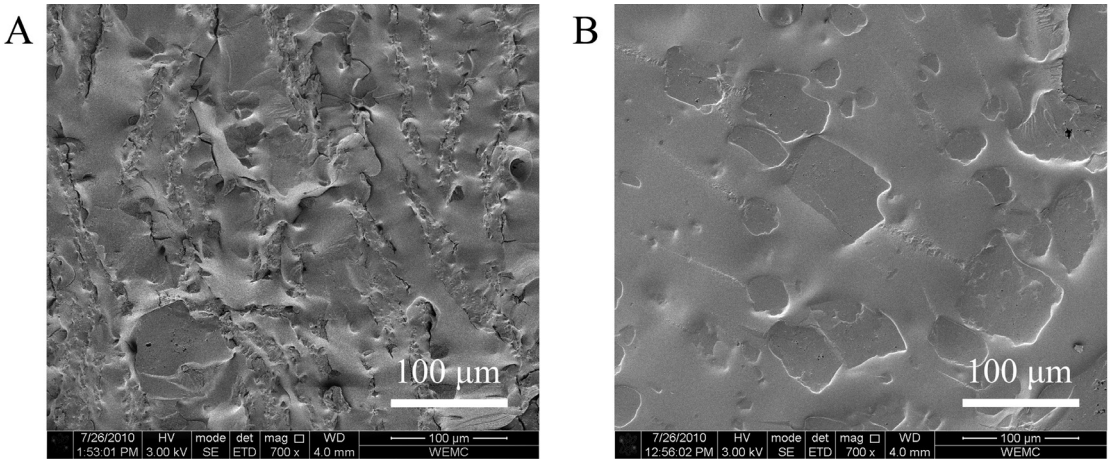

Figure 7. SEM images of composite gels that contained 12.5% w/w WPI–2.5% w/w microparticles (A) and 12.5% w/w WPI–7.5% w/w microparticles (B).

4. Discussion

A production method to modify WPI into microparticles and their properties are presented. Microparticles have an average size of 70 µm. They are irregular in shape and have a dense microstructure. Microparticles have a protein concentration comparable with native WPI powder, which makes them an attractive protein source. The microparticles are denatured and lack gelling ability. They absorbed water and this was enhanced by additional heating. We quantified the effect of water absorption on protein concentration inside microparticles by calculating the mass of swollen particles from the volume of the particles and their volume swelling ratio. The protein concentration inside the microparticles decreased from around 93% w/w in dry condition to around 52% w/w when dispersed in water and to around 25% w/w after further heating. The ability of WPI

microparticles to absorb water and to swell is not new because the water absorption capacity of proteins is commonly known[24]. We also showed that swelling of microparticles depends on time and temperature. The swelling of WPI gels, which is the origin of WPI microparticles, is a kinetic behaviour that depends on the quality of the medium[25, 26].

Dispersions of microparticles did not gel upon heating at any of the concentrations tested. Replacing native WPI by microparticles resulted in weaker gels than those without replacement. This means that the particles can be used to add more protein to a product while suppressing firmness, keeping the total protein concentration constant.

We quantified the effect of adding microparticles by calculating the effective protein concentration in the composite gels. The effective concentration is defined as the protein concentration of composite gel as if it contained only native WPI leading to a similar gel stiffness. For this purpose, the stiffness of composite gels was fitted to the stiffness of WPI gels using a third-order polynomial function. The results are shown in Table 4.

Table 4 shows that microparticles can be used to produce a high-protein gel with a stiffness equal to a protein gel with lower concentration. As an example, a composite gel with a total protein concentration of 20% w/w would have a stiffness that is equal to a WPI gel of 17.3% w/w. This value is in between the concentration of the continuous phase (i.e. 13.5% w/w) and the total concentration (i.e. 20% w/w). It means that addition of microparticles to the continuous phase strengthens the continuous phase. However, a composite gel containing microparticles had a stiffness similar to a gel with a protein concentration that was 1.5–2.7% w/w lower than its total protein concentration (see Table 4). This shows that the weakening effect of microparticles is actually rather limited.

There are two possible explanations for this limited effect. First, microparticles act as fillers with good bonding with the WPI continuous phase, as shown in Fig. 7. Second, microparticles imbibe water from the continuous phase, thereby increasing the local protein concentration in the continuous phase. As a result, the gel of the continuous phase becomes stiffer. This is in line with the finding of a WPI/cassava starch composite in

which the modulus of the gel increased because starch absorbed more water after gelatinization. Hence, the WPI concentration in the continuous phase increased, resulted in a stiffer gel[27]. Both explanations suggest that WPI microparticles are not inert fillers. They are able to influence the continuous phase by absorbing water from it.

Table 4. Quantification of the weakening effect of microparticles in composite gels.

Continuous phase (% w/w WPI)	WPI microparticles (% w/w)	Total protein concentration (% w/w)	Concentration of WPI at the same stiffness (% w/w)
12.8	–	12.8	12.8
12.8[a]	2.5	15.0	13.5
13.2	–	13.2	13.2
13.2[a]	5.0	17.5	15.2
13.5	–	13.5	13.5
13.5[a]	7.5	20.0	17.3

[a] Composite gels.

We evaluated the stiffness of composite gel using a model derived for dispersion of hard spheres[28]. The model was developed for the shear modulus, but it was also valid for Young's modulus[29]:

$$\frac{E_c}{E_m} = \frac{1+AB\phi}{1-B\psi\phi} \qquad (1)$$

where E_c is the modulus of the composite gel, E_m is the modulus of the matrix (continuous phase), ϕ is the volume fraction of the dispersed particles, A is a parameter that is a function of Poisson's ratio (υ) of the matrix, B is a function of the ratio between the modulus of the filler and the matrix, and ψ is a variable that depends on ϕ and the maximum volume fraction (ϕ_{max}). Expressions for A, B, and ψ are as follows[28]:

$$A = \frac{(7-5\upsilon)}{(8-10\upsilon)} \quad (2)$$

$$B = \frac{(E_f/E_m)-1}{(E_f/E_m)+A} \quad (3)$$

$$\psi = 1 + \phi\left(\frac{1-\phi_{max}}{\phi_{max}^2}\right) \quad (4)$$

E_f is the modulus of the filler. The value of B approaches 1 when E_f is much larger than E_m (i.e. for the case of hard-sphere particles), while 0.64 is the usual choice for ϕ_{max}. The effective volume fractions calculated using the particle density when 2.5% w/w and 5% w/w microparticles were used were 0.095 and 0.189, respectively. The swelling effect after heating was included. Those values were used to calculate the stiffness ratio between composite gel and matrix gel, assuming the microparticles to be hard spherical particles. This ratio was then compared with the ratio obtained from the experiments.

Fig. 8 indicates that the gel stiffness increased due to particle addition. A higher particle volume fraction resulted in a higher stiffness both for the theoretical and experimental values. Experimental values are higher than expected based on the assumption of hard spherical particles. Another surprising effect is that at a lower particle volume fraction, the differences between the experiments and the theoretical value are smaller than those at a higher volume fraction. Apparently, the disproportionate effect of the particles is larger for the higher particle volume fraction. Fig. 8 also shows that the behaviour of microparticles approaches that of hard-sphere dispersion with increasing WPI concentration in the continuous phase.

The observation in Fig. 8 can be explained again by considering the ability of microparticles to absorb water from the continuous phase. At lower concentration in the continuous phase, microparticles might absorb more water than those at higher WPI concentration. Therefore, the continuous phase becomes stiffer because of the increased protein concentration in the continuous phase. This effect could partly be compensated by

softening of the particles due to water absorption, but the net effect remains positive. Thus, the resulting composite gel would also be stiffer than the continuous phase alone. At a higher WPI concentration, microparticles swell less because the protein in the continuous phase retains water better, especially upon heating. As a result, the actual concentration in the continuous phase increases less, leading to a smaller deviation from the hard-sphere approach.

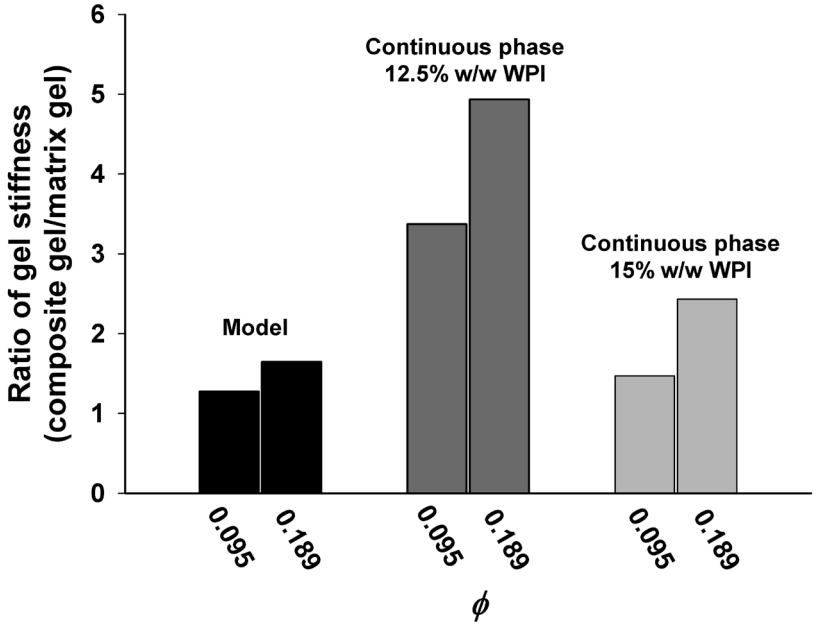

Figure 8. Ratio of gel stiffness between composite and matrix gels. The black bars represent the model calculated for hard spherical particles, the dark and light grey bars represent the experimental values for composite gels containing 12.5% w/w and 15% w/w WPI, respectively.

We thus conclude from Fig. 8 that the effect of microparticles as inert filler is not sufficient to explain their effects in a composite gel. The effects of microparticles are mostly determined by redistribution of the water in the system. Provided bonding between the microparticles and the protein continuous phase is good, the stiffness of the composite gels can be qualitatively summarized as follows: gel stiffness = gel stiffness of the protein continuous phase + increased stiffness due to local increment of the protein concentration in the continuous phase.

5. Conclusion

This article describes a method to modify a concentrated WPI suspension at its natural pH. The procedure involved suspending the protein at high concentration (40% w/w), heating while mixing, drying and grinding to a smaller size. This resulted in so-called WPI microparticles with a high-protein concentration.

A dispersion containing microparticles did not gel upon heating. Thus, microparticles could be used to suppress gelation in a protein system at high concentration, resulting in a weaker gel. However, this effect was limited. One of the aspects contributing to this limited effect is good bonding between microparticles and the protein continuous phase. The final composite gel strength is also affected by redistribution of water from the continuous phase to the microparticles.

Acknowledgements

The authors would like to thank Emmelie Jacobsen (NIZO) for assisting with the pilot plant-scale production of microparticles, Herman de Beukelaer for DSC analysis, and Jacqueline Donkers for performing the SEM.

References

1. Luhovyy, B. L., Akhavan, T., & Anderson, G. H. (2007). Whey proteins in the regulation of food intake and satiety. *Journal of the American College of Nutrition*, *26*(6), 704S-712S.

2. Hayes, A. & Cribb, P. J. (2008). Effect of whey protein isolate on strength, body composition and muscle hypertrophy during resistance training. *Current Opinion in Clinical Nutrition and Metabolic Care*, *11*(1), 40-44.

3. Childs, J. L., Yates, M. D., & Drake, M. A. (2007). Sensory properties of meal replacement bars and beverages made from whey and soy proteins. *Journal of Food Science*, *72*(6), S425-S434.

4. Zhou, P. & Labuza, T. P. (2007). Effect of water content on glass transition and protein aggregation of whey protein powders during short-term storage. *Food Biophysics*, *2*(2), 108-116.

5. Labuza, T. P., Zhou, P., & Davis, L. (2007). Whey to go. *The World of Food Ingredients* Vol. October/November, 108-112.

6. Purwanti, N., van der Goot, A. J., Boom, R., & Vereijken, J. (2010). New directions towards structure formation and stability of protein-rich foods from globular proteins. *Trends in Food Science and Technology*, *21*(2), 85-94.

7. Saglam, D., Venema, P., de Vries, R., Sagis, L. M. C., & van der Linden, E. (2010). Preparation of high protein micro-particles using two-step emulsification. *Food Hydrocolloids*, *25*(5), 1139-1148.

8. Hudson, H. M., Daubert, C. R., & Foegeding, E. A. (2000). Rheological and physical properties of derivitized whey protein isolate powders. *Journal of Agricultural and Food Chemistry*, *48*(8), 3112-3119.

9. Resch, J. J. & Daubert, C. R. (2002). Rheological and physicochemical properties of derivatized whey protein concentrate powders. *International Journal of Food Properties*, *5*(2), 419-434.

10. Havea, P. (2007). Method for preparing a dried modified whey protein. WO/2007/108709.

11. Purwanti, N., Smiddy, M., van der Goot, A. J., de Vries, R., Alting, A., & Boom, R. (2011). Modulation of rheological properties by heat-induced aggregation of whey protein solution. *Food Hydrocolloids*, *25*(6), 1482-1489.

12. Walkenstrom, P., Nielsen, M., Windhab, E., & Hermansson, A. M. (1999). Effects of flow behaviour on the aggregation of whey protein suspensions, pure or mixed with xanthan. *Journal of Food Engineering*, *42*(1), 15-26.

13. Muller, W. H., van Aelst, A. C., Humbel, B. M., van der Krift, T. P., & Boekhut, T. (2000). Field-emission scanning electron microscopy of the internal cellular organization of fungi. *Scanning*, *22*, 295-303.

14. Cerbulis, J., Woychik, J. H., & Wondolowski, M. V. (1972). Composition of commercial wheys. *Journal of Agricultural and Food Chemistry*, *20*(5), 1057-1059.

15. Fleming, S. E., Sosulski, F. W., Kilara, A., & Humbert, E. S. (1974). Viscosity and water absorption characteristics of slurries of sunflower and soybean flours, concentrates and isolates. *Journal of Food Science*, *39*(1), 188-192.

16. Hudson, H. M. & Daubert, C. R. (2002). Functionality comparison between derivatized whey proteins and a pregelatinized starch. *Journal of Texture Studies*, *33*(4), 297-314.

17. Bourne, M. C. (2002). Principles of objective texture measurement in *Food texture and viscosity: concept and measurement* (2nd ed.). London & California: Academic Press.

18. Manski, J. M., van der Goot, A. J., & Boom, R. M. (2007). Influence of shear during enzymatic gelation of caseinate-water and caseinate-water-fat systems. *Journal of Food Engineering*, *79*(2), 706-717.

19. Daubert, C. R., Hudson, H. M., Foegeding, E. A., & Prabhasankar, P. (2006). Rheological characterization and electrokinetic phenomena of charged whey protein dispersions of defined sizes. *LWT - Food Science and Technology*, *39*(3), 206-215.

20. Lowe, L. L., Foegeding, E. A., & Daubert, C. R. (2003). Rheological properties of fine-stranded whey protein isolate gels. *Food Hydrocolloids*, *17*(4), 515-522.

21. Paulsson, M. & Dejmek, P. (1990). Rheological properties of heat-induced betalactoglobulin gels. *Journal of Dairy Science*, *73*, 45-53.

22. Torres, L. M., Calderas, F., Infante, J. A. G., Laredo, R. F. G., Guzman, N. E. R., & Harte, F. (2010). Mechanical properties of ovalbumin gels formed at different conditions of concentration, ionic strength, pH, and aging time. *Food Bioprocess Technology*, *3*, 150-154.

23. Habeych, E., van der Goot, A. J., & Boom, R. (2009). *In situ* compatibilization of starch-zein blends under shear flow. *Chemical Engineering Science*, *64*(15), 3316-3524.

24. Llyod, D. J. (1938). Protein structure and water absorption. *Journal of Physical Chemistry*, *42*(1), 1-10.

25. Gunasekaran, S., Xiao, L., & Eleya, M. M. O. (2006). Whey protein concentrate hydrogels as bioactive carriers. *Journal of Applied Polymer Science*, *99*(5), 2470-2476.

26. Vardhanabhuti, B., Khayankan, W., & Foegeding, E. A. (2010). Formation of elastic whey protein gels at low pH by acid equilibration. *Journal of Food Science*, *75*(5), E305-E313.

27. Aguilera, J. M. & Rojas, E. (1996). Rheological, thermal and microstructural properties of whey protein-cassava starch gels. *Journal of Food Science*, *61*(5), 962-966.

28. Lewis, T. B. & Nielsen, L. E. (1970). Dynamic mechanical properties of particulate-filled composites. *Journal of Applied Polymer Science*, *14*(6), 1449-1471.

29. Manski, J. M., Kretzers, I. M. J., van Brenk, S., van der Goot, A. J., & Boom, R. M. (2007). Influence of dispersed particles on small and large deformation properties of concentrated caseinate composites. *Food Hydrocolloids*, *21*(1), 73-84.

Chapter 5

Hardening in whey protein isolate (WPI) gels: effects of internal structure

Abstract

Textural changes in high-protein gels with a protein concentration of 15% and 20% w/w were evaluated through their mechanical properties. The gels made only from whey protein isolate (WPI) hardened over the first few days and then became constant. However, the protein gels hardened continuously over a longer times when WPI microparticles replaced a part of WPI, keeping the total protein concentration the same. The same continuous hardening of protein gels over time was also observed when a concentrated WPI microparticles was dispersed in a mixture of locust bean gum and xanthan gum. The differences in hardening process between the protein gels without and with WPI microparticles were suggested to be a result of moisture redistribution. This hypothesis was based on the fact that WPI microparticles absorb water, the kinetics of which depends on time and temperature.

This chapter has been submitted for publication.

1. Introduction

Protein-enriched products, for example protein bars, nowadays are formulated for health-conscious consumers[1]. Many studies reveal the positive effects of a higher daily intake of protein for better body weight control[2], higher muscle strength[3], and delay in onset of sarcopenia[4]. However, high-protein products, which mostly consist of a mixture of protein, sugars and water, undergo sensorial changes over time that are not appreciated by consumers. The main changes relate to the hardening of the product with time[5]. Several studies have discussed the mechanisms behind the hardening of these products[1, 6-9]. Li et al. (2008)[6] suggested that an increase in water activity during storage indicates that water becomes less bound by the matrix. Consequently, water may act less as plasticizer and thus hardening occurs. McMahon et al. (2009)[8] proposed that separation between the protein and the carbohydrate in a mixture of protein, carbohydrate, and water causes hardening of the bar and subsequently, increases protein aggregation. Loveday et al. (2010)[9] found no evidence of the formation of additional covalent bonds in protein aggregation, but confirmed that water migration from the protein phase to a glucose−glycerol phase is correlated with the hardening of protein bars.

The questions remain whether hardening is relevant in high-protein systems without ingredients such as sugars or other polyols, and to what extent hardening is a property of the protein matrix itself. A previous study suggested that protein aggregation is responsible for structural and textural changes in a concentrated matrix of whey protein isolate (WPI)[10]. However, this study only explored the changes in a model product made from native WPI (i.e. as received from the manufacturer). A certain extent of hardening probably cannot be avoided in a protein phase. Thus, it is hypothesized that by having the protein phase as a dispersed phase, the hardening of the product might be reduced by concentrating the hardening effects locally in the product. Therefore, we report the role of protein structural elements (WPI microparticles) to retard structural and textural changes in high-protein products. We also took into account that heating might be applied in the preparation of high-protein products, which changes the properties.

The study was carried out to quantify and examine the textural changes, i.e. hardening over time, of a high-protein model product. The model product comprises a protein concentration above the critical gelling concentration of native WPI. We compared a single phase system, i.e. protein gels made from native WPI only, and a multiphase system in which the protein gels were made from dispersions of WPI microparticles in native WPI solution and in a polysaccharide continuous phase.

2. Materials and methods

2.1. Materials

WPI (Bipro) lot no. JE 034-70-440 (Davisco Food International Inc., Le Sueur, MN), with a reported protein content of 97.9% on a dry basis, was used to prepare the native WPI solution and WPI microparticles. A mixture of locust bean gum (LBG) (Degussa, France) and xanthan gum (XG) derived from *Xanthomonas campestris* (Fluka, France) was used as a polysaccharide continuous phase. Isopropanol Emplura® (Merck, Germany) was used as the carrier fluid for WPI microparticles during particle size measurements. Sodium azide (Sigma-Aldrich, Germany) was used at 0.02% w/w as a preservative. Paraffin oil (Merck, Germany) was used as a lubricant during compression tests and as a vapour lock during rheological measurements. Milli-Q water (resistivity of 18.2 MΩ cm at 25 °C, total oxidizable carbon <10 ppb, Millipore, France) was used in all experiments, unless mentioned otherwise.

2.2. Production of WPI microparticles

The WPI microparticles were produced following the method described by Purwanti et al. (2012)[11], but on a laboratory scale. A 40% w/w WPI suspension was centrifuged in 50-ml centrifuge tubes at 78×*g* for 10 min (20 °C) to remove air bubbles. The suspension was then heated at 90 °C for 50 min while mixing in a bowl mixer (type W50) connected to a Brabender Do-corder E330 (Brabender OHG, Duisburg, Germany). The mixer was operated at 0 rpm for 5 min, 5 rpm for 5 min, and 200 rpm for 40 min. The temperature was controlled by circulating water from a water bath through the mixer. The mixer was

cooled down by circulating water at 4 °C for about 5 min before taking the material out of the mixer. The resulting gel pieces were dried in an oven at 50 °C (Termaks) for 16 h. The remaining processing steps were the same as described in the previous study[11].

2.3. Properties of WPI microparticles

The WPI microparticles were characterized in terms of the degree of denaturation, the particle size and density, protein concentration, and the water holding capacity (WHC) according to the procedures described earlier in the previous study[11].

Pieces of WPI gel obtained after heating and mixing were measured with differential scanning calorimetry (DSC). These measurements indicated that the protein in the WPI microparticles was denatured completely.

The microparticle size was measured in triplicate using static light scattering (Mastersizer 2000, Malvern Instruments). The average diameter of the dry microparticles (unswollen condition) was around 70 μm. After dispersion in water, their size increased depending on the contact time with water. The particle size increased to about 97 μm when freshly dispersed in water, to around 105 μm after 1 h, and to around 114 μm after 24 h dispersed in water. Their size increased further by heating the microparticle dispersion at 90 °C for 30 min, to a size that was bigger than that obtained by dispersing the microparticles at room temperature for 24 h. The increase in particle size was in line with previous observations[11]. The details of the size distributions are listed in Table 1.

The protein concentration in the WPI microparticles, measured using the Dumas method (Nitrogen analyser, FlasEA 1112 series, Thermo Scientific, Interscience) in duplicate, was around 93% w/w. This concentration was similar to the protein concentration of native WPI determined using the same method.

The density of the microparticle powder, measured with a manometric gas expansion pycnometer (Quanta Chrome, Ultrapycnometer 1000) in triplicate, was 1.3 g/cm^3. This is similar to the previous result[11].

The WHC was determined using a centrifugation procedure at 845×*g* (Eppendorf-Centrifuge 5424). Five samples per condition were measured and each condition was repeated three times. The WHC of WPI microparticles after hydration at room temperature for 3 h was 3.55 g water/g powder, which gave 3.83 g water/g protein when taking the measured protein concentration of the microparticles into account. The WHC increased to 5.92 g water/g powder (6.38 g water/g protein) after the dispersion was heated at 90 °C for 30 min.

Table 1. Physical properties of WPI microparticles prepared on a laboratory scale.

Properties	**Values**[a]
Protein concentration (% w/w)	92.7 ± 1.2
Density (g/cm^3)	1.3 ± 0.0
Particle size distribution by diameter (*μm*) ($d_{0.1}$–$d_{0.9}$)	
Unswollen microparticles	22 ± 0 – 128 ± 1
Freshly dispersed microparticles	31 ± 1– 176 ± 1
Dispersed microparticles after 1 h	33 ± 1 – 192 ± 2
Dispersed microparticles after 24 h	33 ± 1 – 207 ± 3
Heated dispersed microparticles	35 ± 1 – 231 ± 3
Average microparticle size by diameter (*μm*) ($d_{4,3}$)	
Dry microparticles	70 ± 1
Freshly dispersed microparticles	97 ± 1
Microparticles after 1 h immersion	105 ± 1
Microparticles after 24 h immersion	114 ± 1
Heated dispersed microparticles	125 ± 1

[a] Average ± standard deviation.

2.4. Production of high-protein model product

Three types of model product were prepared:

- Product A: a gel made from a solution of WPI only.
- Product B: a gel made from a dispersion of WPI microparticles in a WPI solution.
- Product C: a gel made from a dispersion of WPI microparticles in a polysaccharide continuous phase.

Product A allowed us to study the hardening in a single phase system; product B allowed us to investigate the hardening in a multiphase protein product. Hardening in a multiphase system was also investigated with product C, in which a polysaccharide (an LBG−XG mixture) was the matrix. The concentrations in all products are listed in Table 2.

Table 2. Composition of model products.

Variant codes	WPI (% w/w)	WPI microparticles (% w/w)	LGB (% w/w)	XG (% w/w)	Total protein concentration (% w/w)
A1	20	−	−	−	20
A2	15	−	−	−	15
B1	17.5	2.5	−	−	20
B2	12.5	7.5	−	−	20
B3	12.5	2.5	−	−	15
B4	7.5	7.5	−	−	15
C1	−	20	0.6	0.6	20
C2	−	15	0.6	0.6	15
C3*	−	−	0.75	0.75	0

* C3 was the matrix for C1.

The samples for the compression tests were prepared as follows. Product A was prepared by dissolving WPI powder in water. The solution was then stirred at room temperature for 2 h and kept at 4 °C while stirring overnight. The WPI solution was centrifuged in 50-ml centrifuge tubes at 78×*g* for 10 min (20 °C) to remove air bubbles. Cylindrical Teflon tubes (diameter 20 mm, length 100 mm) were used to form gels with a uniform cylindrical shape. The WPI solution was poured into the tubes, which were then tightly sealed. The tubes were clamped in a rotating device set at 30 rpm and immersed in a water bath set at 90 °C for 30 min. The tubes were then cooled in an ice−water mixture for 30 min. The resulting gels were carefully removed from the tubes using a cylindrical plunger. The gel was cut with a wire cutter into sections 20-mm long. This resulted in cylindrical gel sections with a diameter/height ratio of 1. These gel sections were tightly wrapped with stretch-plastic foil. This procedure resulted in a number of samples for each variant of product A, which were stored at 20 °C and evaluated at various times within 8 days. The first measurement was done after storing the samples for 2 h at 20 °C; this was defined as time 0.

Product B was prepared by dispersing WPI microparticles in a WPI solution. The dispersion was stirred for 30 min before pouring the dispersion into the cylindrical tubes. The remaining procedures were the same as those for product A. However in this case, rotation of the tubes during heating was important to prevent sedimentation of the WPI microparticles and to retain an even distribution over the product. The homogeneity of the distribution was monitored visually. Product C was prepared by first preparing the LBG−XG mixture. LBG was dissolved in water and stirred at room temperature for at least 1 h. The solution was heated at 80 °C for 30 min in a water bath, followed by cooling to room temperature while stirring. XG was dispersed in the LBG solution while mechanically stirring for 1 h at room temperature. Finally, the WPI microparticles were dispersed in the LBG−XG mixture and mechanically stirred for 1 h. The final dispersion was centrifuged at 78×*g* for 10 min (20 °C) to remove the air bubbles. The remaining steps were the same as those for other products. All variants contained 0.02% w/w sodium azide as a preservative.

For the rheological measurements, the preparation of the WPI solution, the dispersion of WPI microparticles in a WPI solution, and the dispersion of WPI microparticles in an LBG−XG mixture was the same as described above, except that no preservative was added.

2.5. Large deformation tests

All products were subjected to uniaxial compression tests (Instron 5564), unless mentioned otherwise. A sample was placed on a lubricated stainless steel base and compressed with a lubricated stainless steel cylindrical probe with a diameter of 50 mm. A load cell of 2000 N was used. The sample was compressed at a speed of 1 mm/s until 80% compressive strain; the output data were recorded every 10 ms. On average, the number of samples (n) of each product variant being compressed was 7, unless indicated otherwise. The true stress and true strain were determined from the force−distance data provided by Bluehill® material testing software (Instron). The true stress and true strain of the samples at fracture were determined at the first maximum true stress along the true strain, just before the true stress started to drop. Young's modulus of the sample was determined by the slope of true stress at true strains of 0.3−1% for products A and B, and at true strains of 4−8% for product C because of data instabilities below 4% in this product. Young's modulus was used to represent the hardness of the gel.

2.6. Small deformation tests

Textural changes were also investigated using rheological measurements. The samples were prepared *in situ* in the rheometer (AntonPaar Physica MCR301) using a Coutte geometry (CC17). The bob and cup were heated to 90 °C and kept at this temperature for at least 15 min. A WPI solution, a dispersion of WPI microparticles in the WPI solution, or a dispersion of WPI microparticles in an LBG-XG mixture was placed in the cup. The bob was then lowered to 3 mm. This position was chosen to accommodate movement of the bob during measurement. The solutions or dispersions were equilibrated at 90 °C for 10 min, and then kept at this temperature for an additional 30 min. The resulting sample

was cooled down to 20 °C at a rate of 2 °C/min and kept at this temperature for 30 min. A constant strain of 0.01% at a frequency of 1 Hz was applied during heating and cooling. After cooling, the sample was kept in the geometry at 20 °C for 72 h, while a constant strain at 0.1% and frequency of 1 Hz was applied. The changes in storage modulus (G') and loss modulus (G'') were recorded every minute, but plotted every hour.

3. Results

3.1. Large and small deformation properties of product A

Fig. 1 shows typical curves obtained from compression tests of variants of product A, i.e. A1 and A2, containing 20% w/w and 15% w/w native WPI, respectively. The true stress on A1 increased linearly with the true strain up to a maximum level and then dropped quickly. The true stress of A2, with a lower protein concentration, increased more slowly, but more than linearly with the true strain. The changes in Young's moduli of product A over time are depicted in Fig. 2. Both variants hardened for a limited period of about 3 days only. The hardening increase was larger in the case of A1. Fig. 3 (left) shows that the fracture stress of A1 increased in the first 3 days and then stabilized or even decreased slightly. This change was in line with the change in Young's modulus. The fracture stress of A2 remained constant for 8 days of storage. This change was not in line with the change in Young's modulus. This could be due to a subtle change in the hardness, which did not significantly affect the fracture stress. The fracture strains of both variants were relatively constant with the storage time. The results from compression tests showed that protein gels made only from WPI hardened in the first few days, after which the hardness became constant.

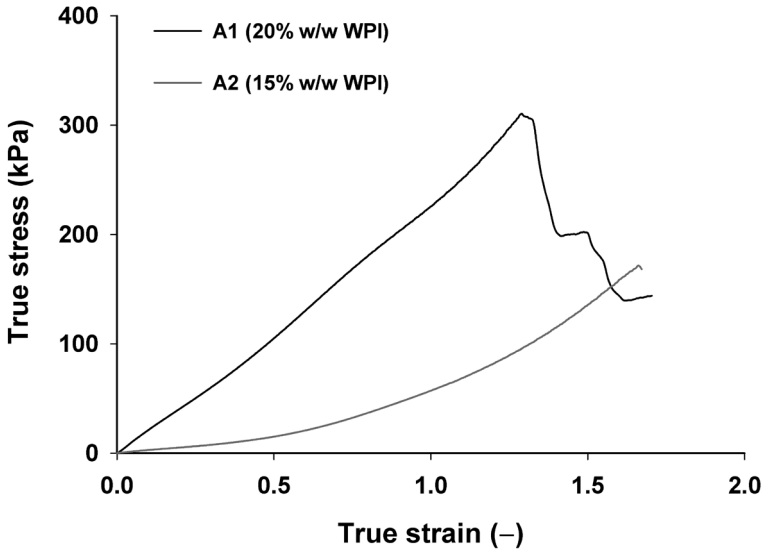

Figure 1. Typical true stress–true strain curves of A1 and A2 containing 20% w/w and 15% w/w native WPI, respectively.

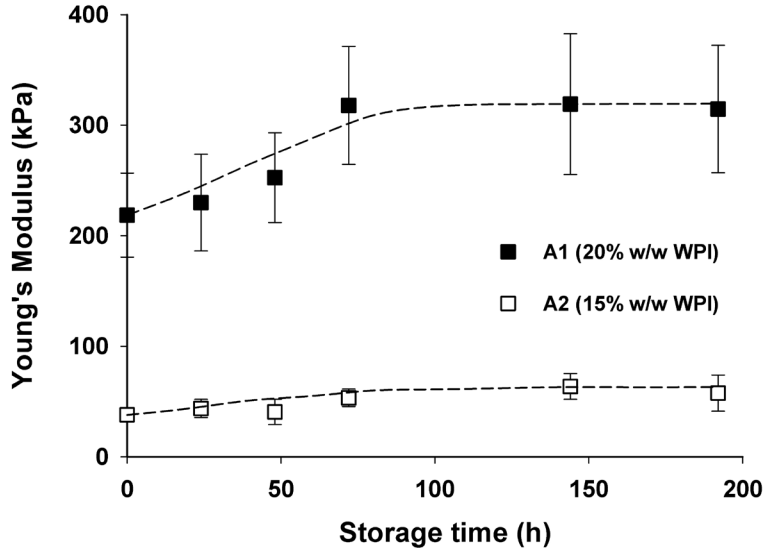

Figure 2. The changes in Young's moduli of product A over time. The lines guide the eyes.

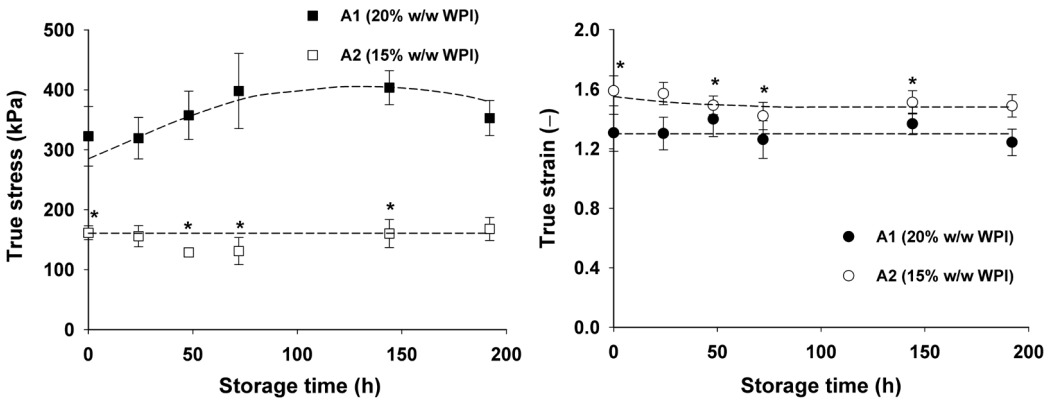

Figure 3. The changes in fracture stresses–strains of product A over time. The lines guide the eyes to the fracture trends over time. *A2, indicates $3 \leq n < 7$.

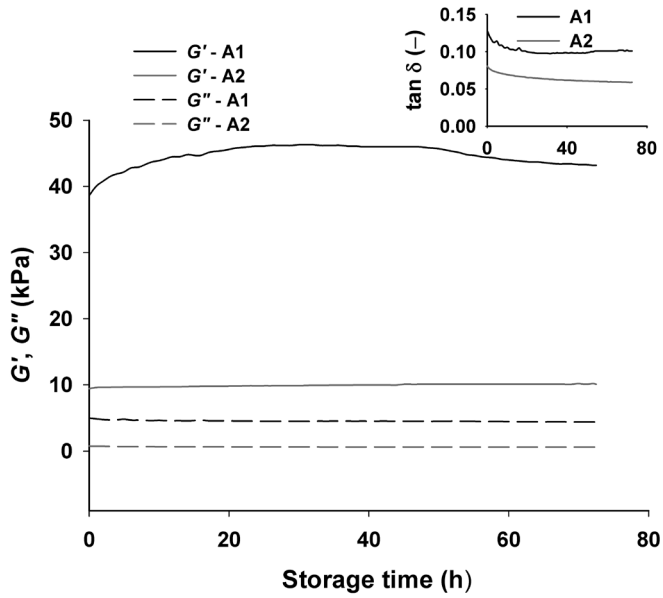

Figure 4. Storage moduli and loss moduli of product A during 72 h at 20 °C. The inset shows the damping factor (tan δ) of the product.

Fig. 4 shows the changes in the storage moduli (G') and loss moduli (G'') of product A at 20 °C over 72-h period. The G' of A1 increased for the first 30 h, after which it seemed to decrease. For A2, the G' increased throughout the time range, but this increase was small. The G'' values for both A1 and A2 tended to decrease slightly. The changes in both G' and G'' resulted in a decreasing damping factor (tan δ), indicating an increasingly solid-like

behaviour. The damping factor of A1 only decreased in the first few hours, but the damping factor of A2 decreased continuously. The change in A2 during the first 3 days at a smaller level of deformation was in line with that observed for Young's modulus in the compression test. However, this was not the case for A1.

3.2. Large and small deformation properties of product B

Fig. 5 shows typical curves obtained from the compression tests of product B. The stress−strain curve for B1 was comparable with that for A1. B2 and B3 behaved similarly as A2, except that B3 did not show a maximum true stress. Young's moduli of product B are depicted in Fig. 6. Young's modulus and its change over time was comparable with that without microparticles (A1) in case 2.5 % w/w of native WPI was replaced by WPI microparticles (B1). Lower values for Young's moduli were obtained when the amount of microparticles was increased at constant total protein concentration (B2) or when the total protein concentration was decreased (B3). However, hardening of the product took place over a longer period for B2 and B3 compared with B1, without any indication of being stable within 8 days of storage.

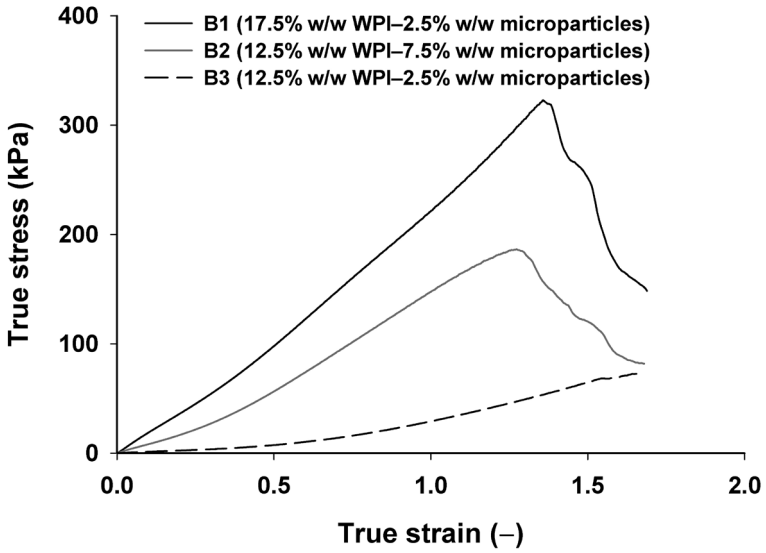

Figure 5. Typical true stress–true strain curves of product B at total protein concentration of 20% w/w (B1 and B2) and 15% w/w (B3).

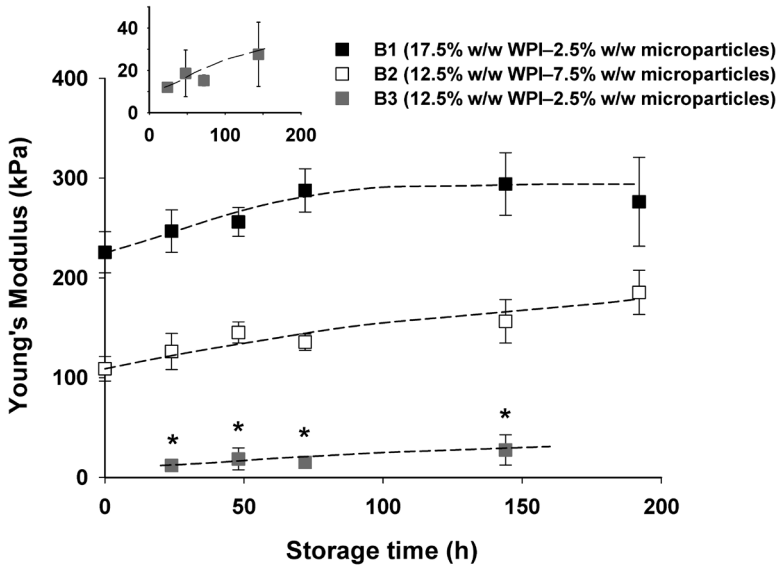

Figure 6. The changes in Young's moduli of product B over time, at total protein concentration of 20% w/w (B1 with 17.5% WPI–2.5% microparticles and B2 with 12.5% WPI–7.5% microparticles) and 15% w/w (B3 with 12.5% WPI–2.5% microparticles). The lines guide the eyes. **n* = 3. Inset is the magnification of B3.

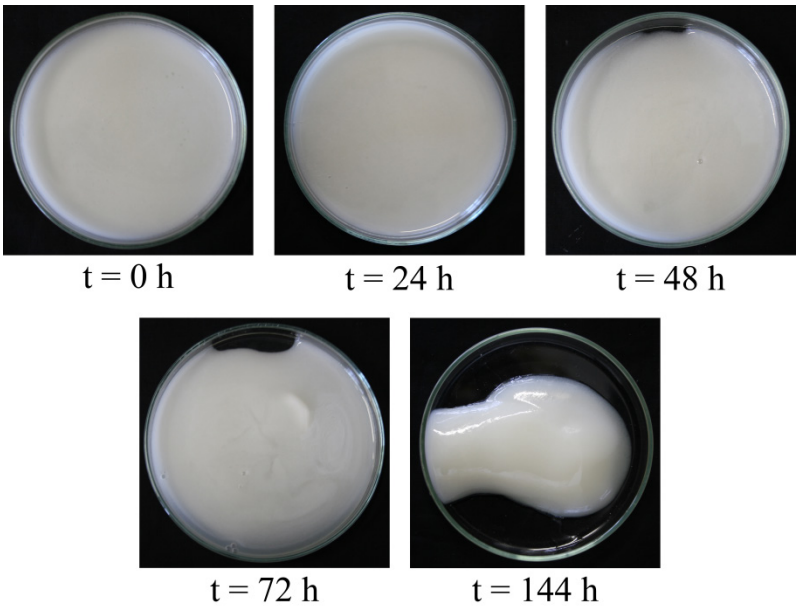

Figure 7. Visual observation of B4 (7.5% w/w WPI–7.5% w/w microparticles) until day 6 of storage at 20 °C. The samples in the Petri dishes had similar volume and all pictures were taken not more than 10 min after pouring the samples.

The use of 7.5% w/w WPI microparticles in B2 resulted in a product variant that showed more hardening over time than B1. This was also the case with B3, which contained 2.5% w/w microparticles with a total protein concentration of 15% w/w. B3 did show a clear hardening trend (Fig. 6, inset), although, it had to be considered that the values for B3 on day 0 and day 8 could not be determined because the samples of this variant were too weak. B4, which contained 7.5% w/w WPI microparticles at 15% w/w overall protein concentration, did not form a gel. Nevertheless, the consistency could be visually observed; it changed over time. Fig. 7 shows that B4 became more viscous during a 6-day storage period, which may be interpreted as being analogous to hardening.

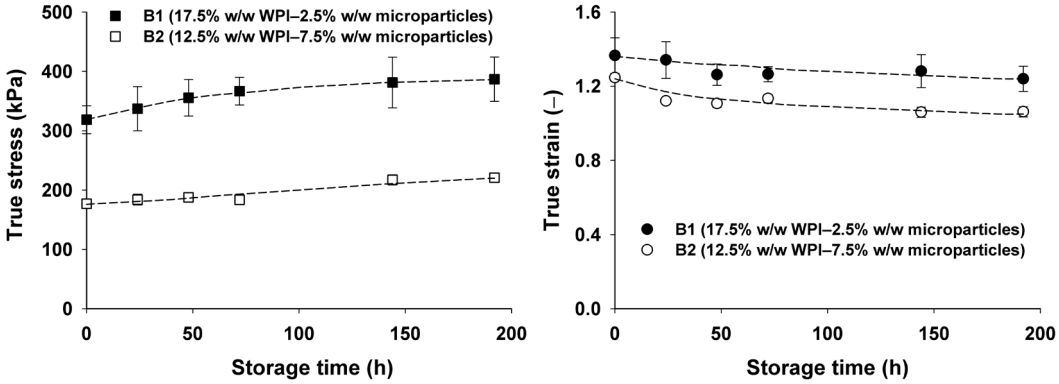

Figure 8. The changes in fracture stresses–strains of product B over time. The lines guide the eyes.

The changes in fracture stress–strain over time for product B are depicted in Fig. 8. The fracture stress of B1 increased over a longer period than its Young's modulus, i.e. it increased until day 6 and then became stable. For B2, the fracture stress increased continuously for 8 days of storage, similar to the changes in its Young's modulus over time. The fracture strains of B1 and B2 decreased slightly over time. This might indicate that the harder gel behaves as a more brittle material, therefore it becomes less stretchable and breaks at a shorter strain. No data are shown for B3 because the samples yielded maximum stresses consistently at day 6 only.

Overall, the results from the compression tests showed that a multiphase protein system hardened continuously during storage. These results were also in agreement with the changes in fracture stresses and fracture strains of the gels.

The concentration of microparticles in the product influenced the rheological properties and their changes over time (Fig. 9). The G' of B1 increased during the first 20 h and then levelled off. The G' values of B2 and B4 increased only during the first 5 h and then decreased again. The G'' values for all B product variants decreased in time. The inset in Fig. 9 shows the damping factor (tan δ). The damping factor decreased for B1 in the first few hours, indicating a more pronounced solid-like behaviour, and then remained constant. The rheological behaviour of product B1 was similar to that of A1. This similarity might be attributed to the relatively small amount of WPI microparticles applied (2.5% w/w) in a concentrated WPI matrix (17.5% w/w). Therefore, the effect that the particles have on the total material was limited. The damping factor for B2 and B4 decreased continuously, implying a continuous hardening process. The change in the damping factor for B2 was in line with the change in large deformation properties observed in the first 3 days, both Young's modulus and fracture properties.

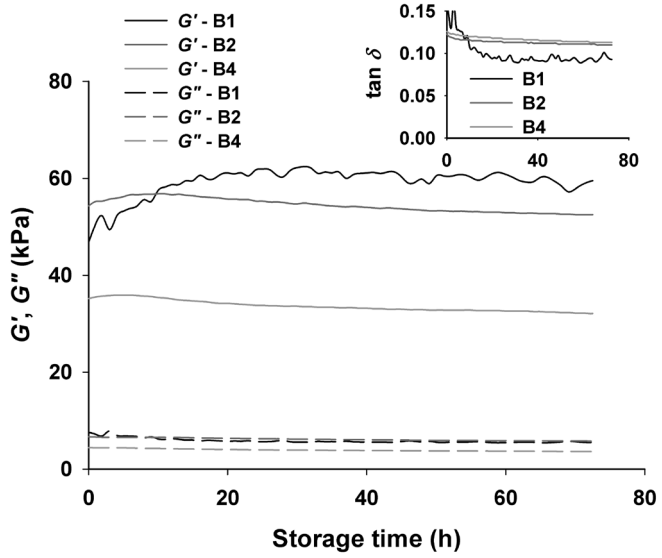

Figure 9. Storage moduli and loss moduli of product B for 72 h at 20 °C. The inset is the damping factor (tan δ).

3.3. Large and small deformation properties of product C

Fig. 10 shows some typical true stress–true strain curves for product C. The polysaccharide matrix (LBG–XG mixture (C3)) yielded a strong non-linear increase in the stress. At the maximum stress, the stress then decreased suddenly, indicating a kind of yielding, shown by the fact that the sample was seen to be squeezed out of the compression probe. The yielding is indicated by the dashed line for C3 in Fig. 10. When WPI microparticles were dispersed in the continuous phase, the stress–strain curve changed. Product C2, which contained 15% w/w total protein concentration, showed a relatively linear increase in the stress with the strain. C1 with 20% w/w protein concentration showed a steep initial increase in stress, followed by a plateau. At high strains, C1 showed a non-linear increase in stress.

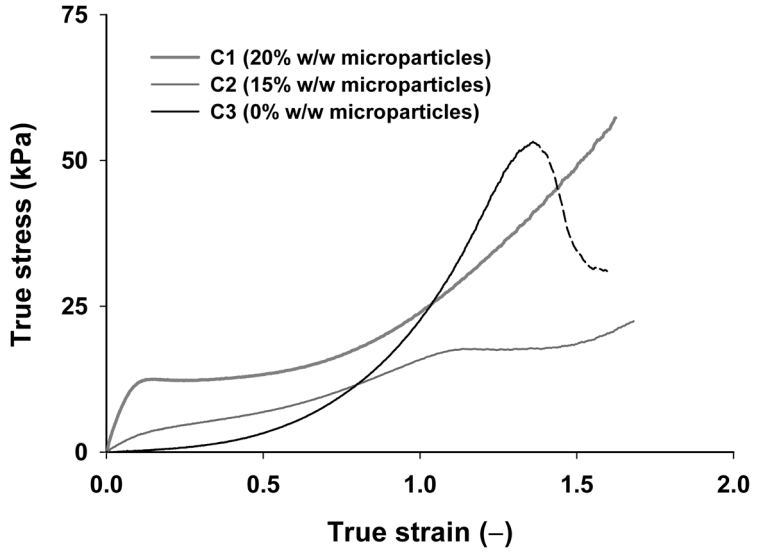

Figure 10. Typical true stress–true strain curves of product C at a total protein concentration of 20% w/w (C1), 15% w/w (C2), and 0% w/w (the polysaccharide matrix, C3).

Fig. 11 shows the Young's moduli of product C versus storage time. As expected from the true stress–true strain curves, the Young's modulus of the matrix was the lowest, followed by C2 with 15% w/w protein concentration, and C1 with 20% w/w protein concentration. The Young's modulus of the matrix (C3) showed some minor variations over time, which

were not significant. Generally, the Young's modulus of C3 was rather stable over time. The modulus of C2 increased slowly, especially in the first 3 days. C1 showed more complex behaviour, but its modulus roughly increased over time. The changes in products C1 and C2 showed that the addition of microparticles resulted in hardening over longer times, even if the property of the matrix alone (C3) did not change over time.

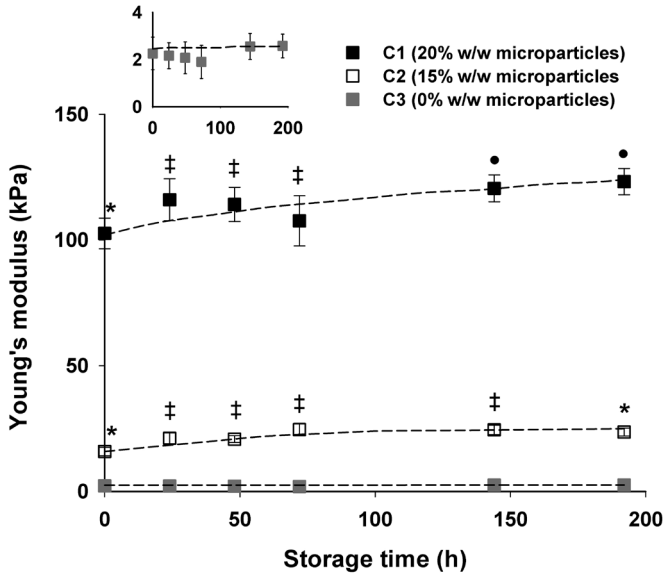

Figure 11. The changes in Young's moduli of product C over time, at a total protein concentration of 20% w/w (C1), 15% w/w (C2) and 0% (the polysaccharide matrix, C3). The lines guide the eyes. •, * and ‡ indicate n = 2, 3 and 4, respectively. The inset is the magnification of C3.

Fig. 12 shows that the G' values increased over time, and the G'' values remained constant for all product variants. The addition of microparticles to the matrix resulted in higher G' and G'' values. This increase is indicative of a filled gel with a dispersed phase that has a higher modulus than the continuous phase, and has good interaction with the continuous phases[12-14]. The insets show that the damping factors decreased over time for all variants. This result was in line with the results obtained for the large deformation tests for C1 and C2, but not for C3. This difference might be attributed to the nature of the LBG–XG mixture that develops more physical cross-links over time[15], and is only observed at small-scale deformation.

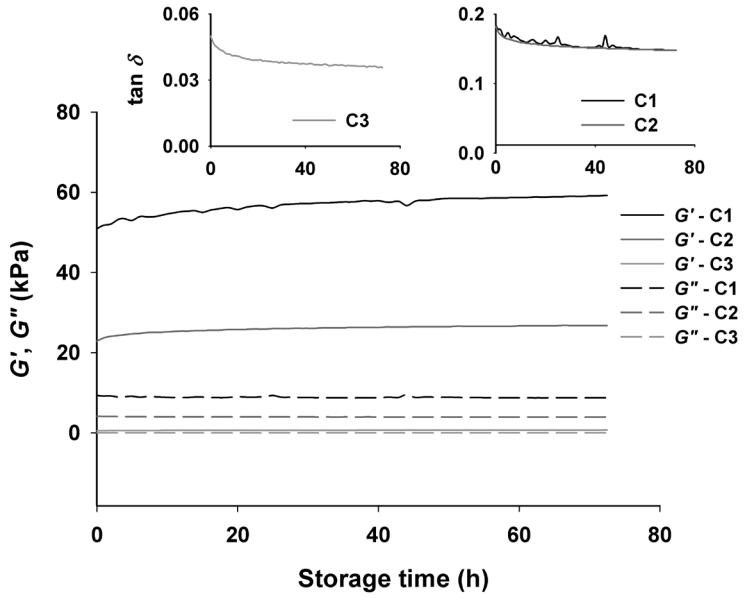

Fig. 12. Storage moduli and loss moduli of product C for 72 h at 20 °C. The insets are the damping factors (tan δ).

4. Discussion

Changes in the textural properties of high-protein gels were evaluated with large-scale deformation tests in terms of Young's modulus (hardness) and fracture properties, and with small-scale deformation tests in terms of the damping factor. From these evaluations, we derive the following conclusions:

- High-protein gels made only from WPI (a single phase protein system) harden in the first few days of storage and then become stable.
- High-protein gels containing WPI microparticles (a multiphase system) harden over a longer time. The composition of the continuous phase (WPI or LBG–XG mixture) does not matter that much.

Previous studies suggested a mechanism of hardening for a concentrated WPI matrix based on protein aggregation through disulphide bond formation[10, 16, 17]. In this study, the formation of disulphide bonds might occur to a certain extent during gel preparation through heat treatment, but could continue if there are free thiol groups remaining after

the heating step. Further disulphide bonds formation during storage would then induces hardening over time. If so, it explains why changes in the gel properties could be observed during the first few days of storage for gels made from WPI only.

Products containing WPI microparticles hardened throughout the storage period tested. It is possible that at longer time scales than used here, the products properties would become stable. Obviously, another mechanism than changes in the protein phase only, such as the formation of additional disulphide bridges, plays a role. We suggest that water migration between the different phases is responsible for hardening over a prolonged period. Water migrating from the matrix to the particles will lead to an increase in the local protein concentration in the matrix resulting in a firmer matrix. Water redistribution within the particles would depend on differences in water activity between the phases, which in this case might be related to differences in protein concentration. In the polysaccharide matrix, separation between the dispersed protein phase and the continuous polysaccharide phase would have an additional effect on hardening. The processes described above are schematically depicted in Fig. 13.

Fig. 13 (left) shows a system without particles in which WPI is well dissolved in water initially. Upon heating, the protein is denatured, followed by aggregation. The aggregates hold a certain amount of water, which will depend on the number of disulphide linkages within the aggregate. When the system contains WPI microparticles (Fig. 13, centre and right), the particles absorb some water from the continuous phase more or less instantaneously. Upon heating, more water is absorbed, which results in an increased local concentration of WPI or further phase separation between the particles and the LBG–XG mixture in the matrix. This process may continue over time after the heating step because water absorption into the microparticles depends on time and temperature. Therefore, this could explain the continuous changes in the gel properties observed for 8 days of storage.

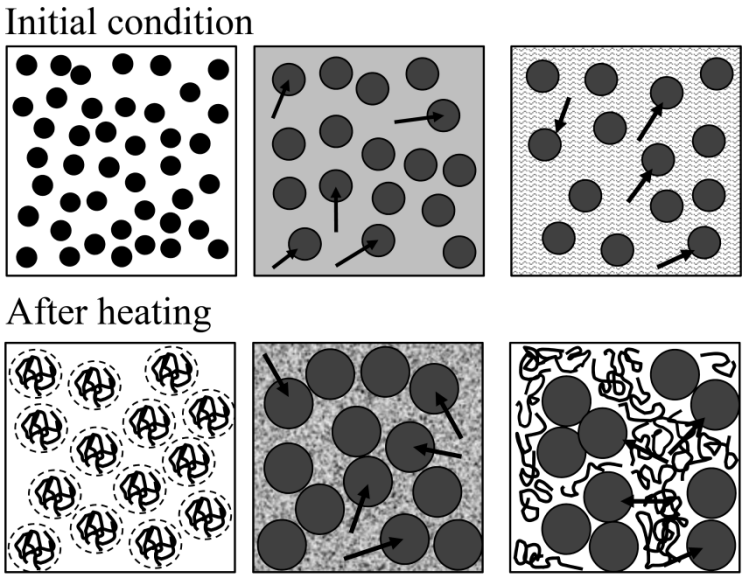

Figure 13. Schematic overview of moisture and/or phase separation in the system containing only WPI (left) and in the system containing WPI microparticles in WPI solution (centre) or WPI microparticles in an LBG–XG mixture (right). The arrows indicate the direction of water migration.

It has already been reported that an increase in hardness based on fracture stress can continue for 50 days for protein bars made with calcium caseinate (CaCas) or milk protein concentrate (MPC)[1, 9]. These bars normally contain sugar or polyol as additional components and do not undergo heat treatment during preparation[1, 6-9]. The absence of a heating step in the preparation could explain the longer period during which hardening occurs.

We thus conclude that hardening over time in products containing WPI microparticles is caused by slow migration of water. This migration induces changes in the mechanical and rheological properties. Stopping or shortening the hardening process in high-protein gels containing microparticles might be achieved by accelerating the moisture transport (and thus avoiding the slow migration over time) and/or the phase separation in the system during the production process. This can be done, for example, by applying a heating step to accelerate the water redistribution to induce all possible changes at the early stage between post manufacturing and product distribution. Another method could be to stop

moisture migration happening. This can be done, for example, by modifying the production of microparticles in such a way that the particles cannot absorb water. This can be achieved by heavily cross-linking the particles or their surface, in which the elastic stress induced by the crosslinks reduces the amount of water that can be absorbed.

5. Conclusion

The increase in hardness over time was investigated in protein gels from WPI only and in gels in which part of the protein was present as microparticles. The products that contained WPI microparticles showed lower initial hardness, compared with the products originating from native WPI only. However, these products showed hardening for a longer period. Prolonged hardening was also observed with products in which WPI microparticles were dispersed in a mixture of LBG–XG.

We conclude that continuous hardening over time cannot be explained by a change in the protein phase only, for example, through the creation of additional bonds. Other effects do play a role; slow water migration from the continuous phase towards the particles may well be an important factor. Due to water migration, re-ordering will take place over a longer period. Better control over the hardening process can be achieved by accelerating the re-ordering and transport during processing, for example, by heating. This could stabilize the products over a shorter period of time.

References

1. Loveday, S. M., Hindmarsh, J. P., Creamer, L. K., & Singh, H. (2009). Physicochemical changes in a model protein bar during storage. *Food Research International*, *42*, 798-806.

2. Luhovyy, B. L., Akhavan, T., & Anderson, G. H. (2007). Whey proteins in the regulation of food intake and satiety. *Journal of the American College of Nutrition*, *26*(6), 704S-712S.

3. Hayes, A. & Cribb, P. J. (2008). Effect of whey protein isolate on strength, body composition and muscle hypertrophy during resistance training. *Current Opinion in Clinical Nutrition and Metabolic Care*, *11*(1), 40-44.

4. Campbell, W. W. & Leidy, H. J. (2007). Dietary protein and resistance training effects on muscle and body composition in older persons. *Journal of the American College of Nutrition*, *26*(6), 696S-703S.

5. Labuza, T. P., Zhou, P., & Davis, L. (2007). Whey to go. *The World of Food Ingredients* Vol. October/November, 108-112.

6. Li, Y., Szlachetka, K., Chen, P., Lin, X., & Ruan, R. (2008). Ingredient characterization and hardening of high-protein food bars: an NMR state diagram approach. *Cereal Chemistry*, *85*(6), 780-786.

7. Liu, X., Zhou, P., Tran, A., & Labuza, T. P. (2009). Effects of polyols on the stability of whey proteins in intermediate-moisture food model systems. *Journal Agricultural Food and Chemistry*, *57*, 2339-2345.

8. McMahon, D. J., Adams, S. L., & McManus, W. R. (2009). Hardening of high-protein nutrition bars and sugar/polyol-protein phase separation. *Journal of Food Science*, *74*(6), E312-E321.

9. Loveday, S. M., Hindmarsh, J. P., Creamer, L. K., & Singh, H. (2010). Physicochemical changes in intermediate-moisture protein bars made with whey protein or calcium caseinate. *Food Research International*, *43*, 1321-1328.

10. Zhou, P., Liu, X., & Labuza, T. P. (2008). Effects of moisture-induced whey protein aggregation on protein conformation, the state of water molecules, and the microstructure and texture of high-protein-containing matrix. *Journal of Agricultural and Food Chemistry*, *56*(12), 4534-4540.

11. Purwanti, N., Moerkens, A., van der Goot, A. J., & Boom, R. (2012). Reducing the stiffness of concentrated whey protein isolate (WPI) gels by using WPI microparticles. *Food Hydrocolloids*, *26*(1), 240-248.

12. van Vliet, T. (1988). Rheological properties of filled gels: influence of filler matrix interaction. *Colloid Polymer Science*, *266*, 518-524.

13. Yost, R. A. & Kinsella, J. E. (1992). Microstructure of whey protein isolate gels containing emulsified butterfat droplets. *Journal of Food Science*, *57*(4), 892-897.

14. Sala, G., van Aken, G. A., Stuart, M. C., & van de Velde, F. (2007). Effect of droplet-matrix interactions on large deformation properties of emulsion-filled gels. *Journal of Texture Studies*, *38*, 511-535.

15. Sandolo, C., Bulone, D., Mangione, M. R., Margheritelli, S., Di Meo, C., Alhaique, F., Matricardi, P., & Coviello, T. (2010). Synergistic interaction of locust bean gum and xanthan investigated by rheology and light scattering. *Carbohydrate Polymers*, *82*, 733-741.

16. Zhou, P. & Labuza, T. (2007). Effect of water content on glass transition and protein aggregation of whey protein powders during short-term storage. *Food Biophysics*, *2*(2), 108-116.

17. Zhou, P., Liu, X., & Labuza, T. P. (2008). Moisture-induced aggregation of whey proteins in a protein/buffer model system. *Journal of Agricultural and Food Chemistry*, *56*(6), 2048-2054.

Chapter 6

Reversing the migration of hard-sphere particles under torsional flow

Abstract

Dispersions of glass spheres in a locust bean gum–xanthan gum mixture at volume fractions (ϕ) of 0.025, 0.02, 0.075, and 0.1 were subjected to shear flow for 5, 15, 30, and 60 min in a cone–cone shearing device. At ϕ = 0.025 and 0.05, the particles migrated outward to the rim of the device. Higher particle volume fractions also resulted in outward migration when sheared for 5 min. However, after prolonged shearing, particles clustered into concentric rings interspaced with regions with less particles. The rings seemed to contract inward, forming a region with concentrated particles in the centre. A theoretical analysis was performed on the driving forces in the system. The driving forces due to concentration, viscosity, and curvature gradients lead to outward migration, but the driving force due to particle interactions at higher particle volume fractions could lead to inward migration.

This chapter has been submitted for publication.

1. Introduction

Particle migration in flowing dispersions has been studied intensively since the 1960s, with emphasis on Poiseuille flow[1, 2] and torsional flow[3], using Newtonian or viscoelastic fluids. Later, Leighton and Acrivos (1987)[4] studied concentrated suspensions of spheres in Newtonian fluids using torsional flow in a Coutte device. They introduced the concept of shear-induced migration based on hydrodynamic diffusion to explain the viscosity changes observed by Gadala-Maria and Acrivos (1980)[5]. Outward particle migration was reported in a dispersion of 9% v/v methyl methacrylate particles in polyisobutylene (PIB) using a cone-plate system[3]. Karis et al. (1984)[6] reported inward migration of a single particle dispersed in a PIB solution at low shear rate in a parallel plate system. This was observed for particles with different radii (141-275 μm). They hypothesized that a critical radius distance (r_c) exists at moderate shear rate: a particle of 200 μm in PIB solution moved inward at $r < r_c$ and migrated outward at $r > r_c$[7].

Since the 1990s, more studies on particle migration have been conducted and some have included numerical simulations of particle migration[8-10]. Phillips et al. (1992)[8] modified the theory proposed by Leighton and Acrivos (1987)[4] to describe the profiles of particle concentration over time using Poiseuille and torsional flow. Shauly et al. (1998)[9] proposed a phenomenological model that accommodates polydisperse suspensions. Kim et al. (2008)[10] investigated the accuracy of the models by Phillips et al. (1992)[8], and predicted that particles migrate outward at low volume fractions, with a particle-free zone in the centre, no migration at $\phi = 0.5$, and particles migrate inward at $\phi = 0.6$ in parallel plates geometry.

Another phenomenon observed in the shear-induced migration of particles was the occurrence of concentric rings[11-14]. Graham et al. (1991)[11] found these concentric rings with a bidisperse concentrated suspension of spheres, with size ratio of 1:4, dispersed in Newtonian oil and sheared in a Coutte geometry. The rings contained the larger spheres, interspaced with fluid and the smaller spheres. Feng and Joseph (1996)[12] observed the formation of concentric rings with polystyrene spheres of 250–850 μm, 2–10% v/v

dispersed in viscoelastic liquids, which were sheared in a parallel plate device. The ring formation started from strings of large spheres that aligned with the flow. At later stages, the rings absorbed the small spheres that were still in the surroundings, leaving a clear liquid between the rings after 20 min of shearing. Kim (2001)[13] observed concentric rings with 10–30% v/v polymethylmethacrylate spheres of 550 μm, dispersed in a polymer solution, sheared in between parallel plates. At longer times, a particle-free region was observed in the centre.

The phenomena described above might also be relevant for food applications. Recent studies showed that separation of gluten from starch (particles) in wheat dough was possible by applying a torsional flow in a cone–cone shearing device[15, 16]. The separation mechanism was explained by a two-step mechanism: first aggregation of the gluten forming larger gluten aggregates, followed by migration of the aggregates to the centre of the cone[16]. Another study showed that the alignment of particles by torsional flow in the direction of the flow might lead to a fibrous structure from a micellar suspension of calcium caseinate[17]. By understanding the behaviour of particles under flow, better insight on the development of structure in foods is generated. Thus, it is interesting to relate the migration properties found for (model) non-food systems to food applications.

This paper studies particle migration under torsional flow in a cone–cone shearing device, in which the generated flow is simple shear flow. A mixture of locust bean gum (LBG) and xanthan gum (XG) was used as the continuous phase. This mixture was chosen because it is widely used in food applications for structuring, stabilizing, or improving functional properties[18, 19]. The LBG−XG mixture can be molten and re-solidified through temperature changes. In the liquid state, the mixture behaves as a viscoelastic material. Glass spheres were used as dispersed model particles. This study investigates how the migration of the glass spheres depends on the particle volume fraction and processing time. The (currently available) theories of Phillips et al. (1992)[8] and Khrisnan et al. (1996)[20] are used to explain the observed phenomena.

2. Materials and methods

2.1. Materials

A mixture of LBG (Degussa, France) and XG (derived from *Xanthomonas campestris*; Fluka, France) was used as the continuous phase. The mixture was prepared by first dispersing LBG slowly in water (Milli-Q, 18.2 MΩ.cm at 25 °C, total oxidizable carbon <10 ppb; Millipore, France). The LBG solution was stirred using a magnetic stirrer for at least 2 h and then, heated at 80 °C for 30 min to solubilize the LBG. The LBG solution was cooled to room temperature while stirring with a magnetic stirrer. After cooling, the LBG solution was stirred with a stirring blade connected to an overhead mixer and XG was slowly dispersed into it. The LBG−XG mixture was stirred for an additional 2 h and kept at room temperature before use. The continuous phase thus contained a mixture of 0.6% w/w LBG and 0.6% w/w XG (pH 5.9).

Non-porous, hydrophilic, spherical glass spheres with an average particle size ($d_{4,3}$) of 76.63 μm and a density of 2.48 g cm^{-3} were used as the dispersed phase. The particles had a distribution size ($d_{0.1}$−$d_{0.9}$) of 54.8−101.8 μm. The particle concentrations, expressed as the volume fraction (ϕ), were 0.025, 0.05, 0.075, and 0.1. The particle dispersions were prepared by mechanical stirring for 1 h. The pH of the particle dispersions was 7.04, 7.9, 8.55, and 9.0 for volume fractions of 0.025, 0.05, 0.075, and 0.1, respectively.

2.2. Rheology

The viscoelasticity of the continuous phase influences the behaviour of dispersed particles under flow[3, 21-24]. Therefore, the continuous phase was characterized at 80 °C in a rheometer (Anton Paar 301). A plate–plate geometry with a diameter of 50 mm (PP-50) was used with a gap distance of 2 mm; shear rate sweeps of 0.1−300 s^{-1} were applied. Twenty-five measurement points per shear rate with a duration of 10 s per point were recorded for shear rates below 1 s^{-1} to avoid transient effects, above which 10 measurement points per shear rate with a duration of 5 s per point were recorded. A transient viscosity experiment was also performed to check the changes of viscosity with

time. Shear rates of 6.49 s^{-1} and 64.93 s^{-1} were applied for 5 and 60 min, respectively, both at 80 °C.

Prior to each measurement, the plate–plate geometry was heated at 80 °C for 15 min. During the measurement, the sample was covered with paraffin oil to avoid water evaporation. The measurements were done with duplicate batches of LBG−XG mixture; each batch was measured in triplicate.

2.3. Shearing device

The in-house shearing device follows the concept of cone and plate geometry in a rheometer. This is a closed device that has a combination of simple shear flow and large shear stresses. The type of the shearing device used in this study has been described by van der Zalm (2011)[25]. The schematic drawings of the shearing device and of the cone–cone part of the device are depicted in Figs. 1 and 2, respectively. The bottom cone, which is in full contact with the sample, has a diameter of 135 mm. The bottom cone is the rotating part; the upper cone is static. The surfaces of the cones are grooved to prevent slippage of the material. The cones are temperature controlled with circulating water. The shearing device is connected to a Brabender Do-corder 330 (Brabender OHG, Duisburg, Germany) to enable speed control and recording of the temperature.

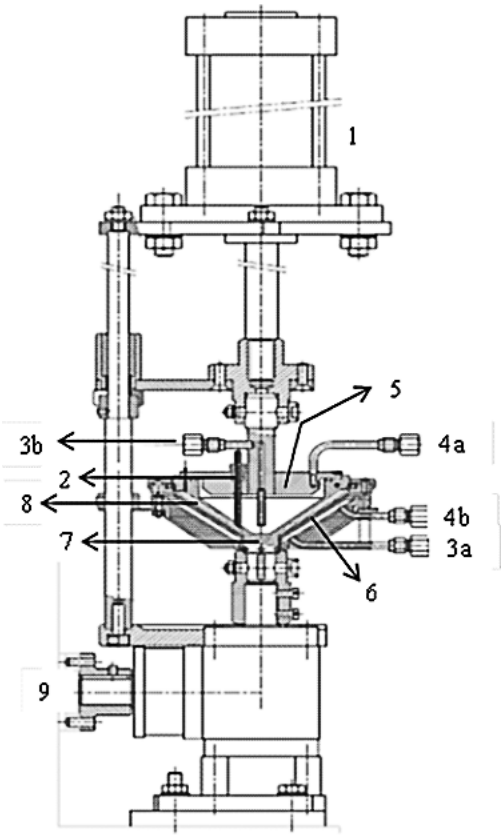

1. Load cell
2. Thermocouple

3a, b. Water inlet circulation

4a, b. Water outlet circulation

5. Variable, stationary cone
6. Rotating cone
7. Axis gap
8. Sample
9. Connection to Brabender

Figure 1. Schematic drawing of the shearing device.

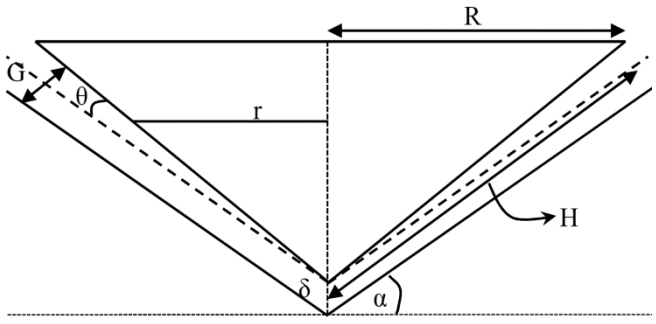

r = radius
R = the maximum radius
H = hypotenuse
δ = axis gap (2 mm)
G = gap along hypotenuse
α = angle of the bottom cone (37.5 °)

Figure 2. Schematic drawing of the cone–cone in the shearing device.

The axis gap between the bottom and the upper cones used in this study was 2 mm and the angle between the two cones was 2.5°. Therefore, the shear rate is not constant, but slowly increases with the distance from the axis. The shear rate profile, calculated using Eq. (1), is depicted in Fig. 3 by taking a rotation speed of 50 rpm.

$$\dot{\gamma} = \frac{2\pi N r}{2H\, sin([1/2]\theta) + \delta\, cos\alpha / cos([1/2]\theta)} \quad (1)$$

where N is number of rotations per second. Using the angles for the chosen configuration, the denominator in Eq. (1) can be simplified to $x_1 r + x_2 \delta$, where x_1 is 0.57 and x_2 is 0.8.

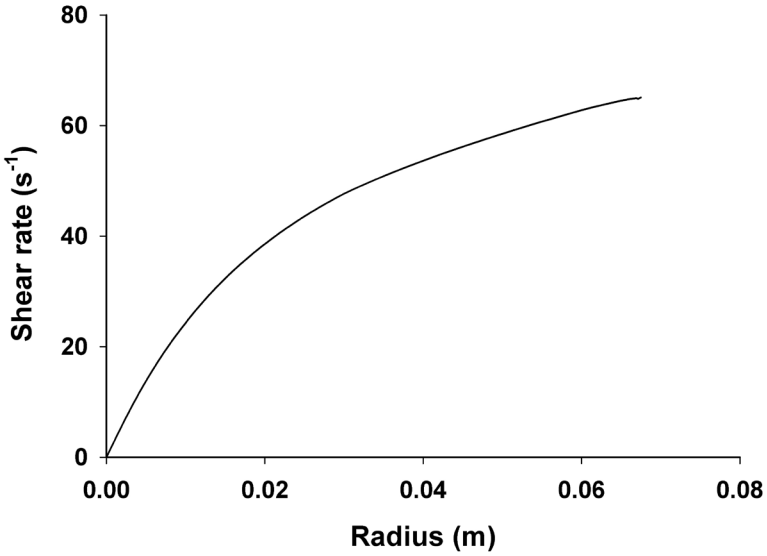

Figure 3. Shear rate profile in the shearing device.

2.4. Shearing process

The shearing device was first heated to 80 °C. The particle dispersion was then placed in the bottom cone and it was closed hydraulically with the upper cone using a pressure of 2.5×10^5 Pa. The particle dispersion was pre-sheared at 5 rpm (shear rate of 6.5 s^{-1} at a radius of 67 mm) for 5 min and then sheared at 50 rpm (shear rate of 64.9 s^{-1} for the same distance). The shearing times at this speed were 5, 15, 30, and 60 min. After shearing, the shearing device was cooled to 10 °C by circulating water at 4 °C for 15 min to fix the arrangement of the particles in the continuous phase. After cooling, the solidified sample was carefully taken out of the device. It was placed on transparent plastic with a circular frame underneath. This circular frame has a radius of 85 mm, which is similar to the hypotenuse of the bottom cone. Pictures of the samples were taken with a Canon EOS

30D camera equipped with Canon EF-S 18–55 mm lens. The shearing experiments for each volume fraction were done in duplicate.

To check the effect of gravity, the particle dispersions were pre-sheared at 5 rpm for 5 min and kept inside the shearing device without further shearing for 60 min. The further procedures for the samples were similar to those in the shearing process.

2.5. Determination of the radial particle distribution

To determine the radial particle distribution in the shearing device, the local particle volume fraction was measured with the total solids fraction of particles as a function of position. Various zones of each sample were cut into pieces, immersed in liquid nitrogen and then stored in the freezer prior to determination of the solid fractions. These pieces were dried in the oven at 105 °C for 5 h. The weight ratio between the dry and wet materials was used to calculate the total solids fraction. The results were calibrated against known particle volume fractions dispersed in the continuous phase.

The grayscale intensity of a sample's picture along its radial distance was used for a qualitative impression of the particle distribution. The grayscale intensity of a sample's picture was scanned radially every 1° throughout the sample (Image J, free software) and was then averaged for all angles. The minimum and maximum grayscale intensity in each initial volume fraction was determined to normalize the intensity values. This normalization was done by subtracting intensity values by the minimum intensity and then dividing by the maximum intensity.

3. Results

3.1. Rheology of the continuous phase

Fig. 4 shows the viscosity and the Weissenberg number of the LBG−XG mixture with increasing shear rates. The continuous phase was shear thinning at 80 °C. The viscosity fitted best with the Carreau-Yasuda model for the first Newtonian plateau and power law region (Eq. 2).

$$\eta = \frac{\eta_o}{(1+(k\dot{\gamma})^b)^{1-(c/b)}} \quad (2)$$

where η_0 = 20.4 Pa s, k = 2.3 s, b = 0.5, and c = 0.37.

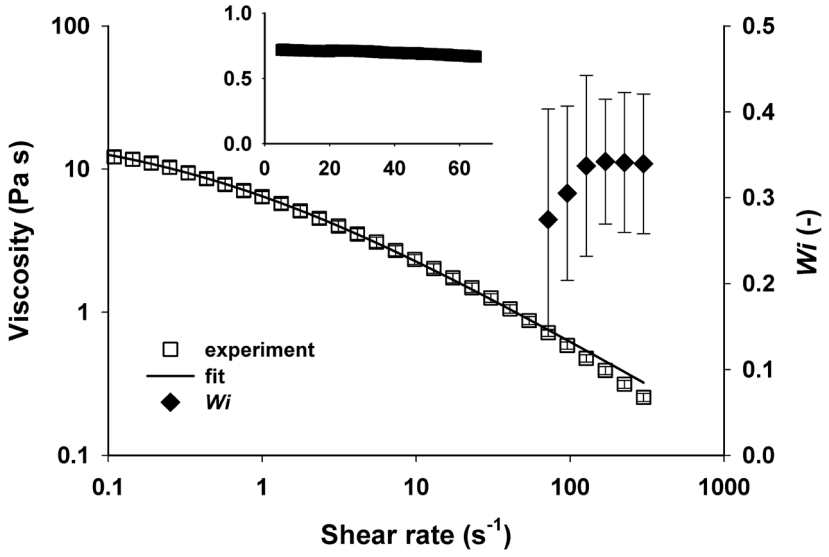

Figure 4. Shear viscosity and Weissenberg number of 0.6% w/w LBG and 0.6% w/w XG mixture at 80 °C. Inset: the transient viscosity at 64.9 s^{-1} for 60 min.

The degree of viscoelasticity of the continuous phase can be expressed with the Weissenberg number (*Wi*), which is determined using the following equation[26]:

$$Wi = \frac{\Psi_1 \omega}{\eta} \quad (3)$$

Ψ_1 is the 1st normal stress coefficient (Pa s^2), ω is the angular velocity (rad s^{-1}), and η is the apparent viscosity. Fig. 4 shows that *Wi* is less than 1 over the shear rates tested. This indicates that the viscoelasticity of the continuous phase is low. For shear rates below 70 s^{-1}, the normal forces were mostly below the sensitivity of the machine and therefore not shown in Fig 4.

The inset of Fig. 4 shows the transient viscosity during constant shearing for 60 min, which reflects the maximum shearing time applied in the shearing device. The viscosity tended to decrease slightly over time. In this measurement, the normal forces were around

the minimum threshold of the equipment (0.01 N), therefore, the resulting *Wi* is not shown.

3.2. Radial particle distribution under shearing

The continuous phase without any particles formed a translucent gel (Fig. 5). Therefore, a black background was chosen to better visualize the particle distributions in the next experiments.

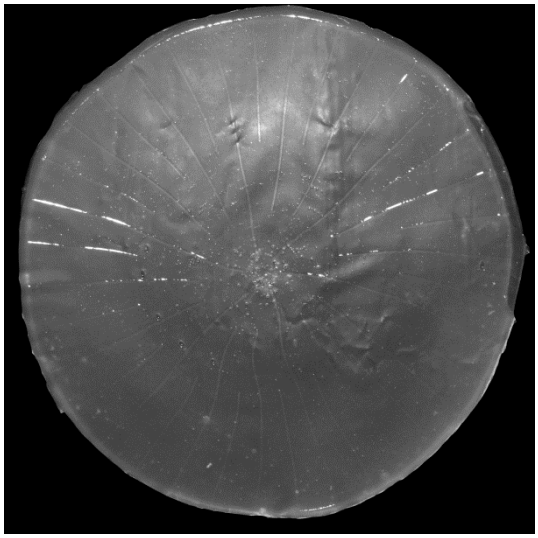

Figure 5. The gel of the continuous phase, i.e. 0.6% w/w LBG−0.6% w/w XG mixture.

Fig. 6 shows the distribution of the glass spheres in the continuous phase when the system was sheared for 5, 15, 30, and 60 min. Qualitatively, a lighter colour implies the presence of more particles. The experiment for each shearing time was done independently, therefore, the pictures for those shearing times represent different samples. The particle distribution from the centre to the rim of the cone is also shown with a normalized grayscale intensity as a function of the normalized radial distance (r/R).

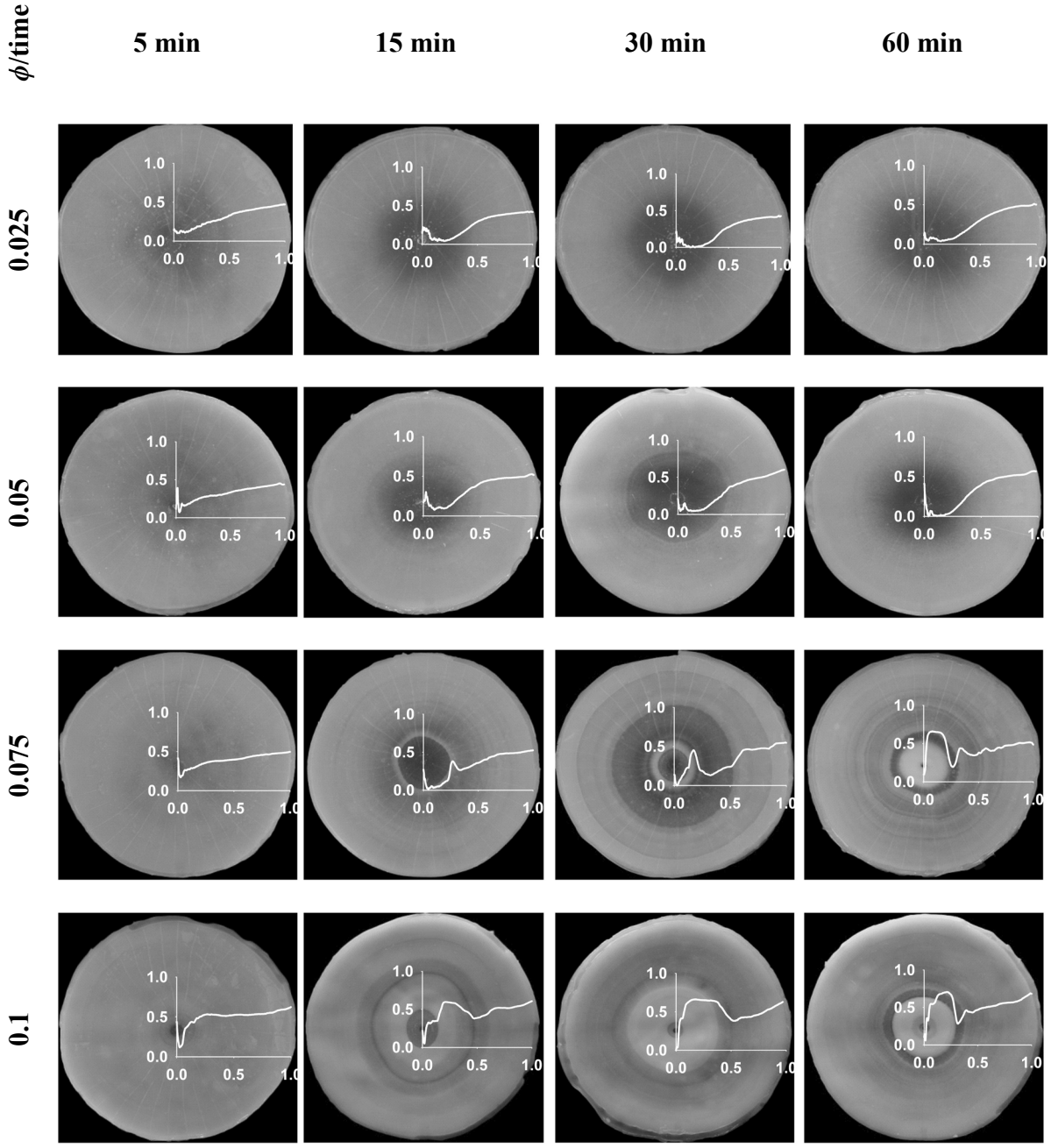

Figure 6. The distribution of glass spheres in the continuous phase after the dispersions were sheared for 5, 15, 30, and 60 min. Inset graphs are the normalized grayscale intensity (*y*-axis, [−]) along the normalized radial distance (*x*-axis, [−]).

Generally, the centre became depleted of particles, leaving a particle-free zone. This is shown by a black area at the centre. At the centre, the grayscale intensity sometimes decreases suddenly before it increases. This might be caused by air bubbles, which were

often found around the centre. For all volume fractions, the particles were homogenously distributed after 5 min shearing. It was observed that the particles migrate outward initially, shown by an increasing grayscale intensity along the radial distance.

After 15 min shearing or longer, the effect of the initial volume fraction on the particle distribution became evident. The particles continued to migrate outward for the lower particle volume fractions (ϕ = 0.025 and 0.05), leading to an increased particle-free zone at the centre. In addition, Fig. 6 suggests that net outward migration stopped after 15 min, as shown by almost similar patterns of the grey intensity along the radial distance.

In the case of a higher particle volume fraction (ϕ = 0.075), the particles clustered into concentric rings, interspaced with more diluted regions. A ring is clearly observed close to the centre. At a longer shearing time, this ring became more concentrated and was positioned closer to the centre. The adjacent diluted region was wider, followed by other rings more outwards. After 60 min shearing, the outer rings seemed to contract, suggesting that particles again migrated inward and formed a particle-rich region at the centre. Adjacent to this region, concentric rings were still observed, interspaced with diluted regions. These dynamics were also observed at the highest volume fraction tested (ϕ = 0.1). Here, an even stronger inward migration of the particles was observed. It seems that the distribution of particles in the continuous phase depends strongly on the volume fraction of particles.

The experiments for each volume fraction at each shearing time were done in duplicate, however for practical reasons, only selected pictures are shown in Fig. 6. All other pictures with their normalized grayscale intensity over the normalized radial distance are given as supplementary material for Fig. 6 at the end of this article. The particle distribution was sometimes slightly different, mainly because of air bubbles and intrusion of stray polyfluoretetraethylene (PFTE) particles used in the shearing device. Nevertheless, all experiments showed that the particles migrated outward at all shearing times at ϕ = 0.025 and 0.05 and migrated inward after 15 min shearing or longer at ϕ = 0.075 and 0.1.

The particle volume fraction at certain positions in the sample is quantified in Fig. 7. Shearing for 5 min resulted in an increased particle volume fraction with the radial distance. At $\phi = 0.025$ and 0.05 and prolonged shearing times, the particle volume fraction at shorter radial distance is lower than that after 5 min shearing. This drop in volume fraction indicates that the centre became depleted of particles. The similarity in the local particle volume fraction between 15, 30, and 60 min shearing suggests that a steady state was reached.

At $\phi = 0.075$ and 0.1, the distribution of particles is more complex when sheared for longer than 5 min. Initially, the same depletion at the centre and enrichment of the rim is observed. At longer shearing times, the migration is reversed and the particles accumulate at a specific radial distance. The peaks in Fig. 7c and d reflect the concentric rings of particles shown in Fig. 6. With longer shearing times, the particles migrated further inward, forming a higher peak near the centre. One should bear in mind that the centre has a very small volume. Even though the centre becomes depleted of particles, it is not a significant part of the total volume. Its volume was even less at a volume fraction of 0.075; the particle-free zone in the centre was in fact too small to be sampled.

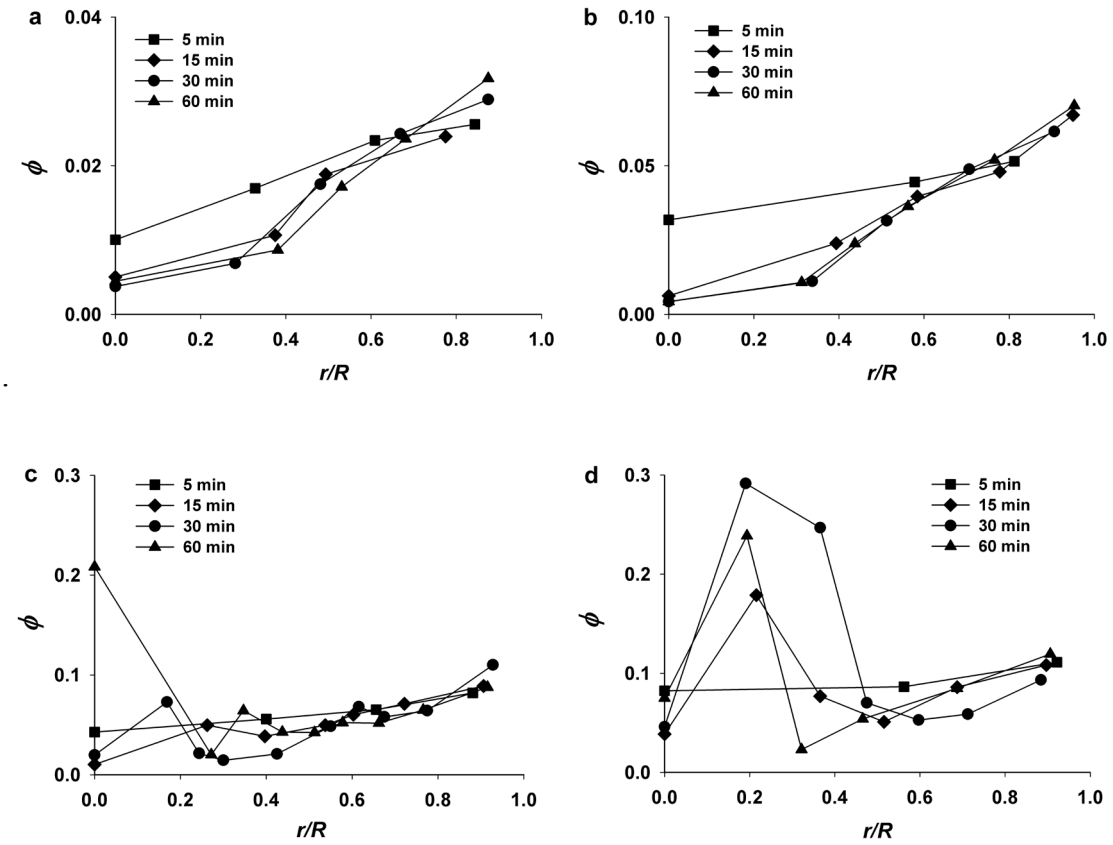

Figure 7. Local particle volume fraction at a specific radial distance at different shearing times at initial ϕ = 0.025, 0.05, 0.075, and 0.1. Lines are guiding the eyes.

3.3. Gravitational effect

To check if gravitation plays a role, experiments were carried out under quiescent conditions for 60 min with ϕ = 0.025, 0.05, 0.075, and 0.1. Fig. 8 shows the distribution of the particles in the continuous phase. The particles indeed tended to migrate to the centre. This migration was more visible at a higher volume fraction. Fig. 8 shows that the gravitation does play a role under quiescent conditions. In the shearing experiments however, the effect of gravitation seems to be very small compared with the other driving forces acting on the particles. Fig. 6 shows no clearance of particles at the rim and no accumulation of particles at the centre of the cone, as shown in Fig. 8.

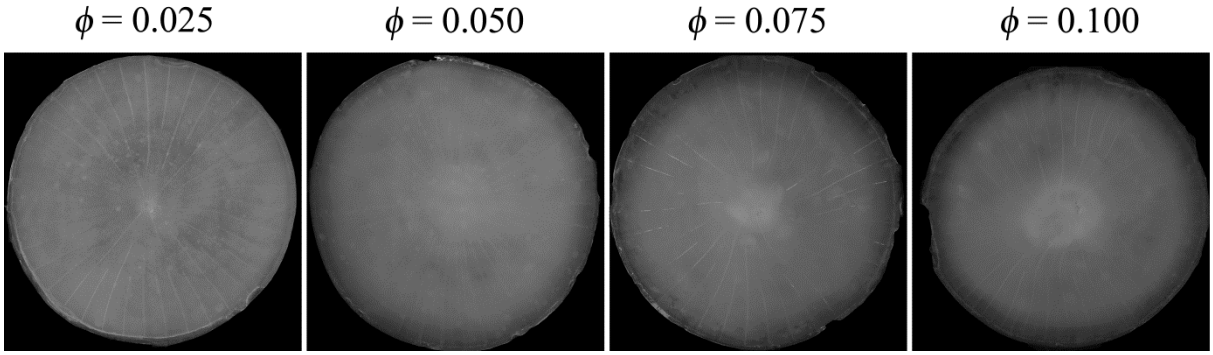

Figure 8. Distribution of particles in the continuous phase under quiescent conditions for 60 min in the shearing device.

4. Discussion

This article describes the migration of spherical particles dispersed in a 0.6% w/w LBG−0.6% w/w XG mixture. Starting from a homogeneous distribution, the particles initially migrated outward upon shearing for all particle concentrations studied. Obviously, the driving force for outward migration is larger than the effect of the gravitational force as this force would result in inward migration. The outward migration continued for longer times at lower particle concentrations. These observations are in line with previous studies in a parallel plate[12, 13, 20] and in a cone–plate system[3, 14].

A higher particle concentration resulted in more complex behaviour. After initial outward migration, concentric rings were formed at certain radial distances. Concentric ring formation of particle dispersions under flow have been reported previously[11-14]. The polydispersity of the particles could be a reason for the ring formation: particles tend to segregate and form clusters according to their size. However, concentric ring formation should then also have been observed at low volume fractions (ϕ = 0.025 and 0.05). Feng and Joseph (1996)[12] observed concentric ring formation at 2% v/v. Unfortunately, there was no firm and general conclusion on the mechanism of concentric ring formation derived in these previous studies.

Some rings that formed at ϕ = 0.075 and 0.1 moved inward and even merged when sheared longer. It seems that the nearest ring from the centre was pushed inward by the

surrounding particles in the outer sides or other rings. Even though the rings observed with ϕ = 0.075 and 0.1 must be due to inward migration, there is concurrent outward migration as well. Outside the first ring (Fig. 6 and 7), the concentration started to increase again with the radial distance. It seems that there is a specific radial distance above which particles move outward and below which they migrate inward. A few studies have reported such bidirectional migration for a single rigid particle in a polymer solution[7, 27, 28]. They proposed the existence of a critical radial distance that is related to a critical shear rate. In other words, the radial migration depends on the local shear rate for a given particle size. The different directions of migration were suggested to be a result of different responses to perturbation of the polymer by the rigid particle[28]. However, those studies were based on a single particle in polymer solutions, which makes it difficult to correlate them to the observations in our system.

The current study clearly shows the existence of reverse particle migration at higher particle volume fractions. We suggest that shear-induced particle migration is the leading mechanism. Shear-induced particle migration is the result of multi-particle interactions[4], leading to a random, diffusion-like migration of particles from their streamlines. Krishnan et al. (1996)[20] proposed a curvature-induced migration mechanism in a parallel plate geometry. Following Phillips et al. (1992)[8], the flux due to particle interactions ($\overrightarrow{J_c}$) is expressed as

$$\overrightarrow{J_c} = -k_c a^2 \phi \vec{\nabla}(\dot{\gamma}\phi) \qquad (4)$$

where k_c is a dimensionless parameter, a is the particle radius, ϕ is the particle volume fraction, and $\dot{\gamma}$ is the shear rate.

The flux of the particles due to a spatially varying viscosity ($\overrightarrow{J_\eta}$) is expressed as

$$\overrightarrow{J_\eta} = -k_\eta a^2 \phi^2 \dot{\gamma} \frac{1}{\eta} \vec{\nabla}\eta \qquad (5)$$

where η is the viscosity and k_η is a dimensionless parameter. The flux due to the curvature gradient in a plate−plate geometry is expressed as follows[20]:

$$\overrightarrow{J_r} = -k_r a^2 \phi^2 \dot{\gamma} \vec{\nabla} \ln \Re \qquad (6)$$

where $\Re$ is the streamline curvature relative to the particle mean curvature, expressed as $a/2r$ where r is the radial distance, and k_r is a dimensionless parameter. We consider the curvature of plate−plate geometry to approach the curvature in the shearing device because both have a shear rate gradient along the radial distance. Although the gradient of the shear rate along the radial distance in plate−plate geometry is linear, it is non-linear in the shearing device (Fig. 3).

The flux ($\overrightarrow{J_T}$) of the particles, therefore, can be expressed as

$$\frac{\overrightarrow{J_T}}{k_c a^2 \phi^2 \dot{\gamma}} = -\vec{\nabla}(\ln \dot{\gamma}\phi) - \frac{k_\eta}{k_c}\vec{\nabla}(\ln \eta) - \frac{k_r}{k_c}\vec{\nabla} \ln \Re \qquad (7)$$

The particle dynamics at the volume fractions tested can be described physically using the mechanisms outlined above. Eq. 4 shows that starting from a homogeneous distribution, the shear rate gradient drives particles to the centre of the device as the shear rate at the centre is zero and then increases with the radial distance. This flux induces volume fraction gradients that lead to a second flux in the opposite direction, towards the rim of the device. The volume fraction gradient also causes a variation in the viscosity spatially (Eq. 5), in which the material at the outer part has a lower viscosity than that at the inner part. This leads to another flux to the rim. Nevertheless, this effect might be insignificant at short shearing times because the increase in viscosity due to spatial differences in particle volume fraction is still small. Finally, the curvature-induced migration (Eq. 6) leads to particle migration to the rim.

At a shorter shearing time, i.e. 5 min, the fluxes leading particles to migrate to the rim seem dominant. This could be attributed to low frequency of particle interactions that might drag particles inward. Therefore, outward migration is observed. At longer shearing times, this net effect continues for low particle concentrations. However, more complex phenomena take place at higher concentrations.

The particle−particle interactions, indicated in $\left[\vec{\nabla}(\ln \dot{\gamma}\phi)\right]$, become more important at the higher volume fractions created by the initial outward migration. As soon as the local

volume fraction exceeds a certain threshold, the collective of particles then experiences a (net) driving force inwards. As the lower volume fractions it encounters still migrate outwards, a sort of front shock is created. When the process is stopped before the steady state condition, we can observe this creation as distinct rings, interspaced with particle-depleted regions at certain positions. It is also evident that the migration is reversed from the first few minutes to longer times.

A hypothesis of what the final particle distribution could look like when a steady state condition is reached ($\overrightarrow{J_T} = 0$) is described below. Eq. 7 can be re-written for steady state as

$$-\vec{\nabla}\left[\ln(\dot{\gamma}\phi(\eta^{\lambda_\eta})(\Re^{\lambda_r})\right] = 0 \text{ or } (\dot{\gamma}\phi\left(\eta^{\lambda_\eta}\right)\left(\Re^{\lambda_r}\right) = constant \qquad (8)$$

where λ_η is k_η/k_c and λ_r is k_r/k_c. Using Einstein's relationship for the viscosity of particle dispersion and substitution of the shear rate expression with Eq. 1, Eq. 8 can be re-arranged as

$$\phi\left(\frac{2\pi\omega r}{x_1 r + x_2\delta}\right)^{1-n\lambda_\eta} \eta_0^{\lambda_\eta}(1 + {}^5\!/_2\,\phi)^{\lambda_\eta}(\frac{a}{2r})^{\lambda_r} = constant \qquad (9)$$

where η_0 is the zero viscosity of the continuous phase and n is the power index of the viscosity. By taking the boundary condition at $r = R$, i.e. the position at the rim, as $\phi_r = \phi_R$, the relation becomes

$$\frac{\phi_r}{\phi_R}\left(\frac{2+5\phi_r}{2+5\phi_R}\right)^{\lambda_\eta} = \left(\frac{r}{R}\right)^{\lambda_r + n\lambda_\eta - 1}\left(\frac{x_1 r + x_2\delta}{x_1 R + x_2\delta}\right)^{1-n\lambda_\eta} \qquad (10)$$

At different particle volume fractions at the boundary condition, the volume fractions as a function of the radial distance ($0 < r < R$) at the steady state condition can be predicted. The values of k_c and k_η are obtained by estimation using experimental data[8], and the value of k_r is often assumed to be similar to k_c[9, 10]. We could not find a good fit with our data, therefore some values reported in the literature are used as a start in this study, i.e. k_c = 0.3075, k_η = 0.64, and $k_r = k_c$ [10], giving λ_η = 2.08 and λ_r = 1.

When the particle dispersions are shear thinning, the predicted particle distributions as a function of the radial distance are depicted in Fig. 9. The maximum particle volume fractions at $r = R$ were around 0.03, 0.07, 0.11, and 0.12 for ϕ = 0.025, 0.05, 0.075 and 0.1, respectively. Therefore those values were chosen for the maximum volume fractions in the prediction.

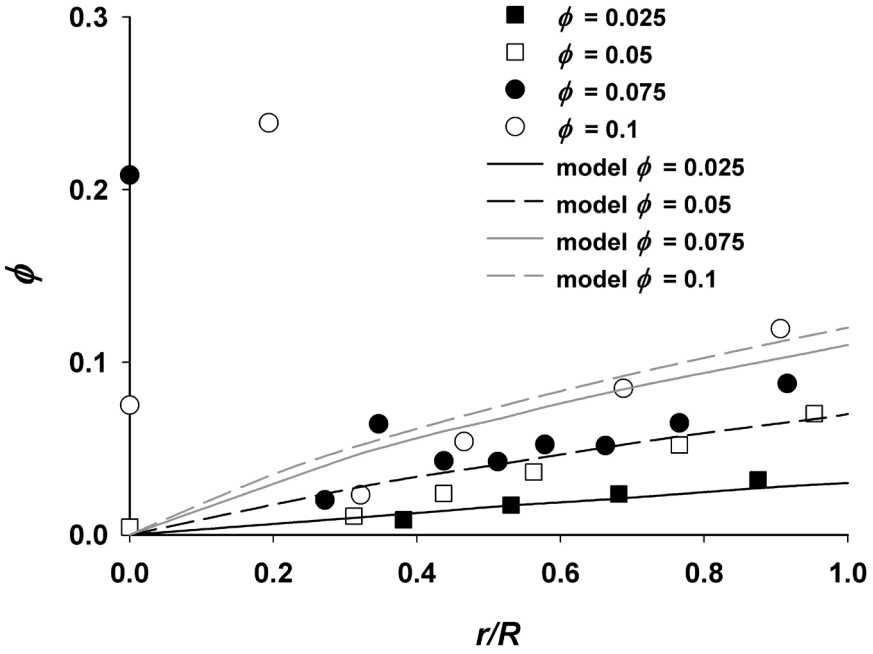

Figure 9. Particle distribution along the radial distance at different ϕ_R under steady state conditions if the particle dispersions behave as shear thinning. The lines are the predictions, the symbols are the experimental results for 60 min shearing.

The predicted results shown in Fig. 9 indicate that the particles tend to migrate outward, i.e. towards the rim of the cones with the chosen parameters. The direction of particle migration and the particle distribution along the radial distance in the predictions are in line with the experimental results for ϕ = 0.025 and 0.05. Fig. 9, however, does not match the experimental results for ϕ = 0.075 and 0.1. At these concentrations, several peaks of particle volume fractions are observed along the radial distance.

Particle distribution under steady state conditions that indicates a reversal of the migration from outward to inward can be predicted if the ratios of empirical parameters, i.e. λ_η and λ_r are changed, keeping in mind that the dispersion is shear thinning. Graham and Mammoli (1998)[29] suggested that k_c is a linear function of ϕ. However, choosing several dependencies of k_c to ϕ did not lead to satisfactory values of λ_η and λ_r. Setting k_c to be much higher than k_r, and then decreasing k_η, resulted in indication of a reversal of the particle migration. However, changing those parameters does not provide better insight. It is possible that the ring formation and inward migration are transient effects, which do not appear in a steady state description. It is clear, however, that this complex behaviour is not yet completely understood at this stage. Further study must be done to reveal the mechanisms behind the observed complexity in behaviour.

5. Conclusion

Dispersions of inert particles (glass spheres) in a dilute biopolymeric mixture were sheared in a cone−cone shearing device. At low particle volume fractions, the particles migrated from the centre to the rim of the device, leading to a steady state distribution after 15 min shearing. At higher volume fractions, the same phenomenon was observed initially but distinct concentrated rings were observed interspaced with more diluted regions after prolonged shearing. These rings tended to contract towards the centre of the device, ultimately leading to a concentrated centre, with a well-defined border. It was shown that the reverse migration behaviour was not the result of the viscoelasticity of the continuous phase.

A theoretical analysis was performed to analyse the various driving forces present in the system. It was concluded that most forces result in outward migration, but the driving forces due to particle interactions may lead to inward migration at higher particle concentration. However, the physical interpretation of the dimensionless parameters involved in the theory is still not clear.

Acknowledgements

The authors would like to thank Maartje Steegmans for a fruitful discussion about shear-induced migration of particles, Dr. Fransisco Rossier Miranda for developing macros in Image-J, and Jimmy Perdana for Matlab programming.

List of symbols

a	radius of the particle (m)
b	1st power index of the Carreau-Yasuda model (−)
c	2nd power index of the Carreau-Yasuda model (−)
$d_{0.1}$	the equivalent diameter where 10% of the particles have a smaller size (μm)
$d_{0.9}$	the equivalent diameter where 90% of the particles have a smaller size (μm)
$d_{4,3}$	volume mean diameter (De Brouckere mean diameter) (μm)
$\overrightarrow{J_c}$	flux of particles (ϕ) due to the gradient of interaction frequency (m s^{-1})
$\overrightarrow{J_\eta}$	flux of particles (ϕ) due to viscosity gradient (m s^{-1})
$\overrightarrow{J_r}$	flux of particles (ϕ) due to curvature gradient (m s^{-1})
$\overrightarrow{J_T}$	overall fluxes of particles due to interaction frequency, viscosity, and curvature (m s^{-1})
k	relaxation time (s)
k_c	a dimensionless parameter for flux due to interaction frequency (−)
k_η	a dimensionless parameter for flux due to viscosity gradient (−)
k_r	a dimensionless parameter for flux due to curvature gradient (−)
n	power law index of viscosity used in the flux expressions (−)
r	radial distance (mm) or (m)
r_c	critical radial distance (mm) or (m)
R	maximum radial distance (mm) or (m)
Wi	Weissenberg number (−)
δ	gap distance between upper and bottom cones (mm)
η	viscosity (Pa s)

η_0 zero viscosity (Pa s)

$\dot{\gamma}$ shear rate (s^{-1})

λ_η k_η/k_c

λ_r k_r/k_c

ω angular velocity (rad s^{-1})

Ψ_1 first normal stress coefficient (Pa s^2)

$\mathfrak{R}$ streamline curvature relative to the particle mean curvature (−)

ϕ particle volume fraction (−)

ϕ_r particle volume fraction at distance r (−)

ϕ_R particle volume fraction at distance R (-)

Supplementary material for Figure 6

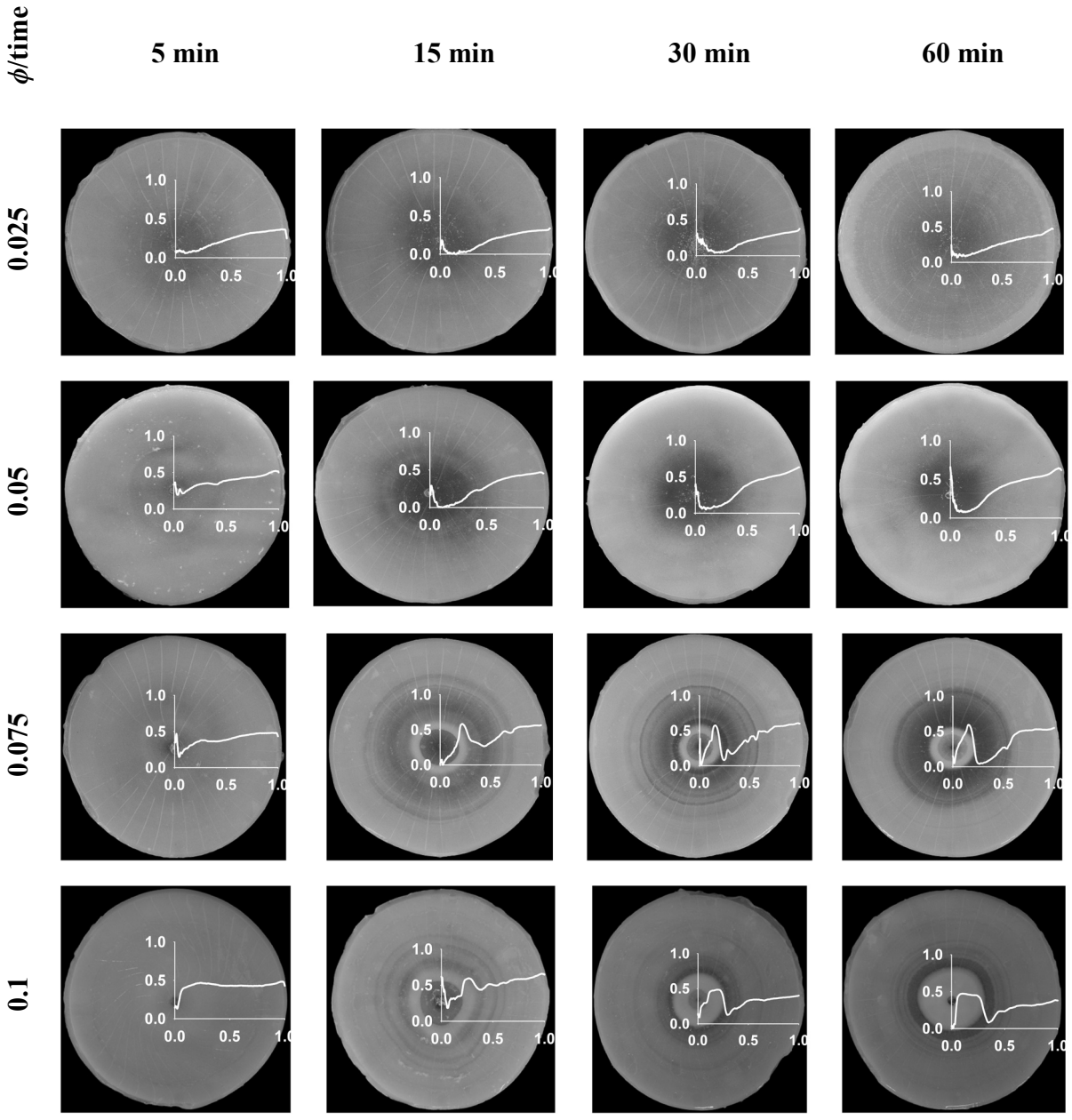

References

1. Karnis, A., Goldsmith, H. L., & Mason, S. G. (1963). Axial migration of particles in poiseuille flow. *Nature*, *200*(4902), 159-160.

2. Segre, G. & Silberberg, A. (1961). Radial particle displacements in poiseuille flow of suspensions. *Nature*, *189*(4760), 209-210.

3. Highgate, D. (1966). Particle migration in cone-plate viscometry of suspensions. *Nature*, *211*(5056), 1390-1391.

4. Leighton, D. & Acrivos, A. (1987). The shear-induced migration of particles in concentrated suspensions. *Journal of Fluid Mechanics*, *181*, 415-439.

5. Gadala-Maria, F. & Acrivos, A. (1980). Shear-induced structure in a concentrated suspension of solid spheres. *Journal of Rheology*, *24*, 779-814.

6. Karis, T. E., Prieve, D. C., & Rosen, S. L. (1984). Lateral migration of a rigid sphere in torsional flow of a viscoelastic fluid. *AICHE Journal*, *30*(4), 631-636.

7. Karis, T. E., Prieve, D. C., & Rosen, S. L. (1984). Anomalous lateral migration of a rigid sphere in torsional flow of a viscoelastic fluid. *Journal of Rheology*, *28*(4), 381-392.

8. Phillips, R. J., Amstrong, R. C., Brown, R. A., Graham, A. L., & Abbot, J. R. (1992). A constitutive equation for concentrated suspensions that accounts for shear-induced particle migration. *Physics of Fluids A*, *4*(1), 30-40.

9. Shauly, A., Wachs, A., & Nir, A. (1998). Shear-induced particle migration in a polydisperse concentrated suspension. *Journal of Rheology*, *42*(6), 1329-1348.

10. Kim, J. M., Lee, S. G., & Kim, C. (2008). Numerical simulations of particle migration in suspension flows: frame-invariant formulation of curvature-induced migration. *Journal Non-Newtonian Fluid Mechanic*, *150*, 162-176.

11. Graham, A. L., Altobelli, S. A., Fukushima, E., Mondy, L. A., & Stephens, T. S. (1991). Note: NMR imaging of shear-induced diffusion and structure in concentrated suspensions undergoing Coutte flow. *Journal of Rheology*, *35*, 191-201.

12. Feng, J. & Joseph, D. D. (1996). The motion of solid particles suspended in viscoelastic liquids under torsional shear. *Journal of Fluid Mechanics*, *324*, 199-222.

13. Kim, C. (2001). Migration in concentrated suspension of spherical particles dispersed in polymer solution. *Korea-Australia Rheology Journal*, *13*(1), 19-27.

14. Ponche, A. & Dupuis, D. (2005). On instabilities and migration phenomena in cone and plate geometry. *Journal of Non-Newtonian Fluid Mechanics*, *127*(2-3), 123-129.

15. Peighambardoust, S. H., Hamer, R. J., Boom, R. M., & van der Goot, A. J. (2008). Migration of gluten under shear flow as a novel mechanism for separating wheat flour into gluten and starch. *Journal of Cereal Science*, *48*, 327-338.

16. van der Zalm, E. E. J., van der Goot, A. J., & Boom, R. (2009). Influence of process conditions on the separation behaviour of starch-gluten systems. *Journal of Food Engineering*, *95*, 572-578.

17. Manski, J. M., van der Goot, A. J., & Boom, R. M. (2007). Formation of fibrous materials from dense calcium caseinate dipersions. *Biomacromolecules*, *8*(4), 1271-1279.

18. Sanchez, V. E., Bartholomai, G. B., & Pilosof, A. M. R. (1995). Rheological properties of food gums as related to their water binding capacity and to soy protein interaction. *Lebensmittel-Wissenschaft & Technologie*, *28*, 380-385.

19. Hua, Y., Cui, S. W., & Wang, Q. (2003). Gelling property of soy protein-gum mixtures. *Food Hydrocolloids*, *17*, 889-894.

20. Krishnan, G. P., Beimfohr, S., & Leighton, D. (1996). Shear-induced radial segregation in bidisperse suspensions. *Journal of Fluid Mechanics*, *321*, 371-393.

21. Michele, J., Putzold, R., & Donis, R. (1977). Alignment and aggregation effects in suspensions of spheres in non-Newtonian media. *Rheologica Acta*, *16*, 317-321.

22. Lyon, M. K., Mead, D. W., Elliott, R. E., & Leal, L. G. (2001). Structure formation in moderately concentrated viscoelastic suspensions in simple shear flow. *Journal of Rheology*, *45*(4), 881-890.

23. Scirocco, R., Vermant, J., & Mewis, J. (2004). Effect of the viscoelasticity of the suspending fluid on structure formation in suspensions. *Journal of Non-Newtonian Fluid Mechanics*, *117*(2-3), 183-192.

24. Gunes, D. Z., Scirocco, R., Mewis, J., & Vermant, J. (2008). Flow-induced orientation of non-spherical particles: Effect of aspect ratio and medium rheology. *Journal of Non-Newtonian Fluid Mechanics*, *155*(1-2), 39-50.

25. van der Zalm, E. (2011). Concentrated separation of wheat floud into starch and gluten. Wageningen University.

26. Steffe, J. F. (1996). Rheological methods in food process engineering (2nd ed.). East Lansing, MI: Freeman Press.

27. Prieve, D. C., Jhon, M. S., & Koenig, T. L. (1985). Anomalous migration of a rigid sphere in torsional flow of a viscoelastic fluid. *Journal of Rheology*, *29*(6), 639-654.

28. Choi, H. J., Prieve, D. C., & Jhon, M. S. (1987). Anomalous lateral migration of a rigid sphere in torsional flow of a viscoelastic fluid-effect of polymer concentration and solvent viscosity. *Journal of Rheology*, *31*(4), 317-321.

29. Graham, A. L. & Mammoli, A. A. (1998). Effects of demixing on suspension rheometry. *Rheologica Acta*, *37*, 139-150.

Chapter 7

General discussion

1. Introduction

The aim of the work reported in this thesis was to explore the potential of protein structuring to create attractive food products having an increased protein content. The overall conclusion from the thesis is that structuring of protein can lead to new products with novel properties. In addition, the thesis shows that the stability of the products is not strongly improved by protein structuring.

2. Main findings and conclusions

Products with an increased protein content are of interest to specific groups of consumers. However, preparing a concentrated protein product is a challenge because a high concentration of protein in a product generally results in a firm product that hardens over time[1-7]. Such a product would not be palatable to consumers. In this thesis, it was therefore investigated whether structuring of the protein could be a way to overcome those shortcomings.

The existing knowledge on structuring globular proteins in model products containing proteins above 10% w/w was summarized into a review, described in **chapter 2** of this thesis. Only recently, studies appeared that addressed the factors causing the undesired physical properties of products at an increased protein content.

Based on the literature study, it was concluded that several promising methods exist to reduce the toughness and further hardening of high-protein products over time. The most promising options are the addition of plasticizer, of a disulphide reducing agent, of a free-thiol group blocking agent, and the use of structural elements. These structural elements may be formed through pre-processing of a single protein phase or a multiphase system in which other ingredients are involved, such as sugar, fat, and polysaccharides. Then, they can be further processed in a final processing step to make a complete product. The final processing step will allow the formation of a more complex structure. This thesis explored the creation of structural elements, and subsequent application of these elements into a complete product.

Chapter 3 describes a first method to prepare structural elements. Native (i.e. as received from the manufacturer) whey protein isolate (WPI) was transformed by heating into protein aggregates at a concentration below the gelling concentration. The protein aggregate suspension obtained was then concentrated into a higher protein concentration and reheated to form a gel. This resulted in a softer gel than one made from native whey protein only at a similar concentration. By this method, whey protein was first clustered using short-range attractive interaction forming aggregates. Then, these aggregates interacted within a longer range in the system to form a gel network. The results suggested that gel strength is lowered most with large, dense and non-reactive protein aggregates.

Chapter 4 reports on a procedure in which WPI was heated, while mixing. The gels obtained were then dried and ground. This procedure resulted in so-called WPI microparticles that fulfilled the criteria mentioned in chapter 3 (large, dense and non-reactive). Replacing part of the native WPI by microparticles led to a gel that was softer, while having the same overall protein concentration. This effect was complicated by the fact that the WPI microparticles absorbed water from the surrounding continuous phase and in this way increased the overall firmness of the resulting product.

Chapter 5 describes the effects of the WPI microparticles on the stability of high-protein gel over time. Both a high-protein gel made only from WPI and one made from WPI microparticles hardened over time. However, the hardening process was different. The gel made from WPI hardened in the first few days after production, after which the hardening stopped. The gel containing WPI microparticles in a WPI matrix or in a polysaccharide matrix also hardened, but this hardening continued for a longer period. We concluded that hardening in a high-protein gel containing only WPI does occur due to the properties of the protein, such as the ability to form additional disulphide bridges. In multiphase systems that contained WPI microparticles, additional factors such as moisture redistribution are probably responsible for longer term effects.

Chapters 2 to 5 focus on isotropic high-protein gels. For foods however, anisotropic structuring may be attractive because it would yield more freedom in designing palatable

products. Previous research showed that an anisotropic structure could be induced in a caseinate suspension by using well-defined shear flow[8]. **Chapter 6** presents a study in which a model material (glass spheres dispersed at various concentrations in a weakly viscoelastic medium) was used to investigate the potential of flow-induced structuring further. When subjected to torsional flow (simple shear flow in a rotating device), the particles at all volume fractions tested initially migrated outward. The final structure strongly depended on the initial particle volume fractions. At higher volume fractions, the particle migration reversed from outward to inward after prolonged shearing. In addition, concentric rings were formed interspaced with more diluted regions. A theoretical basis was presented that accounted qualitatively for most of the effects. Even though it is clear that the model dispersions are far from a real food product, this chapter shows the potential to create a broad range of product structures using flow-induced structuring. Nevertheless, more research is necessary to fully understand and explore this effect, and to translate it to food-type formulations.

3. Evaluation of the approaches

3.1. Material

Whey protein isolate was chosen as the model material in this study. It is frequently applied for high-protein foods, amongst others due to its good amino acids composition. Whey protein contains all essential amino acids, and is a rich source of branched chain amino acids (BCAA), i.e. isoleucine, leucine and valine[1, 9, 10], which are essential for growth and recovery of muscle tissue[11-13]. In that sense, whey protein is an interesting ingredient to make high-protein foods.

Whey protein also offers a number of technological advantages. It is available as an isolate with high purity and with a high degree of un-denatured protein. This allows us to use it in both un-denatured or in denatured state depending on the functional properties needed. In addition, whey protein is available in large volumes. For research purposes, it

is important that extensive knowledge is available on whey protein. About 19,000 papers[14] can be found on studies with whey protein, dated from the 1950s.

Thus, whey protein is a good model material. Nevertheless, translating the results obtained with whey protein to other protein sources (e.g. plant protein) is not trivial. The intrinsic properties of those proteins, the presence of other components in case of concentrates, or the severity of fractionation process might well result in different functional properties.

As a model protein to study flow-induced structuring, whey protein in its original form is not an appropriate model. In the un-denatured (globular) state, whey protein typically has a size of a few nanometers. On this scale, shear flow has no effect. To use flow for structuring, one should create domains that have a size that is susceptible to the flow. Therefore, transformation of the protein into aggregates or microparticles is necessary. However, concentrated dispersions of these aggregates or microparticles in water behaved differently compared with calcium caseinate suspensions, which was shown by Manski et al. (2007) to form anisotropy under flow-induced structuring[8].

3.2. Methodology

Aggregation of whey protein at relatively low protein concentrations, i.e. below 12% w/w, has been studied extensively. However, there are two reasons why aggregation of proteins in the dilute regime may not be a good starting point for preparing high protein foods. First, starting with a dilute protein solution to prepare aggregates would imply a significant stream of water to be removed. A product having 30% w/w protein, prepared out of an aggregate suspension in which the protein is aggregated in a 1% w/w solution, would require 30 tons of protein solution initially for every ton of product. Twenty-nine tons of water has to be removed and as an additional problem, the concentration of electrolytes for buffering and other components would increase to unacceptably high levels. That is why it is necessary to work at higher concentration initially. In case the aggregates could be formed in a 12% w/w protein solution, only 2.5 tons of protein solution is needed and only 1.5 tons of water has to be removed. A final reason is that

aggregation leads to protein particles which do not have a high protein content due to solvent inclusion into the aggregates. As a result, the ultimate gain in concentration by using these aggregates is not optimal.

Based on these considerations, a second route was chosen. A protein gel at relatively high concentration was prepared, mechanically ground into small particles, and subsequently dried. The fact that a concentrated solution is used makes this approach suitable for production on larger scale. The initial protein concentration used is more flexible than in the production of aggregates since higher protein concentrations than 12% w/w can be used. The powder that is obtained after the drying step can easily be stored and transported, and the final particle size can be mechanically controlled by the grinding process.

The research discussed in chapters 4 and 5 show that indeed the use of microparticles leads to products (gels) that are weaker than those made from native protein. However, the increase in hardness over time could not be avoided.

4. Scientific implication

4.1. Hardening and stability of high-protein foods

The study showed that hardening in WPI gels occurs over a few days. This is much shorter than the typical hardening times that are generally assumed to be valid for other high protein products. Some studies on whey protein suggested that disulphide bonds formation is responsible for hardening in concentrated protein matrix[2, 15]. However, the study by Loveday et al. (2010)[7] showed that a model product made with 20% w/w WPI remained soft for 50 days with no evidence of covalent cross-linking. Here, we observed that multiphase systems containing WPI microparticles showed hardening over a longer period than a single phase system containing only WPI (chapter 5). This is in line with the fact that many authors observed hardening in multiphase systems containing sugar or polyols[4-7, 16]. Our conclusion is therefore that hardening in high-protein systems take place by other effects than internal protein cross-linking.

In general, structuring may reduce the initial firmness of the product (chapter 3, 4 and 5). However, the heterogeneity in the product leads to phases or domains that are often not yet at thermodynamic equilibrium with each other. Therefore, there are driving forces for redistribution in the product matrix. While transfer of protein or other macromolecular components is not probable, water is easily redistributed, especially if the continuous phase is aqueous as well. Moisture will be transferred from one domain to the other when differences in water activity are present. This will change the overall mechanical properties of the product. This transfer apparently takes place over a timescale of a few days. If we would take a low estimate of the diffusivity of water in the particles at 10^{-12} m^2 s^{-1}, we would have over two days as typical diffusion-length of 800 μm. This is around 11 times the average size of dry microparticles. Thus, diffusion may not be limiting, but it may be that internal relaxation of the protein matrix inside the microparticles is the rate limiting step in the moisture redistribution.

To prevent water redistribution, the driving force for redistribution, i.e. the difference in water activity, has to be reduced or eliminated. A reduction of the water activity in the continuous phase would reduce the difference with the protein particles. A reduced water activity can be achieved by adding sugar or polyelectrolytes in the continuous phase, which are not able to enter the protein particles. Alternatively, the microparticles might be heavily cross-linked, which would lead to an elastically-induced increase in the water activity within the microparticles, or the protein might be modified to become more hydrophobic. However, the side effect of that last option could be syneresis or even further separation of the protein from the rest of the materials.

4.2. The potential of flow-induced structuring

Most of the work described in chapters 3, 4 and 5 is on the preparation and application of structural elements as a dispersed phase into a product. However, positioning of the structural elements in a specific fashion could generate other textural properties, relative to random stacking.

Anisotropy might be required for a product that is meant as a replacement for meat (a natural high protein food), and it would create a better reservoir for flavour and (micro)nutritional ingredients. Even though product hardening over time may still occurs, anisotropy can give better sensorial properties in one direction (i.e. parallel to the alignment) than the other direction (i.e. perpendicular to the alignment). For this purpose, we studied the behaviour of microparticles in a polysaccharide matrix under simple shear flow. We decided to use glass spheres as model particles for the WPI microparticles because the microparticles are irregular and relatively polydisperse in size. Use of the micoparticles would introduce too many variables at the same time. Chapter 6 shows that glass particles in a weakly viscoelastic matrix migrate perpendicular to the shear flow. They form enriched and depleted concentric rings when the initial particle volume fraction is sufficient. The formation of those rings in simple shear flow is often attributed to the existence of attractive interactions between the particles. However, those interactions are unlikely in this case due to the fact that the glass spheres themselves will repel each other due to their negative charge. The use of hollow glass spheres with smaller size (10 μm) and density (1.1 g/cm^3), dispersed in a locust bean gum (LBG)–xanthan gum (XG) mixture resulted in a fully anisotropic structure after subjection to simple shear flow at 50 °C (Fig. 1, left). The same experiment at 80 °C did not lead to any anisotropy (Fig. 1, right). This difference might be attributed to the different flow properties of LBG–XG mixture at these two temperatures. This implies that inter-particle interaction is probably not the determining factor in the formation of anisotropy.

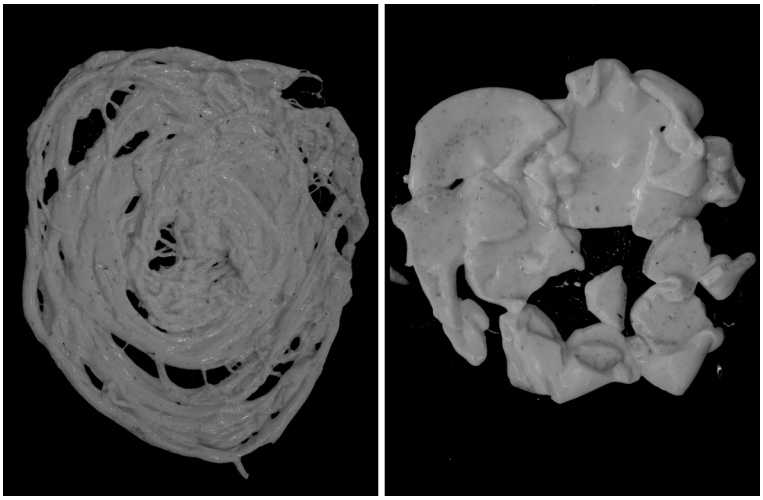

Figure 1. Structure formation of glass spheres (10 µm, 1.1 g/cm^3) in a LBG−XG mixture under simple shear flow in a shearing device at 50 °C (left) and at 80 °C (right).

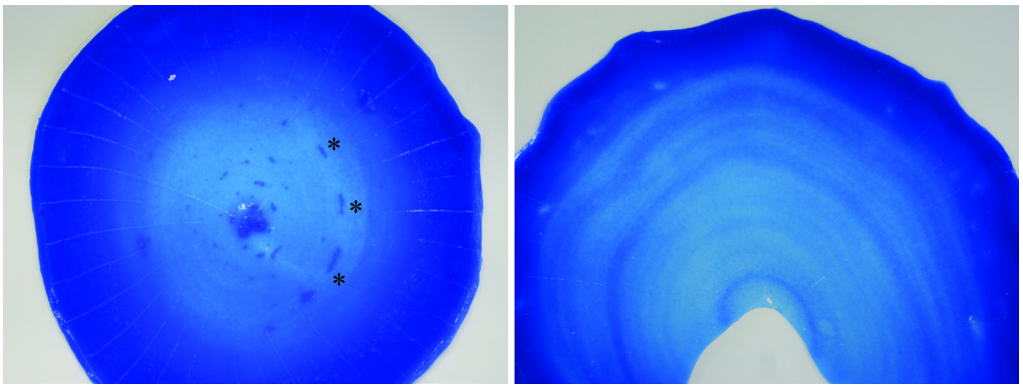

Figure 2. Distribution of WPI microparticles in a LBG−XG mixture under simple shear flow in a shearing device. The particles were dyed in blue. * indicates elongation of particle clumps and alignment with the flow.

The next step after the experiments with glass spheres is to translate the results to the systems with WPI microparticles. Fig. 2 shows the distribution of WPI microparticles dispersed in an LBG–XG mixture after being sheared with a simple shear flow. The left picture shows that clumps of particles aligned with the flow. Even though the visual distinction between the particles and the continuous phase is more difficult with these particles, it can be observed that the particles formed concentric rings along the radial distances with more particles located at the rim (Fig. 2, right). This is in line with the

distribution of glass spheres at certain volume fractions in **chapter 6**. This figure also shows that it might be possible to extrapolate the findings in chapter 6 to systems with WPI microparticles, even though the effects have not been optimized to any extent.

5. Future prospective

5.1. Protein structuring

The creation of whey protein into small particles prior to their assembly into a product is a useful tool to modify the properties of the overall (whey) protein product. Protein aggregation at low concentration might be an option to increase the protein content of liquid products, in which a protein increase of a few per cent might be of interest already. The production of protein aggregates that should be applied at a high protein content (e.g. > 15%) is only possible by using several subsequent processes, e.g. a concentration process or drying. By choosing appropriate processes, e.g. applying a combination of microfiltration and drying instead of only drying, energy consumption can be reduced to a certain extent. However, the method above will always lead to large liquid by-product streams. The formation of WPI microparticles, as described in this thesis, can be started at much higher protein concentration than the gelling concentration of WPI. Therefore, it is feasible to dry them at large scale with relatively high in energy efficiency, without losing too much raw materials.

Fig. 3 gives Sankey diagrams (an overview of the sizes of the mass streams and energy consumption required) for a product containing 15% w/w WPI in the form of aggregates and microparticles. The calculations are based on 1 kg WPI powder. Furthermore, it is assumed that the aggregates are prepared by heating a 9% w/w WPI solution at 68.5 °C for 24 h (1) or 90 °C for 30 min (2). The aggregates are then either concentrated (Fig. 3a) or dried (Fig. 3b). The microparticles are prepared from a 40% w/w WPI suspension. Here, the energy consumption is calculated based on pilot-scale equipment. The stream from left to right is the material stream and the stream from the top is the energy stream. The sizes of the arrows represent the size of the streams.

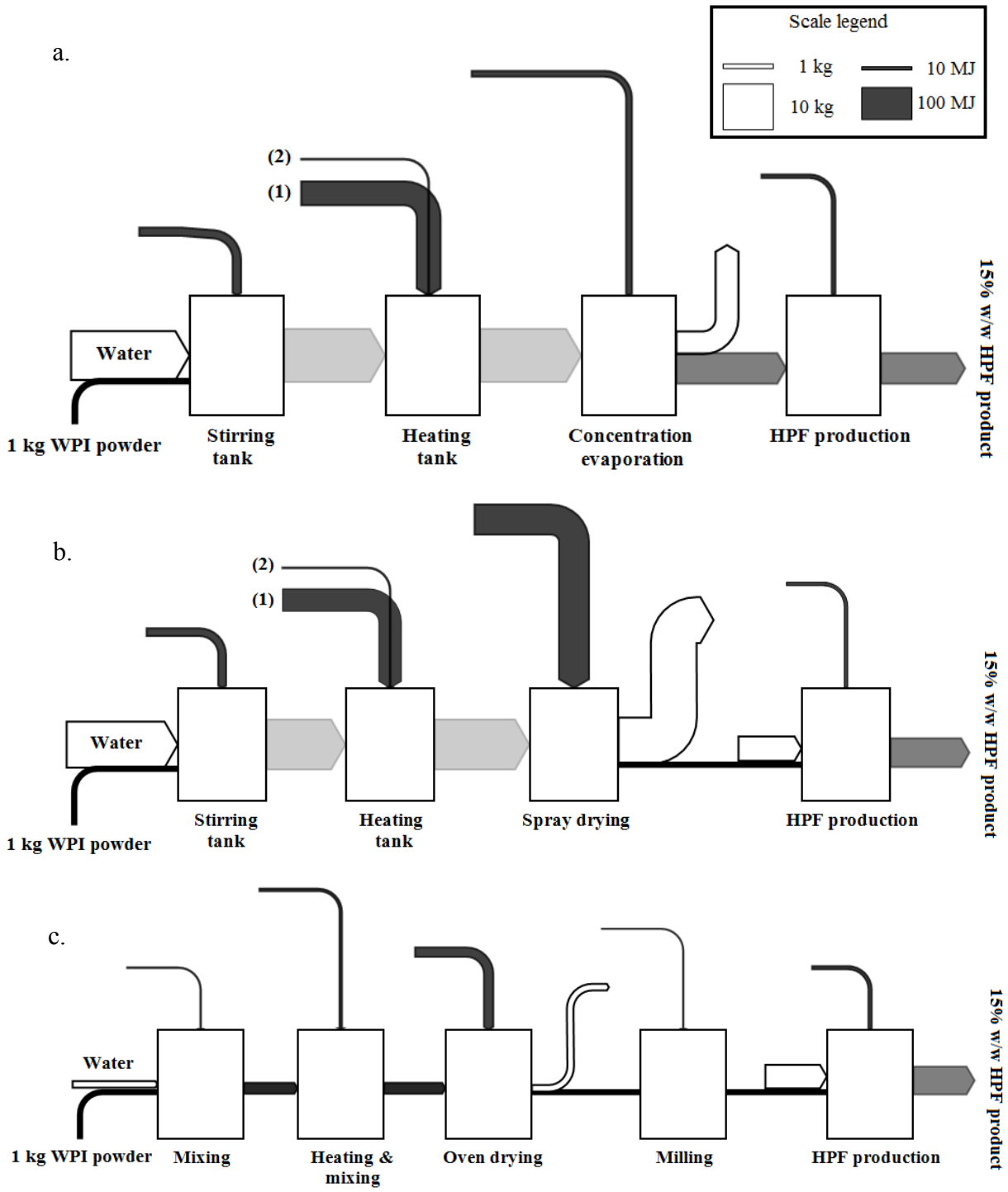

Figure 3. Production schemes of high-protein foods (HPF), made from WPI aggregates (a, b) and WPI microparticles (c). The material stream: white is water, black is WPI powder, the colour deviation from black represents less concentration of WPI powder in the stream. Arrows entering vertically represent energy stream. The scale legend for mass and energy streams applies for all graphs. (1): when heated at 68.5 °C for 24 h, (2): when heated at 90 °C for 30 min.

5.2 Application of microparticles

Microparticles are readily applied in soft solid or solid food products. In this case, the hardness difference between the particles and the solid matrix is minor, therefore the sensorial properties of the products will be less influenced by the presence of the particles. The particle size is important to avoid a gritty perception of the products. The size of the microparticles reported in chapter 4 and 5 may be reduced further by appropriate technologies. Several studies reported that the use of a homogenization process or high shear process[17-19], or the use of a jet mill grinding with fine separation[20] resulted in small particle sizes, even submicron sizes. Fig. 4 shows the size distribution of Simplesse®, commercial protein microparticles made from whey protein concentrate (WPC), and the corresponding sensorial properties of the particle size. It should be noted that this figure is very schematic and oversimplifies the situation. Other aspects than the particle size have to be considered as well such as other ingredients, properties of the particles other than only the size, and matrix that the particles are applied into.

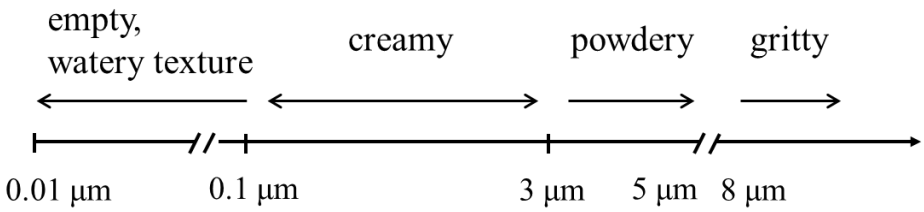

Figure 4. Particle size distribution of Simplesse®, WPC microparticles, from Singer and Dunn (1990)[19].

5.3 Novel structuring techniques

The understanding of how shear flow may induce structure in foods consisting of concentrated suspensions is still in its infancy. Some effects have been shown for concentrated sodium caseinate and calcium caseinate in the presence of transglutaminase under simple shear flow[21], but the wealth of structures obtained in this thesis shows that there is further potential. The protein microparticles developed in this thesis might well be useful for this type of structuring.

In the case of WPI microparticles, sedimentation, water absorption, and irregular shape are several factors that influence the particle behaviour under simple shear flow. Although it was observed that these particles formed concentric rings in a weakly viscoelastic matrix (Fig. 2), just as observed with glass spheres, it is still difficult to predict how anisotropic structure has to be formed under simple shear flow. The development of a practically applicable theory on these phenomena would be of great value here, and should be a research aim in the near future.

5.4. Stable high-protein foods; *is it possible*?

In this study, high-protein model products were produced at high water activity. The inclusion of WPI microparticles resulted in the driving force of water redistribution from the continuous phase (often called matrix) to the particles, leading to hardening of the model product over time. The role of the water activity on hardening is not clear yet. It has been reported that the changes of water activity and moisture content correlate poorly with hardening of high-protein product during storage[22]. On the other hand, Li et al. (2008)[4] reported that hardening of the product was associated with an increase in water activity. The later was explained as the result of more water that initially plasticises the polyol syrup becomes free water, giving the higher water activity. Both studies stressed the importance of mobility of proton-containing compounds, which in this case are water and polyols, in the hardening process of high-protein products. Higher mobility of protons indicates a higher susceptibility of the product to physicochemical changes. Loveday et al. (2009, 2010)[6, 7] suggested that water migration from the protein surface to the hydroxyl groups of low molecular weight of polyol compounds leads to a protein-rich phase and a phase rich of water-polyol. The decreased molecular mobility of polyol compounds was observed consistently with glucose crystallization during storage.

From those studies, the possibility to engineer the ingredients of high-protein products and their properties such that the products are completely stable over time still needs further study. Protein itself does not seem the determining factor for the product stability, but its interaction with water. Water redistribution leads to changes in the overall properties of

the total product. Water mobility is only completely stopped in its glassy state, but this is incompatible with the required product properties. As quoted from Boerhaave (1745)[23] "*as water is common to be met with and comes to be used on every occasion, men are apt to imagine they thoroughly understand its nature: but those who have carefully applied themselves to the examination thereof, find it one of the most difficult subjects in all natural philosophy to be acquainted with*".

The use of polyol or sugar with water, engineered properties of proteins, or the use of other ingredients do help to soften high-protein products and slow down their hardening over time. In these ways, it is possible to deal with the changes of product properties normally associated with this type of product. Loveday et al. (2010) [6, 7] found that water migrated from the protein phase to a glucose-glycerol phase, and found hardening of the total product as a result. In this thesis, we reported that the protein microparticles absorb water from the continuous phase, which in this case could be a dilute solution of either protein or carbohydrates (locust bean gum and xanthan gum). Thus, we notice that in the study by Loveday et al. (2010) [6, 7], the protein loses water, while we found that the protein microparticles gain water.

The difference between the two findings is probably due to the concentration in the continuous phase. If we assume that the water redistribution is the result of developing local differences in water activity, we hypothesize that it would be possible to completely stop water redistribution by having a continuous phase that is more concentrated than in this work, but less concentrated than in the work by Loveday et al. (2010) [6, 7]. Of course, care should be taken that now the continuous phase itself should not show hardening.

References

1. Labuza, T. P., Zhou, P., & Davis, L. (2007). Whey to go. *The World of Food Ingredients* Vol. October/November, 108-112.

2. Zhou, P., Liu, X., & Labuza, T. P. (2008). Effects of moisture-induced whey protein aggregation on protein conformation, the state of water molecules, and the microstructure and texture of high-protein-containing matrix. *Journal of Agricultural and Food Chemistry*, *56*(12), 4534-4540.

3. Baier, S. K., Guthrie, B. D., Elmore, D. L., Smith, S. A., Lendon, C. A., Muroski, A. R., Porter, M. A., Engleson, J. A., Arudi, R. L., Zupfer, J., & Aimutis, W. R. (2007). Influence of extrusion on protein conformation and shelf-life extension of nutritional bars. International symposium on the properties of water X, September 2-7, Bangkok, Thailand.

4. Li, Y., Szlachetka, K., Chen, P., Lin, X., & Ruan, R. (2008). Ingredient characterization and hardening of high-protein food bars: an NMR state diagram approach. *Cereal Chemistry*, *85*(6), 780-786.

5. McMahon, D. J., Adams, S. L., & McManus, W. R. (2009). Hardening of high-protein nutrition bars and sugar/polyol-protein phase separation. *Journal of Food Science*, *74*(6), E312-E321.

6. Loveday, S. M., Hindmarsh, J. P., Creamer, L. K., & Singh, H. (2009). Physicochemical changes in a model protein bar during storage. *Food Research International*, *42*, 798-806.

7. Loveday, S. M., Hindmarsh, J. P., Creamer, L. K., & Singh, H. (2010). Physicochemical changes in intermediate-moisture protein bars made with whey protein or calcium caseinate. *Food Research International*, *43*, 1321-1328.

8. Manski, J. M., van der Goot, A. J., & Boom, R. M. (2007). Formation of fibrous materials from dense calcium caseinate dipersions. *Biomacromolecules*, *8*(4), 1271-1279.

9. Luhovyy, B. L., Akhavan, T., & Anderson, G. H. (2007). Whey proteins in the regulation of food intake and satiety. *Journal of the American College of Nutrition*, *26*(6), 704S-712S.

10. Siso, M. I. G. (1996). The biotechnological utilization of cheese whey: a review. *Bioresource Technology*, *57*, 1-11.

11. Fujita, S. & Volpi, E. (2006). Amino acids and muscle loss with aging. *Journal of Nutrition*, *136*(1), 277S-280S.

12. Hayes, A. & Cribb, P. J. (2008). Effect of whey protein isolate on strength, body composition and muscle hypertrophy during resistance training. *Current Opinion in Clinical Nutrition and Metabolic Care*, *11*(1), 40-44.

13. Paddon-Jones, D., Short, K. R., Campbell, W. W., Volpi, E., & Wolfe, R. R. (2008). Role of dietary protein in the sarcopenia of aging. *American Journal of Clinical Nutrition*, *87*(5), 1562S-1566S.

14. http://apps.webofknowledge.com. October 31, 2011.

15. Zhou, P., Liu, X., & Labuza, T. P. (2008). Moisture-induced aggregation of whey proteins in a protein/buffer model system. *Journal of Agricultural and Food Chemistry*, *56*(6), 2048-2054.

16. Liu, X., Zhou, P., Tran, A., & Labuza, T. P. (2009). Effects of polyols on the stability of whey proteins in intermediate-moisture food model systems. *Journal Agricultural Food and Chemistry*, *57*, 2339-2345.

17. Singer, N. S., Yamamoto, S., & Latella, J. (1988). Protein product base. US Patent, 4734287.

18. Onwulata, C. I., Konstance, R. P., & Tomasula, P. M. (2002). Viscous properties of microparticulated dairy proteins and sucrose. *Journal of Dairy Science*, *85*(7), 1677-1683.

19. Singer, N. S. & Dunn, J. M. (1990). Protein microparticulation: the principle and the process. *Journal of the American College of Nutrition*, *9*(4), 388-397.

20. Hayakawa, I., Yamada, Y., & Fuji, Y. (1993). Microparticulation by jet mill grinding of protein powders and effects on hydrophobicity. *Journal of Food Science*, *58*(5).

21. Manski, J. M., van Riemsdijk, L. E., van der Goot, A. J., & Boom, R. M. (2007). Importance of intrinsic properties of dense caseinate dispersions for structure formation. *Biomacromolecules*, *8*(11), 3540-3547.

22. Lin, X., Ruan, R., Chen, P., Chung, M., Ye, X., Yang, T., Doona, C., & Wagner, T. (2006). NMR state diagram concept. *Journal of Food Science*, *71*(9), R136-R145.

23. Boerhaave, H. (1745). Elementa Chemiae (2nd ed.). Basel: Im-Hoff.

Summary

This thesis describes the role of structuring to control the rheological and mechanical properties of high-protein model foods. By altering the internal structure of the model systems, textural properties of the model systems at initial stage (fresh products) can be improved.

C**hapter 2** reviews existing studies related to high-protein foods. The effects of ingredients and processing were evaluated with respect to food products having a high protein content. Some studies indicated typical problems occurring in products or model systems with an increased protein content such as product hardening over time. Ingredients that might be added to ameliorate product properties were plasticizers, peptides made from whey proteins, disulphide reducing agents, and components that block the free thiol groups in proteins.

The chapter provides guidelines for structuring high-protein foods aimed at avoiding or reducing the unfavourable changes in properties over time. Concentrated proteins in their native (unmodified) form can be replaced by protein domains or structural elements with altered properties. These domains or elements mitigate the changes in product structure, resulting in a product that is softer than the one made from native proteins only.

Structuring native protein into structural elements and applications

In **chapter 3**, we studied the aggregation of WPI at neutral pH using different heating conditions. Generally, a higher concentration and a higher temperature resulted in bigger and less dense aggregates. A higher temperature also resulted in a higher reactivity (a larger number of available thiol groups). Heating a suspension containing 15% w/w aggregates led to a weaker gel than a gel made from native (i.e. as received from the manufacturer) protein. This result was hypothesized to originate from the lower number of contact points formed with larger aggregates. The most pronounced weakening effect could be obtained with aggregates that are large, dense, and non-reactive.

In **chapter 4**, we presented microparticulation as a second method to structure native WPI. Microparticles were created by gelling a concentrated WPI solution, drying the gel

and milling it into small particles. Partial replacement of native WPI with WPI microparticles resulted in a weaker gel than a gel made from native WPI only at the same total protein concentration. This result was attributed to the inability of the microparticles to form a gel. However, the weakening effect of these particles in the model system was limited due to water redistribution and the good bonding between the particles and the protein continuous phase.

Chapter 5 describes how the properties of high-protein gels containing WPI microparticles change over time. A high-protein gel made from native WPI was used as a reference. The firmness and fracture stress of the gel made from WPI only increased during the first few days and then stabilized. The gel consisting of WPI microparticles in WPI or in a mixture of locust bean gum (LBG)–xanthan gum (XG) tended to harden for a longer period. Most likely, water redistribution is responsible for this observation.

Chapter 6 presents the application of torsional flow to a dispersion of glass spheres in an LBG– XG mixture. The glass spheres were used as a model for the more complex WPI microparticles. The continuous phase was weakly viscoelastic under the experimental condition. The glass particles migrated to the rim of the shearing device at low particle volume fractions. At higher volume fractions (ϕ = 0.075 and 0.1) and prolonged shearing times, a part of the particles then re-migrated to the centre. In addition, rings of particles were observed and the effect was interpreted as the onset of particles to migrate to the centre. The existing theory for shear-induced particle migration was used to explain the observations. In case particles are homogeneously distributed in a concentrated suspension, a shear rate gradient drives the particles inward. This results in a concentration gradient that embodies a second, opposite, driving force for particles to migrate outward. Additional driving forces, i.e. gradients in viscosity and curvature, support the outward migration. As a result, the net effect of outward migration is observed at a shorter shearing time, but shearing for a longer time could give rise to the particles migrating inwards under certain conditions.

The results from all previous chapters and the methodology applied were discussed in **Chapter 7**. An overall conclusion is that structuring is an important tool to improve the properties of high-protein foods, but it cannot be used to stop the hardening of the products over time. For completely stopping or at least controlling the hardening process, more scientific research is necessary to fully understand the underlying mechanisms leading to hardening in high protein foods. Finally, a number of additional results described in this chapter shows that structuring using shear flow offers new possibilities for influencing product properties and creating new product structures.

Samenvatting

Dit proefschrift beschrijft hoe structurering kan worden toegepast om de reologische en mechanische eigenschappen van geconcentreerde eiwitproducten te controleren. Het blijkt dat verandering van de structuur in het product mogelijkheden biedt om de textuur van het verse product te verbeteren.

Hoofdstuk 2 geeft een overzicht van bestaande wetenschappelijke studies op het gebied van geconcentreerde eiwitproducten. Er is gekeken wat de mogelijkheden zijn om de eigenschappen van deze producten te veranderen door het toevoegen van ingrediënten en aanpassingen in het verwerkingsproces. Ook is een overzicht gegeven van studies die de karakteristieke problemen van het harder worden van dit soort producten beschrijven. Dit probleem kon worden verminderd door ingrediënten zoals weekmakers, hydrolyseproducten van wei-eiwit, reducerende stoffen of componenten die de vorming van nieuwe zwavelbruggen verhinderen, toe te voegen.

In het hoofdstuk worden ook richtlijnen gegeven hoe geconcentreerde eiwitproducten moeten worden gestructureerd om ongewenste verandering in textuur te reduceren of tegen te gaan. Natief eiwit kan worden vervangen door eiwitdeeltjes, waardoor de veranderingen in productstructuur onderdrukt kunnen worden en een zachter product verkregen wordt. Deze deeltjes worden ook wel structuurelementen genoemd.

De productie en toepassing van eiwitstructuurelementen

Hoofdstuk 3 beschrijft de vorming van wei-eiwit aggregaten door het verhitten van de eiwitoplossing bij neutrale pH. Het bleek dat een hogere eiwitconcentratie of een hogere temperatuur leidde tot grotere aggregaten met een lagere dichtheid. Aggregaten die gemaakt zijn bij een hogere temperatuur bleken reactiever, wat betekent dat deze in staat zijn meer zwavelbruggen te vormen. Vervolgens werd de oplossing geconcentreerd tot een 15% aggregaat-oplossing. Het verhitten van deze oplossing gaf een zwakkere gel dan een gel gemaakt van 15% natief eiwit. Het vermoeden is dat deze verzwakking een gevolg is van het feit dat door de toepassing van aggregaten meer lokale eiwitinteracties zijn

ontstaan en daardoor een zwakker eiwitnetwerk. De meeste verzwakking werd verkregen met grote aggregaten die een hoge dichtheid hadden en non-reactief waren.

In **hoofdstuk 4** presenteren we microdeeltjes als een tweede methode om natief wei-eiwit te structureren. Microdeeltjes worden gemaakt door een geconcentreerde wei-eiwitoplossing te geleren en vervolgens te drogen. De gedroogde gel wordt gemalen tot een fijn poeder dat bestaat uit microdeeltjes. Het vervangen van natief eiwit door microdeeltjes, bij gelijke eiwitconcentratie, leidt tot een zwakker gel door het feit dat microdeeltjes geen gel meer kunnen vormen. Het verzwakkend effect was minder dan verwacht doordat de deeltjes veel water absorberen en zo de eiwitconcentratie in de matrix verhogen.

Hoofdstuk 5 beschrijft hoe de eigenschappen van geconcentreerde eiwitgellen met microdeeltjes veranderen in de tijd. Hierbij werd een gel gemaakt van natief eiwit als vergelijkingsmateriaal genomen. De stijfheid en spanning bij breuk van een wei-eiwitgel namen toe in de eerste dagen, maar daarna veranderden de eigenschappen nauwelijks. Een gel met microdeeltjes in een wei-eiwitgel of een in gel bestaande uit johannesbroodpitmeel en xanthaan leek harder te worden over een langere periode. Waarschijnlijk wordt dit veroorzaakt door waterherverdeling in het product.

Hoofdstuk 6 presenteert het effect van torsiestroming op een dispersie van glasdeeltjes in een johannesbroodpitmeel-xanthaan (JB-X) gel. De glasdeeltjes waren gekozen als modeldeeltjes voor de microdeeltjes uit de vorige hoofdstukken. De continue fase bij deze experimentele conditie is enigszins visco-elastisch. De glasdeeltjes bewogen naar de rand van het afschuifapparaat bij lage deeltjesvolumefracties. Een hogere deeltjesfractie (ϕ =0.075 en 0.1) en langere afschuiftijden leidde tot migratie van deeltjes naar de punt van de kegel, wat een tegengestelde beweging is. Bovendien werden nog concentrische ringen van deeltjes gevormd, wat is geïnterpreteerd als het begin van de omkering van de deeltjesbeweging. De deeltjesbeweging is vergeleken met bestaande theorieën van deeltjesbewegingen onder stroming. Deze theorieën geven aan dat een gradiënt in de afschuifsnelheid leidt tot een beweging van deeltjes naar de punt (centrum) van de kegels.

Dit leidt tot een concentratiegradiënt, die weer aanleiding geeft tot een andere drijvende kracht voor deeltjesmigratie. Deze kracht is naar buiten gericht. Ook andere krachten, ontstaan door verschillen in viscositeit en kromming van het afschuifveld leiden tot een beweging van deeltjes naar de rand van de kegel. Deze krachten verklaren een deeltjesbeweging naar buiten bij korte procestijden. Bij bepaalde proces condities en langere procestijden maken deze krachten ook een migratie mogelijk naar binnen.

In **hoofdstuk 7** worden alle resultaten en de methodes uit de vorige hoofdstukken nog eens beschreven. Er kan geconcludeerd worden dat structurering een belangrijke methode is om eigenschappen van geconcentreerde eiwitproducten te verbeteren, maar het aanbrengen van structuur stopt niet het hardingsproces. Om het hardingsproces volledig te stoppen of tenminste te controleren is meer begrip nodig van de mechanismen die leiden tot harding in geconcentreerde eiwitproducten. Dit vraagt meer wetenschappelijk onderzoek. Tenslotte worden nog extra resultaten beschreven die aangeven dat het gebruik van afschuifstroming nieuwe mogelijkheden biedt om nieuwe productstructuren te maken, resulterend in producten met wellicht interessante eigenschappen.

Acknowledgements

Publication list

Training activities

Acknowledgements

In the midst of 2007, an informal conversation with Dr. Atze Jan van der Goot in De Wit's coffee corner after completion of my thesis (MSc) exam brought me to the next step of education, i.e. being a PhD student. About four years later, here is the end of this step in the form of a PhD thesis. Although the thesis cover only mentions my name, the works in this book would not have been accomplished without support, help, and encouragement of many people. Therefore, I would like to acknowledge them here.

First of all, I would like to express my gratitude to my co-supervisor, Dr. Atze Jan van der Goot. Dear Atze, thank you for offering me the opportunity to do a PhD under your supervision in the first place. In the project, you gave me freedom to answer my curiosities in many things about the subject. On the other hand, you also helped me to come back on track when I was drawn in my own curiosities. Your scientific insight helped me to understand the project, to decide which direction should be taken, and to accomplish the works in the project. Thank you for continuous guidance and unconditional support, especially during hard times that I had to pass during the project.

I would like to thank my promoter, Prof. Remko Boom. Dear Remko, thank you for your smart and endless scientific thoughts. Although I could not execute them all, your thoughts gave me different perspectives in seeing scientific challenges. Your kindness, politeness, and humility as a professor really impressed me. I always remember our first email contact when you asked me not to call you "Sir".

I would like to express my appreciation to my students Rea Joanne-Zijp, Anouk Moerkens, and Emma van der Veen. Thank you very much for your valuable contributions to this thesis. It was a pleasure working with all of you.

I would like to thank the technical support from Herman de Beukelaer, Jacqueline Donkers, Adriaan van Aelst, Emmelie Jacobsen, Mary Smiddy, Jos Sewalt, and Maurice Strubel during my project. Jos and Maurice: I am sorry for extra time you had to spend when I broke things in the lab.

Many thanks to my roommates in Room 607: Jan, Janneke, and Edwin as the "first generation", and then Jimmy, Ruben, Kashif, and Karolina as the "second generation". Thanks for the pleasant and joyful atmosphere in the room. It was really helpful to share thoughts and ideas with all of you guys! Teruntuk Jimmy, terima kasih sudah banyak membantu mengedit gambar dan mengecek beberapa tulisan disaat-saat terakhir pembuatan buku ini. Terima kasih juga atas dukungan moralnya saat aku sedang krisis percaya diri selama mengerjakan project.

I might not have had much social life during my stay in Wageningen, but I really enjoyed during my stay in Food Process Engineering Group. The people in the group were serious when came to work, but they were fun during coffee break, labuitje, and PhD trip. A special thank is given to Fransisco who has helped me in the first stage of preparing this book. Certainly, I had fun working in the Food Structuring Group. I thank Lieke, Elsbeth, and Kasia for discussion about your projects and mine that we often did in the lab. This gave me different insights of how things should be done. Lena, Nicholas, and Jacqueline, I thank you for the joyful time in the lab. To Jorien and Laura: welcome to the group! I wish you great success with your projects. I would also like to acknowledge Joyce Krauss and Martin de Wit for their helpful hands with all administrative things.

I would like to express my appreciation to my paranymphs Dilek Saglam and Anna van Dinther for arranging the necessary things for my promotion day. I thank you for to be part of this important occasion (for me).

It was a great experience for me to be a team member in B1002 project. Although the project was tough, it was a pleasure for me working with many people with different expertise. To be part of this project taught me lessons not only about how to handle my own project, but also about how to work in a multidisciplinary environment. Many thanks to Johan, Arno, Stacy, Renko, Hans, Paul, Peter, Dilek, Mary, Emmelie, Emma, Anke, and Harry for this great experience.

I am also grateful to all members PPI whom I knew since my stay in the Netherlands for our togetherness. It did not feel like staying far from home when we gathered. Many

thanks to Pak Djaeni, Pak Hadiyanto and Mbak Adian, Mbak Wahyuni, and especially members of PPI 2005-2007 (Pipit, Oly, Obeth, Puput, Evi, Dowty, Gladys, dkk) for their great encouragement and support. I also thank Milkha for her time to fulfil my wish for the reception and Melliana for her time to discuss things related to Chemistry. My stay in the Netherlands was also more colourful because of Bang Enade and Myradiati. Bang E, I wish you the best for your promotion in the midst of 2012!

A special acknowledgement is given to the family of Marco Traa who always welcomed me in their house during my stay in the Netherlands. Pak Marco and Mbak Ina, I thank you for your hospitality and especially, your time to listen and to accompany me when I was in vulnerable moments.

Great appreciation is also given to my family for this achievement. I thank my parents for their unconditional love and support so that I become who I am now. I owe you so much that I cannot return in any ways. To my sisters, Wahyuni and Hartini, thanks for your encouragement during my stay in the Netherlands. All the jokes and stories you shared to me always cheered me up. The distance that took us apart made our sisterhood becomes stronger.

Last but not least, I would like to express my truthful acknowledgement to my beloved husband, Anton Ady Susanto. Dear Anton, it was a big sacrifice you did for me. You let me go to pursue my dream after we married for only 3 months. You always supported me when I was down, you were happy when I was in joy, and your unconditional love gave confidence in me. The long-distance relationship was never to be the boundary between us, instead, it strengthens our relationship even more. Without you, I would not have reached this stage in my life.

I might not have mentioned all people who have helped me in the last four year in this acknowledgements. Nevertheless, I sincerely thank you all for your direct or indirect assistances during my project.

Publication list

Peer reviewed journals

Purwanti, N., Venema, P., van der Goot, A. J. and Boom, R. Reversing the migration of hard-sphere particles under torsional flow. *Submitted for publication*.

Purwanti, N., van der Veen, E., van der Goot, A. J. and Boom, R. Hardening in whey protein isolate (WPI) gels: effects of internal structure. *Submitted for publication*.

Purwanti, N., Moerkens, A., van der Goot, A. J. and Boom, R. 2012. Reducing the stiffness of concentrated whey protein isolate (WPI) gels by using WPI microparticles. *Food Hydrocolloids*, *26*(1), 240-248.

Purwanti, N., Smiddy, M., van der Goor, A. J., de Vries, R., Alting, A. and Boom, R. 2011. Modulation of rheological properties by heat-induced aggregation of whey protein solution. *Food Hydrocolloids*, *25*(6), 1482-1489.

Purwanti, N., van der Goot, A. J., Boom, R. and Vereijken, J. 2010. New directions towards structure formation and stability of protein-rich food from globular proteins. *Trends in Food Science and Technology*, *21*(2), 85-94.

Purwanti, N., Fox, M., Schroen, K. and de Jong, P. 2009. The microheater: a new tool for rapid determination of food kinetics. *Journal of Food Engineering*, *91*(1), 78-84.

Sawalha, H., **Purwanti, N.**, Rinzema, A., Schroen, K. and Boom, R. 2008. Polylactide microspheres prepared by premix membrane emulsification – effects of solvent removal rate. *Journal of Membrane Science*, *310*(1–2), 484-493.

Purwanti, N., Setiawan, B. I. and Nelwan, L. O. 2004. Model of temperature control system for silkworm (Bombyx mori L.) cultivation. *Jurnal Keteknikan Pertanian*, *18*(1), 9-17.

Conference proceedings

Purwanti, N., Moerkens, A., van der Goot, A. J., Boom, R. 2011. Potential application of pre-processed whey protein isolate (WPI) for high-protein food. *11th International Congress on Engineering and Food*. May 22–26, Athens.

Purwanti, N., van der Goot, A. J., Boom, R. 2009. Susceptibility of whey protein dispersions to flow-induced structuring. *3rd International Symposium on Delivery of Functionality in Complex Food Systems*. October 18–21, Wageningen.

Purwanti, N., van der Goot, A. J., Boom, R. 2009. Towards improved texture properties of protein-rich foods. *5th International Symposium on Food Rheology and Structure*, June 15–18, Zürich.

Training activities

Overview of completed training activities

Courses

Discipline specific activities

Sustainability Analysis in Food Production, Wageningen	2011
Unbiased Stereology, Bern, Switzerland	2010
Rheological Measurement, Leuven, Belgium	2009
Food Hydrocolloids: Fundamentals & Application, Wageningen	2009
Macroscopical Physical Chemistry, Han-sur-lesse, Belgium	2009
Thermodynamics for the Process Technology, Delft	2008
Food Enzymology, Wageningen	2008
Macroscopical Physical Chemistry, Han-sur-lesse, Belgium	2008

General courses

Writing grant proposal, Wageningen	2011
Career assessment, Wageningen	2011
Teaching methodology and skills for PhD student , Wageningen	2011
Conversation skill in one-to-one, Wageningen	2011
Project & time management, Wageningen	2009
Supervising & organizing MSc thesis project, Wageningen	2009
Technique for writing & presenting a scientific paper, Wageningen	2009
VLAG-PhD week	2008

Conferences

International Conference on Engineering and Food, Athens, Greece	2011
Symposium Delivery of Functionality in Complex Food System, Wageningen, The Netherlands	2009
The International Symposium on Food Rheology and Structure, Zürich, Switzerland	2009

Optional

Project Meetings "High Protein Food", TIFN	2008 – 2010
PhD trip Food Process Engineering, USA	2010
Symposium Food Process Engineering	2010
Brain & Game Session Food & Bioprocess Engineering	2008, 2009
PhD trip Food & Bioprocess Engineering, Japan	2008

The research described in this thesis was financially supported by Top Institute Food and Nutrition.

Financial support from Wageningen University and Top Institute Food and Nutrition for printing this thesis is gratefully acknowledged.

Cover Design : Nanik Purwanti and Rais Diosdado

Layout Design : Nanik Purwanti and Rais Diosdado

Printing : GVO drukkers & vormgevers B.V. | Ponsen & Looijen

Front cover : the word ‘structuring’ is represented by a couple of gears.

Back cover : microscopy images of WPI microparticles, taken with a light microscope and SEM.